

Synthesis and evaluation of small molecule inhibitors of pre-mRNA splicing to effectively modify gene expression

A dissertation submitted to the University of Manchester for the degree of Master's of
Science by Research in the Faculty of Science & Engineering.

2019

Olivier A Kirchhoffer

**Department of Chemistry, School of Natural Sciences, Faculty of Science and
Engineering**

Table of Contents

| | |
|---|----|
| Table of Contents | 2 |
| List of Figures | 5 |
| List of Tables..... | 7 |
| List of Abbreviations..... | 8 |
| Abstract | 11 |
| Declaration | 12 |
| Copyright Statement..... | 12 |
| Acknowledgments | 13 |
| 1.0 - Introduction..... | 14 |
| 1.1 - The Spliceosome | 14 |
| 1.1.1 – The pre-mRNA..... | 14 |
| 1.1.2 – The Splicing mechanism | 15 |
| 1.1.3 - U2 snRNP: previously discovered inhibitors..... | 17 |
| 1.1.4 - U5 snRNP as a splicing regulator | 19 |
| 1.2 - Inhibition of <i>Snu114</i> : From fusidic acid to lithocholic acid | 20 |
| 1.2.1 - Fusidic acid | 20 |
| 1.2.2 - A new hit compound derived from fusidic acid | 21 |
| 1.2.3 - Lithocholic acid | 22 |
| 1.3 - Protection of the <i>C-24</i> free acid group..... | 23 |
| 1.3.1 - POM protection of <i>C-24</i> | 23 |
| 1.3.2 - Isopropanol protection of <i>C-24</i> | 24 |
| 1.3.3 - <i>Tert</i> -butanol protection of <i>C-24</i> | 25 |
| 1.4 - Functionalization at the <i>C-3</i> position | 26 |
| 1.4.1 - Anhydrides | 26 |
| 1.4.2 - Acids | 27 |

Table of Contents

| | |
|--|----|
| 1.4.3 - Mitsunobu Inversion | 28 |
| 1.4.4 – Fluoro-deoxygenation | 29 |
| 1.5 - Biological Assays | 31 |
| 1.5.1 - Thermal Shift Assay (TSA) | 31 |
| 1.5.2 - Splicing Assay | 32 |
| 2.0 - Project Aims | 34 |
| 3.0 - Results & Discussion | 35 |
| 3.1 - Protection of the C-24 Acid moiety | 35 |
| 3.2 - Esterification with anhydrides | 37 |
| 3.2.1 - DMAP mechanism in the initial procedure | 37 |
| 3.2.2 – Alternative reaction conditions for esterification with anhydrides | 38 |
| 3.2.3 – Saturated anhydrides | 38 |
| 3.2.4 – Unsaturated anhydrides | 40 |
| 3.3 - Esterification with acids..... | 42 |
| 3.4 - N-Acylation at C-24..... | 43 |
| 3.5 - Mitsunobu Inversion | 44 |
| 3.6 - 'Butyl deprotection to restore the C-24 acid moiety | 46 |
| 3.7 - Fluoro-deoxygenation reactions | 47 |
| 3.7.1 - DAST | 48 |
| 3.7.2 - XtalFluor-E + DBU | 49 |
| 3.7.3 - XtalFluor E + TEA·3HF | 50 |
| 3.8 - Biological Assays | 52 |
| 3.8.1 - Thermal Shift Assays (TSA)..... | 53 |
| 3.8.2 - Splicing assays – 1 mM | 54 |
| 3.8.3 – Splicing assays - 1 mM and 100 μ M..... | 56 |
| 4.0 - Conclusion & Future work | 57 |
| 4.1 – New lead compound..... | 57 |

Table of Contents

| | |
|---|----|
| 4.2 – Recently developed alternative to Mitsunobu inversion reagents..... | 58 |
| 4.3 – Stereocontrol in fluoro-deoxygenation mechanism | 58 |
| 5.0 - Experimental | 60 |
| 5.1 – Instrumentation, Software, Techniques and Apparatus | 60 |
| 5.1.1 - Structures | 60 |
| 5.1.2 - Thin Layer Chromatography (TLC) | 60 |
| 5.1.3 - Chromatography | 60 |
| 5.1.4 - Nuclear Magnetic Resonance Spectroscopy (NMR) | 60 |
| 5.1.5 - Infra-Red Spectroscopy | 60 |
| 5.1.6 - Melting points | 60 |
| 5.1.7 - Optical rotation | 60 |
| 5.1.8 - Experimental Terms..... | 61 |
| 5.1.9 - Baths | 61 |
| 5.1.10 - Solvents and Reagents | 61 |
| 5.2 – Experimental Procedures | 62 |
| 5.3 - <i>In-Vitro</i> pre-mRNA Splicing Assay | 91 |
| 5.3.1 - Yeast; Gel electrophoresis | 91 |
| 5.3.2 - Yeast; qRT-PCR quantification | 92 |
| 6.0 - References..... | 93 |

Word count - 21,044

List of Figures

| | |
|---|----|
| Figure 1 - Pre-mRNA structure with important features of the intronic sequence..... | 14 |
| Figure 2 - The Spliceosome assembly/disassembly mechanism..... | 15 |
| Figure 3 - Structures Spliceostatin A (1) and E7107 (2), two active inhibitors of SF3b.... | 17 |
| Figure 4 - The five different alternative splicing patterns..... | 18 |
| Figure 5 - Steps III and IV of the splicing cycle, with the sub-units of the U5 snRNP ¹ | 19 |
| Figure 6 - Fusidic acid 1 and its 3D chair-boat-chair (trans-cis-trans) structure..... | 20 |
| Figure 7 - Structure of the hit compound 4 derived from fusidic acid..... | 21 |
| Figure 8 - 3D structure of lithocholic acid 5 (cis-trans-trans) and the hit compound 4. | 22 |
| Figure 9 - Mechanism of the carboxylic acid protection with chloromethyl pivalate (7)..... | 23 |
| Figure 10 - Reaction conditions proposed for the isopropanol protection of lithocholic acid..... | 24 |
| Figure 11 - Reaction conditions used for the tert-butanol protection of lithocholic acid..... | 25 |
| Figure 12 - Reaction scheme for the C-3 functionalization starting with anhydrides..... | 26 |
| Figure 13 - Mechanism of the DCC-mediated (27) coupling of acids to form esters..... | 27 |
| Figure 14 - The Mitsunobu inversion reaction, with the S _N 2 transition state. | 28 |
| Figure 15 - Reactivity of an equatorial (α) and an axial (β) leaving group at C-3..... | 29 |
| Figure 16 - Mechanistic pathways for the deoxo-fluorination using DAST (37)..... | 30 |
| Figure 17 - Structures of XtalFluor-E (41)/-M (42) and TEA·3HF (43)..... | 31 |
| Figure 18 - Evolution of an enzyme's binding state and shape in a TSA..... | 31 |
| Figure 19 - Sequence of the forward primers used and the associated reverse primer..... | 32 |
| Figure 20 - Summary of the attempted modifications on lithocholic acid..... | 34 |
| Figure 21 - Carboxylic acid protecting groups for lithocholic acid..... | 35 |
| Figure 22 - Reaction conditions used to protect lithocholic acid with chloromethyl pivalate..... | 36 |
| Figure 23 - Mechanism of the DMAP-catalysed cleavage of succinic anhydride (17)..... | 37 |
| Figure 24 - Alternative procedure adopted for esterification reactions with anhydrides..... | 38 |
| Figure 25 - Tautomerism between itaconic (24) & citraconic anhydrides (23) and their ring-opened analogs. | 41 |
| Figure 26 - Esters obtained through EDCI coupling of the corresponding carboxylic acid. | 42 |
| Figure 27 - Amide formation at the C-24 acid moiety of lithocholic acid..... | 43 |

| | |
|--|----|
| Figure 28 - The two-step Mitsunobu inversion reaction..... | 44 |
| Figure 29 - Reaction conditions for the deprotection of a tert-butyl ester..... | 46 |
| Figure 30 - Selected region of the ¹ H NMR spectra of all the attempted fluoro-deoxygenations. | 47 |
| Figure 31 - Fluoro-deoxygenation reaction with DAST (37)..... | 48 |
| Figure 32 - Fluorination reaction with XtalFluor-E (41) and DBU (84) as an additive..... | 49 |
| Figure 33 - Fluorination reaction with XtalFluor-E (41) and TEA·3HF (86) as an additive. | 50 |
| Figure 34 - 3D-Structure of DHEA (87) and both α-(13) & β-(75) hydroxyl groups..... | 51 |
| Figure 35 - Thermal shift assay results of some compounds of interest (Error bars indicate SD, n = 3)..... | 53 |
| Figure 36 - Splicing inhibition displayed by some of the most promising new compounds. Splicing Efficiency (%) calculated as a percentage of the DMSO control. Error bar indicates SD, n = 2..... | 55 |
| Figure 37 - Splicing inhibitory activity of the hit compound (4) compared to compounds (47+48) and (51+52). Splicing Efficiency (%) calculated as a percentage of the DMSO control. Error bars indicate SD, n = 3 (**** = P<0.00001)..... | 56 |
| Figure 38 - Structures of the new lead compounds..... | 57 |
| Figure 39 - (A) Newly developed organocatalyst for the Mitsunobu inversion reaction. (B) Structures of the dimethylsuccinate esters of LA with unnatural C-3 configuration. (C) Structure of the 3α- deoxo-fluorinated compound..... | 58 |
| Figure 40 - Structures of DAST, XtalFluor-E and AlkylFluor..... | 59 |

List of Tables

| | |
|---|----|
| Table 1 - Structures resulting from all the attempted C3-functionalisation reactions with varying anhydride reagents. The corresponding C-24 protecting group is given in brackets next to the yield, where the yield reads "-" the reaction was not attempted. | 39 |
| Table 2 – Structures of the molecules used in thermal shift assays and splicing assays.... | 52 |

List of Abbreviations

| | |
|-------------------|---|
| A | adenine |
| AS | alternative splicing |
| ATP | adenosine triphosphate |
| BPS | branch point sequence |
| ¹³ C | carbon 13 |
| C | cytosine |
| cDNA | complementary deoxyribonucleic acid |
| C _T | cycle time |
| DAST | diethylaminosulfur trifluoride |
| DBU | 1,8-Diazabicyclo[5.4.0]undec-7-ene |
| DCC | <i>N,N'</i> -dicyclohexylcarbodiimide |
| DCM | dichloromethane |
| DCU | <i>N,N'</i> -dicyclohexylurea |
| DHEA | dehydroepiandrosterone |
| DMAP | 4-dimethylaminopyridine |
| DMF | dimethylformamide |
| DMSO | dimethylsulfoxide |
| DNA | deoxyribonucleic acid |
| dNTP | deoxy nucleotide triphosphate |
| DTT | dithiothreitol |
| E ₂ | Elimination 2 |
| EDCI | 1-ethyl-3-(3-dimethylaminopropyl)carbodiimide |
| EDTA | ethylenediaminetetraacetic acid |
| EF-2 | elongation factor 2 |
| EF-G | elongation factor G |
| ES (+/-) | electrospray (positive or negative) |
| Et ₂ O | diethyl ether |
| G | guanine |
| GDP | guanosine diphosphate |
| GTP | guanosine triphosphate |
| ¹ H | proton |
| HRMS | high-resolution mass spectrometry |

| | |
|-----------------------------------|--|
| HSQC | heteronuclear single quantum coherence |
| Hz | hertz |
| Kb | kilobase |
| LA | lithocholic acid |
| LRMS | low-resolution mass spectrometry |
| m.p. | melting point |
| mRNA | messenger ribonucleic acid |
| NMR | nuclear magnetic resonance |
| NTC | nineeen-complex |
| PCA | phenol chloroform-isoamyl alcohol |
| PCR | polymerase chain reaction |
| PEG ₆₀₀₀ | polyethylene glycol 6000 g.mol ⁻¹ |
| POM | pivaloyloxymethyl |
| pre-mRNA | pre-messenger ribonucleic acid |
| Py-tract | polypyrimidine-tract |
| qPCR | quantitative polymerase chain reaction |
| qRT-PCR | quantitative reverse transcription polymerase chain reaction |
| R _f | retention factor |
| RNA | ribonucleic acid |
| RQ | relative quantity |
| RT | reverse transcription |
| SAR | structure-activity relationship |
| SD | standard deviation |
| SDS | sodium dodecyl sulfate |
| SF3b | splicing factor 3b |
| S _N 1/S _N 2 | nucleophilic substitution 1/2 |
| snRNP | small nuclear ribonucleoprotein |
| SSA | spliceostatin A |
| SSIV | superscript IV |
| T | thymine |
| TBE | tri borate ethylenediaminetetraacetic acid |
| TEA | triethylamine |
| TEA·3HF | triethylamine ·3 hydrogen fluoride |
| TFA | trifluoroacetic acid |

List of Abbreviations

| | |
|--------------------|---------------------------|
| TLC | thin layer chromatography |
| T _m | melting temperature |
| TSA | thermal shift assay |
| tRNA | transfer ribonucleic acid |
| U | uracyl |
| U2AF ⁶⁵ | U2 auxiliary factor 65 |
| UV | ultra-violet |

Abstract

The spliceosome is a highly complex molecular machine that still holds a lot of secrets for contemporary biology. It plays a crucial role as one of the various mechanisms involved in generating a plethora of different proteins, from a limited amount of genetic information, sealed in the form of DNA in the nucleus of living cells.

Previous studies have tried to dissect this complex mechanism by inhibiting the spliceosome, in order to study its biological properties. Interestingly a significant number of inhibitors found, which target the specific U2 snRNP unit of the spliceosome, have been reported to have anti-cancer activity. Some of the most promising compounds, which resulted from this drug development approach, have almost made it to the drug market at the time of writing, for their antitumor activity. A vast amount of research has emerged concerning the biological processes that ultimately led to this activity.

Previous work within the Whitehead group, which focused on developing inhibitors of the U5 snRNP unit of the spliceosome, has led to the discovery of a compound derived from the steroidal antibiotic fusidic acid that displayed significant splicing inhibitory activity. Lithocholic acid later emerged as another potential starting point for developing small molecule inhibitors of the U5 snRNP, as it was found to have similar levels of inhibition as the hit compound derived from fusidic acid.

Lithocholic acid was a good starting point for further SAR studies, as it isn't heavily functionalised, making it a robust compound that can easily be diversified. A variety of compounds were generated from it, with new structural features and additional functional groups that unravelled new information about the target protein. Splicing assays also revealed that several of these compounds have superseded the level of inhibition achieved by the previously outlined hit compound.

Declaration

No portion of the work referred to in this dissertation has been submitted in support of an application for another degree or qualification of this or any other university or other institute of learning.

Copyright Statement

- i. The author of this dissertation (including any appendices and/or schedules to this dissertation) owns certain copyright or related rights in it (the “Copyright”) and s/he has given The University of Manchester certain rights to use such Copyright, including for administrative purposes.
- ii. Copies of this dissertation, either in full or in extracts and whether in hard or electronic copy, may be made **only** in accordance with the Copyright, Designs and Patents Act 1988 (as amended) and regulations issued under it or, where appropriate, in accordance with licensing agreements which the University has from time to time. This page must form part of any such copies made.
- iii. The ownership of certain Copyright, patents, designs, trademarks and other intellectual property (the “Intellectual Property”) and any reproductions of copyright works in the dissertation, for example graphs and tables (“Reproductions”), which may be described in this dissertation, may not be owned by the author and may be owned by third parties. Such Intellectual Property and Reproductions cannot and must not be made available for use without the prior written permission of the owner(s) of the relevant Intellectual Property and/or Reproductions.
- iv. Further information on the conditions under which disclosure, publication and commercialisation of this dissertation, the Copyright and any Intellectual Property and/or Reproductions described in it may take place is available in the University IP Policy, in any relevant Dissertation restriction declarations deposited in the University Library, The University Library’s regulations and in The University’s policy on Presentation of Dissertations

Acknowledgments

First of all I would like to thank Dr Roger Whitehead, for his pedagogy and attention to detail that made me learn a lot throughout this project, while also making me feel trusted for this task. My co-supervisor Dr Ray O'Keefe and Dr Huw Thomas both deserve my gratitude for the enlightments provided on the biological parts of the project. Dr Richard Bryce, who also works on that project, did provide me with great support when the moment came and I wish to thank him for his trust. Megan Eadsforth also deserves special thanks; on top of productive professional collaborations, you've also been an amazing friend this year and I can't thank you enough for having had my back when I needed help! Thanks also to all other members of the Whitehead and O'Keefe groups I've had the pleasure of collaborating with!

Then I would like to thank my dad particularly for his unconditional support in whatever decisions I have been taking so far. Feeling safe and backed-up, while sliding along the learning curve of life, is an invaluable force that I feel grateful for having had. Thanks to Claudia also for being always supportive and optimistic! Special thanks to Jean, Irene and Aline who have been there since the earliest years, your trust and financial support throughout my studies mean a lot to me.

In another perspective, Coop (CH) also deserves my thankfulness for providing me with a job, without which I wouldn't have been able to self-fund this degree. Juliane, Liridona, Nathalia and Gradi, it has been a pleasure being part of your team; time really flies at work when you have nice colleagues!

Finally, Yass and Soph, the two pillars of my Mancunian life, boredom is never a thing around you! I'm grateful for some amazing friendships from Strasbourg that have lasted over the years and the distance: Gabriel, Eugenia, Michael, Lola, Edouard, Mathilde and Cedric, I can't plan a trip home without crossing your way! Leocadie, Oskar, Joseph, Ludovica, Elan, Stanley, Masud, Joe, Andrea, Freddie, Marie, Victor, Aurelien, Peter, Charlotte and so many other people that I would like to thank for the amazing time I've had in this city!

1.0 - Introduction

1.1 - The Spliceosome

1.1.1 – The pre-mRNA

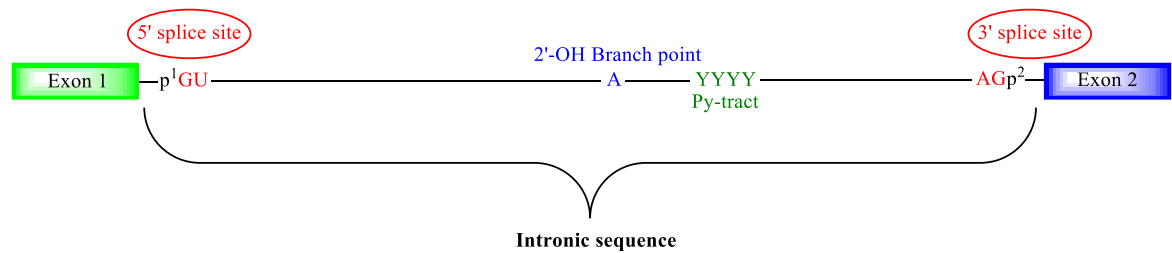


Figure 1 - Pre-mRNA structure with important features of the intronic sequence.

Despite all the knowledge acquired nowadays over transcription and translation mechanisms, the splicing process, which occurs between these two, has not yet been fully elucidated. The spliceosome, made up of five small nuclear ribonucleoprotein complexes (snRNPs: U1, U2, U4, U5 and U6) and over 150 non-snRNP proteins, is the molecular machinery carrying out the splicing reaction.

The entity created from the transcription of DNA is called "pre-mRNA" and is made up of exons (coding sequences) and introns (non-coding sequences). In essence, the splicing mechanism consists of the removal of the non-coding introns, resulting in a "mature" mRNA.¹ There are two different modes in which splicing can be carried out, known as constitutive and alternative splicing. Constitutive splicing refers to when exons are spliced in a conserved manner by the spliceosome, always generating the same mRNA from each pre-mRNA, as opposed to alternative splicing, which can produce multiple proteins from a single gene. Alternative splicing contributes in adding diversity to the phenotype of living systems.²

1.1.2 – The Splicing mechanism

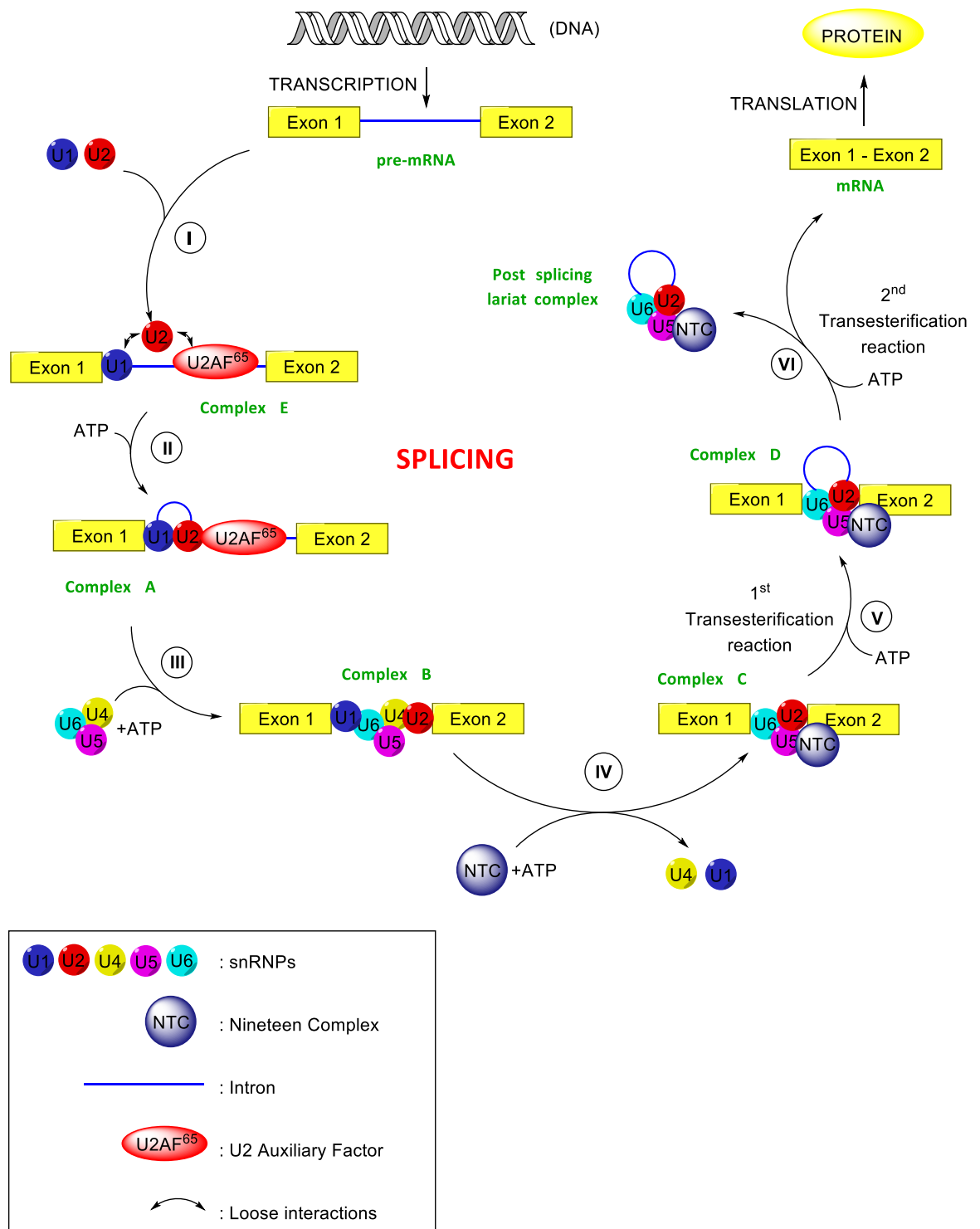


Figure 2 - The Spliceosome assembly/disassembly mechanism.³

Splicing occurs in a stepwise manner as depicted on Figure 2: the first step **(I)** is the addition of U1 on the 5' splice site of the intron, while U2 is thought to be loosely bound to U1 as well as an auxiliary factor called "U2AF⁶⁵". This auxiliary factor is itself bound to a specific and conserved portion of the intron sequence, called the polypyrimidine-tract (Figure 1, Py-tract). In contrast to every other step of the splicing mechanism, formation of complex E does not require the presence of ATP.⁴ Introduction of ATP therefore initiates step **II**, where U2 base pairs with the branch point sequence (BPS, Figure 1), effectively forming complex A. Eventually, addition of the U4/U6·U5 tri-snRNP complex (step **III**), another ATP-fuelled process, leads to the formation of complex B, which contains all five snRNPs.

One last step is required to generate the catalytically active complex C, requiring addition of the Nineteen Complex (NTC) and a remodelling of the spliceosome driven by eight ATPases and one GTPase (step **IV**). The elimination of U1 & U4 resulting from this step suggests that the previously bound U4/U6 complex had to be unwound and this process is effectively controlled by the U5 snRNP.^{5,6}

Complex C then carries out the splicing reaction, which consists of two consecutive transesterification reactions. The first reaction happens with cleavage at the 5'-end of the intron (step **V**), resulting in a free exon 1. In addition, the intron forms a "lariat structure" (blue curve on figure 2) while still being attached to exon 2. This circular intronic structure results from the 5'-guanosine nucleotide attaching onto the branch point, characterised by an adenosine nucleotide, via a phosphodiester bond linkage. Subsequently, a chemically similar reaction occurs at the 3' splice site (step **VI**), which involves cleavage of the intron lariat and tethering of exon 1 to exon 2 to generate the mature mRNA.⁷

1.1.3 - U2 snRNP: previously discovered inhibitors

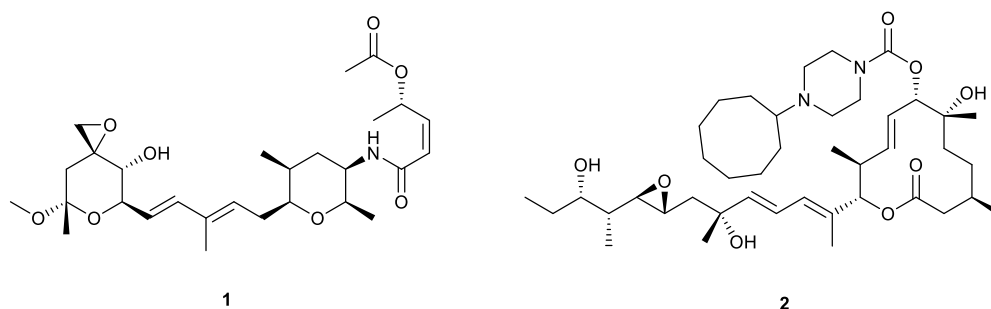


Figure 3 - Structures *Spliceostatin A (1)* and *E7107 (2)*, two active inhibitors of *SF3b*.⁸

To this day, several inhibitors of the U2 snRNP displaying antitumor activity have been identified. All of these inhibitors were found to target the *SF3b* unit, a subcomplex of the U2 snRNP⁸, however the mechanism leading to antitumor activity remained unclear. Two undeniable consequences of the inhibition of *SF3b* have been largely documented: *SF3b* inhibitors induced alternative splicing pathways and also induced leakage of pre-mRNA from the nucleus of a cell into its cytoplasm.⁹

Alternative splicing (AS) consists of 5 different variants in the way a pre-mRNA strand is spliced: exon skipping, alternative 5' splice site, alternative 3' splice site, mutually exclusive exons and intron retention, as depicted on Figure 4. Opinions diverged however when it came to determining which event of AS happened most frequently when *SF3b* was inhibited. Wu & co-workers¹⁰ provided data that support a predominance of exon skipping events, regardless of which inhibitor was used, while others argued that intron retention was the predominant event resulting from the *SF3b* inhibition induced by Spliceostatin A (R. Yoshimoto, 2016).⁹ The outcome of the splicing mechanism upon inhibition of *SF3b* does nevertheless also depend on other external factors, such as the nature of the cell line used in the assays. In that way, one inhibitor could display different alternative splicing events, depending on whether yeast pre-mRNA or human pre-mRNA was used.

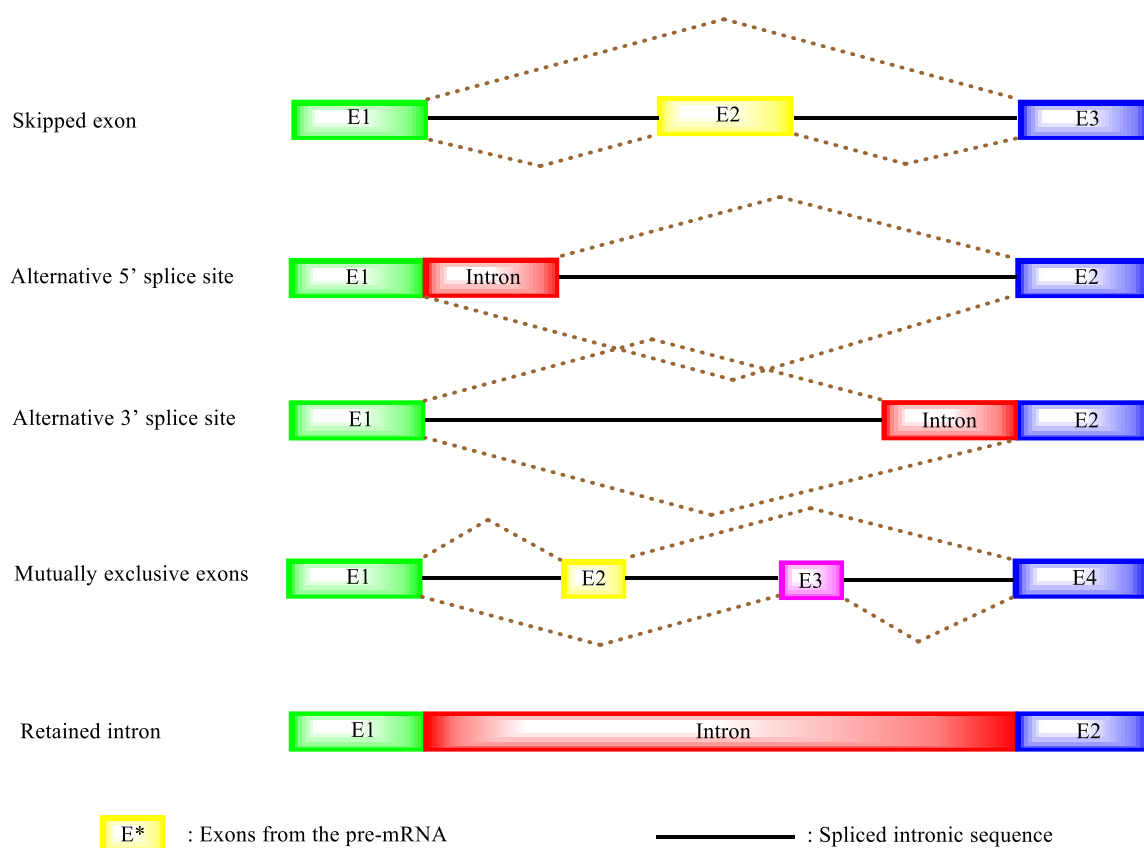


Figure 4 - The five different alternative splicing patterns.⁹

Spliceostatin A (SSA, **1**, Figure 3) is one example of an *SF3b* inhibitor that is reported to have promising antitumour activity. In fact, binding of SSA to the *SF3b* complex was thought to affect branch point sequence (BPS) recognition by the U2 snRNP, which was thought to induce alternative splicing events. In other words, SSA alters the splicing mechanism rather than simply inhibiting it as a whole, leaving an entire new grey zone for biological mechanisms to happen. In addition, pre-mRNA leakage from the nucleus to the cytoplasm was also a consequence observed following inhibition of *SF3b*, with leaked pre-mRNAs being predominantly short and with weak 5' splice sites. This suggested that SSA treatment also had a certain degree of selectivity towards particular pre-mRNA sequences.⁹

Pladienolides were also a family of compounds derived for their activity on SF3b, despite their structures showing notable differences when compared to Spliceostatin A. E7107 (**2**, Figure 3) was a particularly interesting member of this family that has already made it to first-in-human clinical trials. It was thought to act in a similar way as SSA, by preventing U2 snRNP from being bound to the BPS.¹¹

The discovery of small molecule inhibitors of the U2 snRNP has enabled a whole range of studies on the biological activity induced by these compounds and has revealed more detail on the role of U2 snRNP within the spliceosome. The Whitehead group has therefore focused on developing inhibitors of the U5 snRNP in order to open an entirely new area for investigations into the mechanism of the spliceosome as a whole.

1.1.4 - U5 snRNP as a splicing regulator

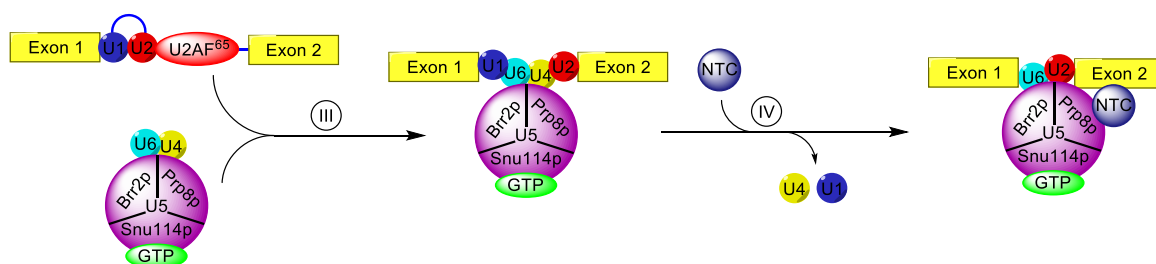


Figure 5 - Steps III and IV of the splicing cycle, with the sub-units of the U5 snRNP¹.

As stated earlier, U5 is a crucial snRNP as it is mostly responsible for the control of the final activation step (IV) of the spliceosome. During this step, three sub-units of particular importance, *Prp8*, *Snu114* and *Brr2*, are associated with the U5 snRNA (Figure 5). *Prp8* holds a central position in the spliceosome, allowing it to interact with entities located beyond the boundaries of the U5 snRNP itself⁵, meanwhile both *Brr2* & *Snu114* interact with the N and C termini of *Prp8*.⁴ While *Prp8* is thought to be the principal regulator of the splicing mechanism as a whole¹, both *Snu114* and *Prp8* actually regulate the ATPase *Brr2*, with *Snu114* believed to have overall control of *Brr2* activity. *Brr2* is eventually responsible for the ATP-dependent U4/U6 unwinding; any changes made on other entities linked with its activity can have an influence on the rate of completion of the final activation step (IV) of the spliceosome.^{3,12}

Snu114 is a GTPase that was found to allow *Brr2* activity when in a GTP-bound state, as opposed to a GDP-bound state, in which it displays an inhibitory effect. Despite GTPases usually catalysing hydrolysis reactions, the use of non-hydrolyzable GTP analogs also allowed *Brr2* activation, which proved that GTP hydrolysis is unnecessary in this process. Consequently, *Snu114* was considered as a "classic signalling G protein" that regulates *Brr2* activity, rather than being directly involved in the dynamics of the RNA rearrangements during splicing.¹³

Snu114 also has a very similar sequence identity with the translation elongation factors *EF-G* and *EF-2*. Unlike *Snu114*, *EF-G* and *EF-2* catalyse the hydrolysis of GTP to drive translocation of tRNA and mRNA through the ribosome, consequently qualified as "chemomechanical motors" rather than signalling proteins. This similarity was nevertheless used as a starting point for further research on *Snu114*, after it had been established that fusidic acid, an inhibitor of *EF-G*, had also shown promising inhibition of yeast and human *in vitro* splicing at 1 mM.³

1.2 - Inhibition of *Snu114*: From fusidic acid to lithocholic acid

1.2.1 - Fusidic acid

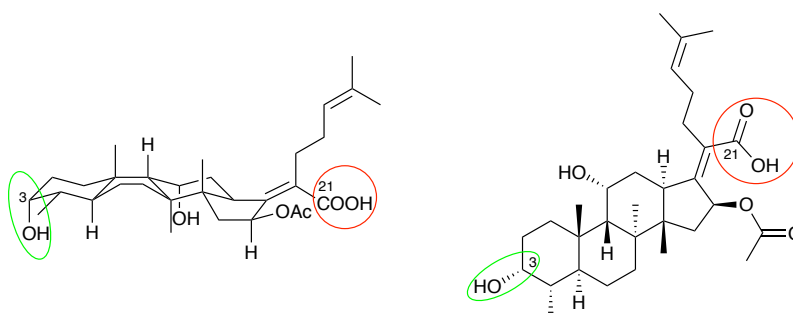


Figure 6 - Fusidic acid **1** and its 3D chair-boat-chair (*trans-cis-trans*) structure.

Fusidic acid is a steroidal antibiotic that adopts an unusual *trans-cis-trans* (chair-boat-chair) conformation (3, Figure 6), compare to the common *trans-trans-trans* (chair-chair-chair) conformation of other steroids. An extensive Structure Activity Relationship (SAR) study on fusidic acid derivatives for their antibacterial activity has been reported.¹⁴ This study directed S. Harte¹⁵ and R. Soltysiak³ in making chemical modifications to fusidic acid, with the aim of increasing its potency and specificity for *Snu114*. It was found that the binding pocket surrounding the C-3 hydroxyl group is not conserved between *Snu114* and *EF-G*, therefore this position was chosen as the most suitable for modifications. Unfortunately, most modifications resulted in decreased potency compared to fusidic acid. It was also found that esterification of the C-21 acid moiety (red circle, Figure 3), was particularly detrimental to the splicing inhibition activity of fusidic acid. Interestingly, esterification of the C-21 acid moiety also results in a decrease in antibacterial activity of fusidic acid. This suggests that the carboxylate ion forms crucial interactions within the active site of *EF-G* and *Snu114*.

Notably, in the crystal structure of EF-G bound by fusidic acid the carboxylate ion is in close proximity to the Mg^{2+} ion within the GTP active site.¹⁶ The same Mg^{2+} ion is found within the active site of Snu114, it is therefore possible that the acid group within the molecule interacts with this ion. It is possible that such interactions disturb GTP/GDP binding to Snu114 and result in deactivation of the U5 snRNP which would ultimately lead to a blocked splicing mechanism.

Efforts were taken to try and further elucidate the binding mode of fusidic acid to Snu114 via photo-crosslinking studies. Whilst attempting to incorporate a photocross-linking moiety into fusidic acid, an intermediate was found which was significantly more potent than fusidic acid, inhibiting both yeast and human *in vitro* splicing at approximately 100 μ M.

1.2.2 - A new hit compound derived from fusidic acid

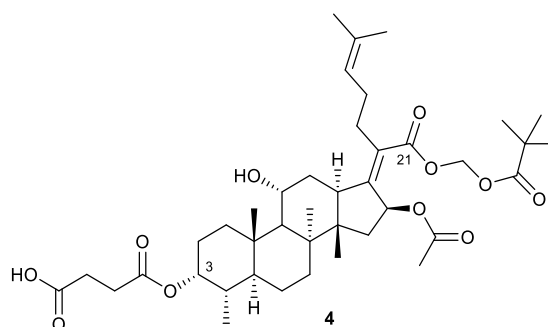


Figure 7 - Structure of the hit compound **4** derived from fusidic acid.

Among all the C-3 functionalized derivatives of fusidic acid, the succinate ester stood out with a promising improvement in activity (**4**, Figure 7). Interestingly, its C-21 free acid moiety was protected, which should have led to a decrease in activity. The presence of a new free acid group on the added succinate ester did however compensate for that loss in activity and provided strong evidence of the potential interchangeability of the acid group on either end of the molecule.

Following that observation, other carboxylic acid-containing steroid structures were also tested for splicing inhibition and lithocholic acid was chosen as a new lead compound, as it was shown to inhibit human *in vitro* splicing at 100 μ M. Furthermore, no inhibition of EF-G was exhibited by compound **4**, which proved that it might also have good specificity towards binding the spliceosome. This specificity could also be verified for lithocholic acid using thermal shift assays.³

1.2.3 - Lithocholic acid

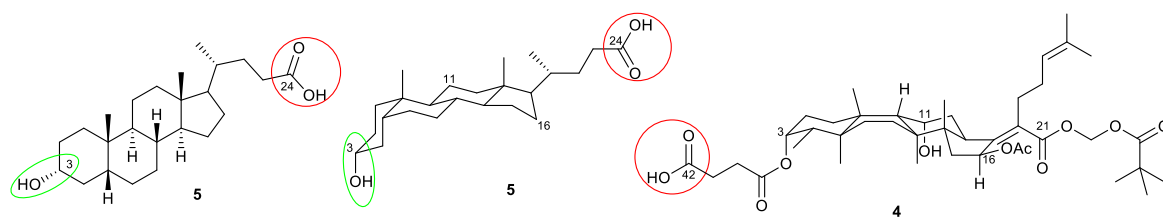


Figure 8 - 3D structure of lithocholic acid **5** (*cis-trans-trans*) and the hit compound **4**.

Despite their differences in ring conformations (Figure 8), the distance between C-3 and C-21 in fusidic acid is comparable to that between C-3 and C-24 in lithocholic acid. In addition to that, both lithocholic acid (**5**) and the hit compound (**4**) had closely overlapping molecular volumes when both acids (C-24 & C-42 red-circled on Figure 5) were overlaid (unpublished communication, Ray O'Keefe, University of Manchester).

From another perspective, the lack of any C-11-hydroxyl or C-16-acetyl group in lithocholic acid could be seen as disadvantageous, as these moieties could potentially form interactions with the binding pocket of *Snu114*. When making an analogy with the homologous EF-G binding site, Godtfredsen & co-workers¹⁴ found that functionalising these two groups on fusidic acid only resulted in a slight decrease in binding affinity. The presence of these two groups might therefore not be fundamental to the binding affinity.

In terms of reactivity, the absence of both C-11 & C-16 functionalities is actually advantageous, as the only location found to tolerate structural changes in fusidic acid was the C-3 hydroxyl group, which is also present in lithocholic acid. Consequently, lithocholic acid was thought to be a more robust starting point for C-3 functionalization, as any additional functional group in a molecule creates potential for side reactions to occur. Chemical stability also implies that an additional range of chemical reactions could be achievable, which would proceed in more forcing conditions.

1.3 - Protection of the C-24 free acid group

1.3.1 - POM protection of C-24

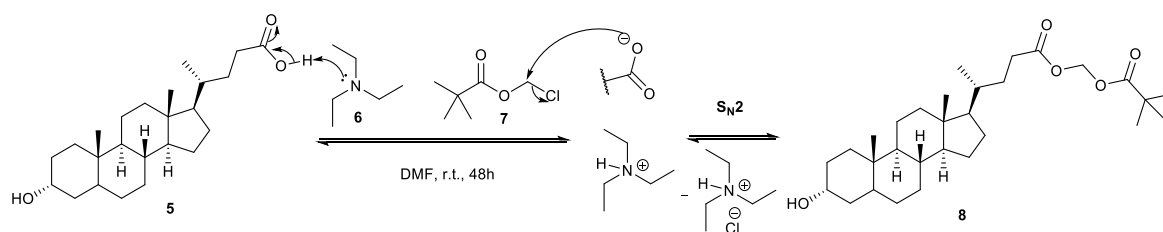


Figure 9 - Mechanism of the carboxylic acid protection with chloromethyl pivalate (7).

For comparative purposes, the starting point chosen for C-24 protection was the pivaloyloxymethyl (POM) group, a selection made by R.J. Soltysiak based on its lability under basic conditions, that would allow controlled deprotection if required.^{3,17} This protecting group was also reported in the structure of previously developed prodrugs, which suggested that it could be suitable for use in biological systems.¹⁸ In another perspective, additional binding interactions like hydrogen-bonding could also be thought to occur with the POM-protected compound, as two new hydrogen-bond acceptors were generated compared to a simple *methyl*-protection.

The straightforward S_N2 mechanism of this protection step was facilitated by the deprotonation of the carboxylic acid group (5, Figure 9). Chlorine is also a good leaving group, which favours this type of mechanism. One of the major drawbacks of this synthesis however, would be the use of DMF with its particularly high boiling point, which may prompt the need for additional purification methods. Besides, the reaction proceeded in gentle conditions in terms of pK_a, which was probably also an important factor for this reaction to work in the case of fusidic acid. Lithocholic acid on the other hand, could enjoy greater freedom for the protecting mechanisms to be chosen, by potentially widening the array of possible protecting groups used.

1.3.2 - Isopropanol protection of C-24

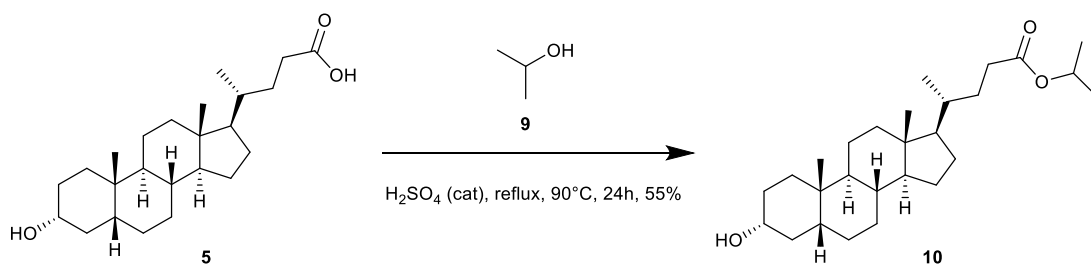


Figure 10 - Reaction conditions proposed for the isopropanol protection of lithocholic acid.

In an attempt to diversify the protecting groups used on the C-24 acid moiety, a procedure for isopropyl protection of C-24 was proposed by P. G. G. do Nascimento.¹⁹ Sulfuric acid was used in catalytic amount, while it contained isopropanol (9) acting as both a reagent and a solvent (Figure 10). Completion of this reaction essentially relied on Le Chatelier's principle to favour product formation via the large excess of reagent used, despite the unfavourable kinetics of this reaction, highlighted by the high temperatures required.

Additionally, for comparative purposes, generation of the *tert*-butyl ester was also planned and due to the very similar reactivity of isopropanol (9) and *tert*-butanol (12), interrogations as to whether this procedure could also be used to *tert*-butyl-protect lithocholic acid were therefore raised. The main difference in reactivity between both alcohols could nevertheless be highlighted when considering nucleophilic substitutions that could occur as side-reactions: *tert*-butanol being a tertiary alcohol, the *tert*-butyl ester formed upon esterification would react via a $\text{S}_{\text{N}}1$ mechanism, going through a carbocation intermediate, favoured under acidic conditions and in the presence of a nucleophile (*tert*-butanol in excess). Meanwhile, isopropanol is a secondary alcohol, for which S_{N} reactions could proceed through either $\text{S}_{\text{N}}1$ or $\text{S}_{\text{N}}2$ mechanisms, depending on the reaction conditions.

1.3.3 - *Tert*-butanol protection of C-24

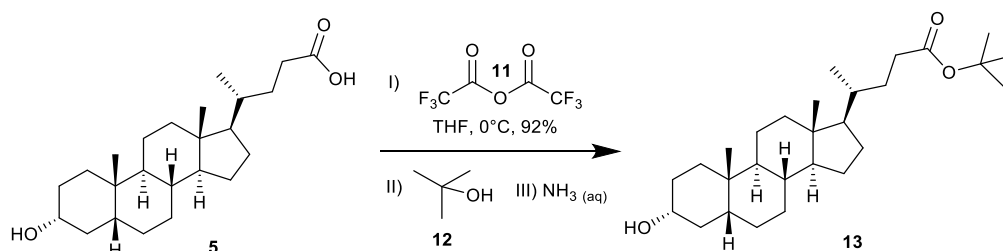


Figure 11 - Reaction conditions used for the *tert*-butanol protection of lithocholic acid.

The assumption that the acid catalysed reaction may not be suitable for use with *tert*-butanol prompted further investigations into finding potential alternatives. R. P. Bonar-Law and co-workers²⁰ had reported a multistep procedure for the esterification of lithocholic acid with *tert*-butanol, which did not require acidic conditions (Figure 11). Furthermore, this reaction did not require the alcohol to be used as a solvent, which reduced the expense and waste of the reagents, especially when the latter had to be used in anhydrous form.

Additionally, there was no apparent reason that would prevent this reaction from being reproducible with methanol or isopropanol instead of *tert*-butanol. Even though concentrated 35% (w/w) solution of ammonium hydroxide was used in this procedure, the resulting pKa of the reaction mixture should not be basic enough to allow cleavage of the supposedly formed *methyl-isopropyl*- ester.

Formation of either *tert*-butyl-, *isopropyl*- or *methyl*-protected lithocholate esters was necessary in order to allow reactions proceeding in basic media, such as the second step of a Mitsunobu inversion reaction to be carried out on the C-3-hydroxyl group.

1.4 - Functionalization at the C-3 position

1.4.1 - Anhydrides

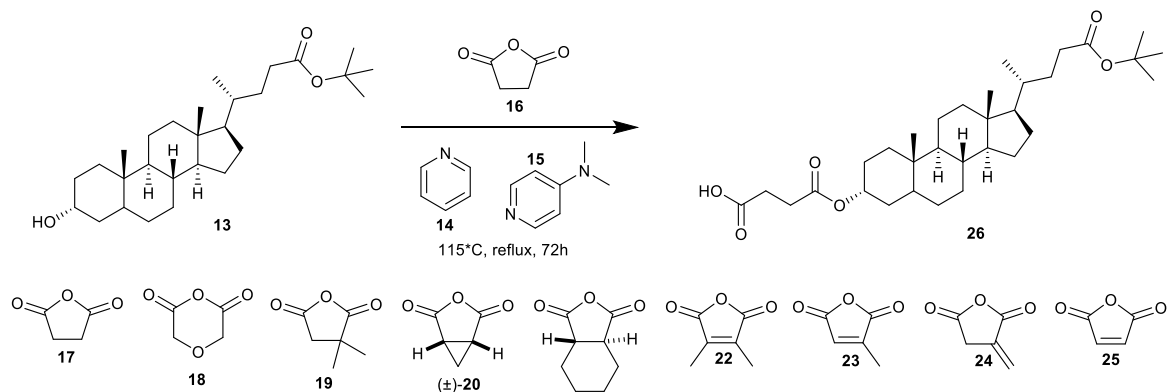


Figure 12 - Reaction scheme for the C-3 functionalization starting with anhydrides.

Functionalization of the C-3-hydroxyl group was initiated at the stage where R.J. Soltysiak left his research on fusidic acid.³ Initially, the same procedure using pyridine (**14**) as both a solvent and a base, along with DMAP (**15**) only added in catalytic amount, was adapted to lithocholic acid (Figure 12). This method resulted in the formation of an ester upon opening of the cyclic anhydride, while it also generated a free acid group, which was of particular interest as stated earlier.

Anhydrides were particularly interesting for the fact that they can undergo esterification reactions without requiring any coupling agent. The reactivity of their carbonyl groups is enhanced, when compared to that of the corresponding di-acid formed upon hydrolysis. Still, their reactivity also contributed in making the stereochemistry of the products hard to control in the case of unsymmetrical anhydrides. Chiral anhydrides would therefore have two distinct electrophilic-sites of addition, which resulted in two different regioisomers/diastereoisomers upon addition of a nucleophile on one of the carbonyl carbons.

1.4.2 - Acids

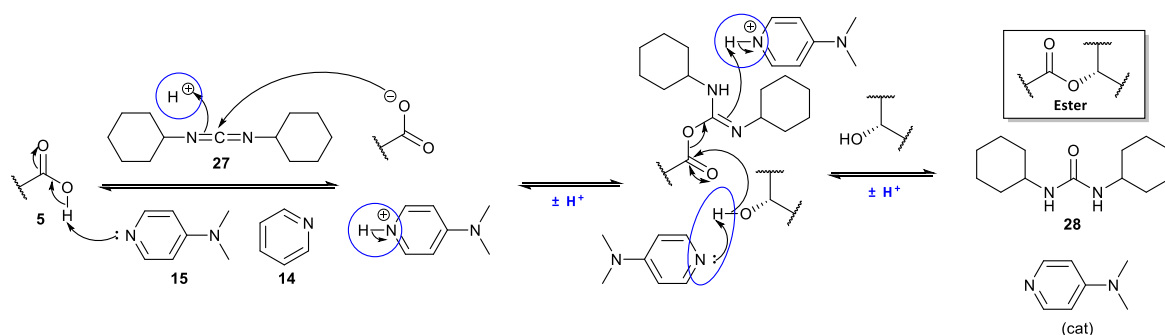


Figure 13 - Mechanism of the DCC-mediated (**27**) coupling of acids to form esters.

In an attempt to diversify the functional groups that can be added onto C-3, a DCC-mediated coupling mechanism of several acid reagents was carried out, inspired by B. Neises and W. Steglich's method.²¹ The most common issue encountered with the use of N,N'-dicyclohexylcarbodiimide (DCC, **27**) was purification of the side products of the reaction, especially N,N'-dicyclohexylurea (DCU, **28**, Figure 13).

This procedure was previously conducted on fusidic acid with success¹, but fusidic acid has several polar functionalities along its steroid chain that effectively reduced its interactions with the lipophilic cyclohexyl groups of DCU. Lithocholic acid on the other hand only has two distal polar groups attached on either end of the steroid backbone, making it much more lipophilic and therefore more prone to interact with the cyclohexyl groups of DCU.

1.4.3 - Mitsunobu Inversion

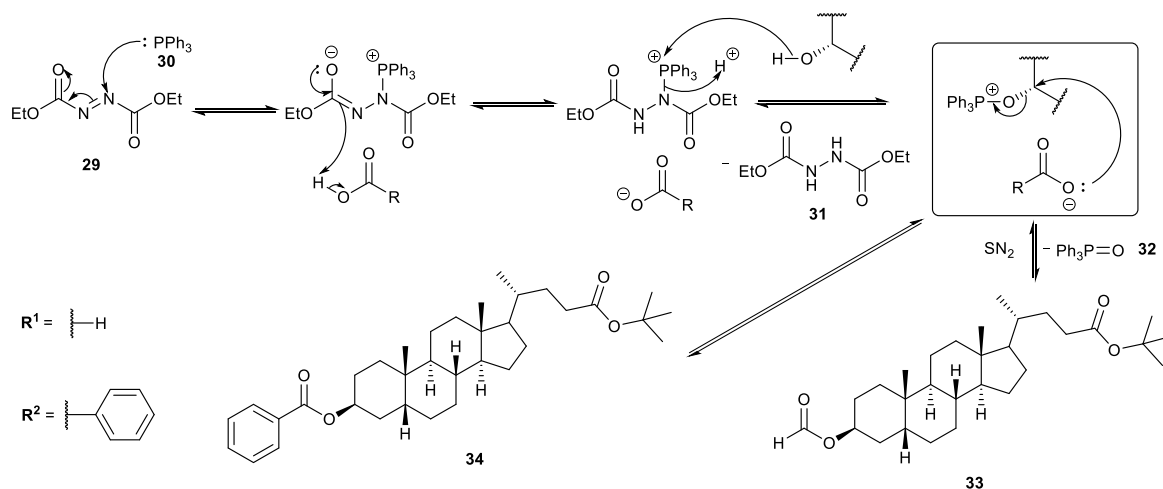


Figure 14 - The Mitsunobu inversion reaction, with the S_N2 transition state.

Stereochemistry can have a significant impact on the binding affinity of a molecule with an enzymatic target, especially in molecules having a relatively rigid backbone (e.g. steroids). The *C*-3 configuration of the steroids used was even more crucial, as it was the bridging bond between the lipophilic polycyclic skeleton and the usually more hydrophilic fragments that were added to the initial structure.

Fortunately, Oyo Mitsunobu's inversion technique has now been reported as successful on a lot of different secondary alcohols, achieving good yields without requiring any expensive catalysts in the process.^{22,23,24} Lithocholic acid has a three-dimensional structure that could potentially have created issues when it came to the kinetics of the reaction. In fact, the S_N2 transition state of this reaction relied on the interaction between the σ^* orbital of the C-O bond on lithocholic acid and the p orbital of O^- on the conjugate base of formic/benzoic acid (Figure 15). When it comes to energy barriers however, lithocholic acid has its hydroxyl group in an equatorial position on the chair structure (**35**), which could make it harder for a nucleophile to approach its σ_{C-O}^* orbital. Three axial hydrogens present on the A-ring induce steric clashes with the nucleophile, which would not occur if the nucleophile approached from the backside of an axial σ_{C-O}^* orbital (**36**).

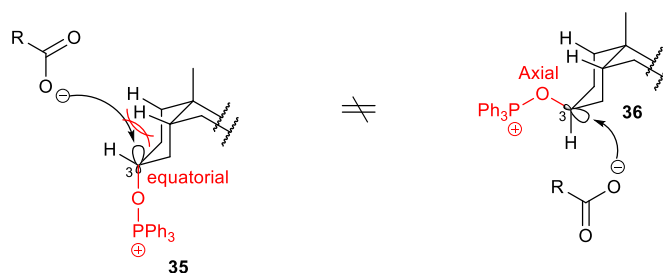


Figure 15 - Reactivity of an equatorial (α) and an axial (β) leaving group at C-3.

Secondly, cleavage of the ester formed had to be performed in order to restore the hydroxyl group with its inverted configuration. A straightforward hydrolysis in basic conditions was enough to cleave this type of ester.

1.4.4 – Fluoro-deoxygenation

Introduction of fluorine atoms into drug molecules is of particular interest in medicinal chemistry: due to its small size and very high electronegativity, a fluorine atom can add unique features to a compound. It can act as a weak hydrogen-bond acceptor as well as having attractive polar interactions with certain functional groups, thereby increasing binding affinities with proteins.

Furthermore, fluorine adds metabolic stability to a drug due to its insensitivity to metabolic oxidation mechanisms that are carried out by *P450* cytochromes. This also correlates with the absence of any known fluoroperoxidase to this day, even though a lot of naturally occurring haloperoxidases have been discovered for the formation of organochlorides/bromides.²⁵ Rarity of fluorine in naturally occurring compounds can nevertheless be a good factor of novelty for drug discovery.

Investigations were carried out in order to find a procedure that would be the most appropriate to the structure of lithocholic acid. The oldest procedures found dated back as far as the mid-nineties, while the most recent ones were from 2017, showing that deoxo-fluorination reactions are still not completely developed. In fact, the "black sheep" of the deoxo-fluorination field would probably be the competing elimination reaction, almost unanimously mentioned in studies of this type of reaction.^{26,27,28}

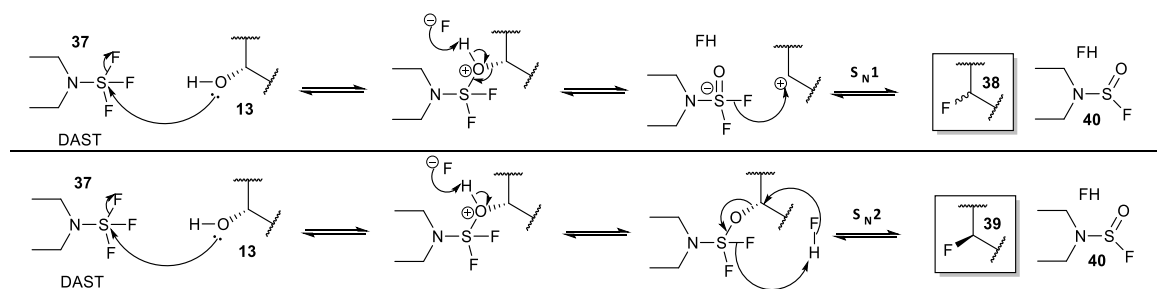


Figure 16 - Mechanistic pathways for the deoxy-fluorination using DAST (**37**).

Stereospecificity of the fluorine incorporation is also subject to dispute, as most of the deoxy-fluorinating reagents are thought to react through an S_N2 pathway and/or an S_N1 pathway depending on the reaction conditions. As depicted in Figure 16, the stereochemical outcome of the reaction will depend on the type of pathway that is taken. As such, it will generally be more convenient to favour an S_N2 pathway, which will be stereoselective with respect to formation of the inverted configuration when fluorine is incorporated into the structure. The S_N1 mechanistic pathway in contrast, would lead to uncertainty about the reaction's stereochemistry. Not to mention that, on top of the stereochemical uncertainty of a S_N1 mechanistic pathway, the carbocation intermediate formed is also very prone to elimination reactions, via the release of a proton attached to one of the adjacent carbon atoms.

Hydrogen fluoride (HF) is produced in both reaction pathways and is rather unpredictable in terms of reactivity. Having a $pK_a = 3.2$, it is not anywhere near as acidic as other hydrogen halides, due to the H-F bond being very strong (570 kJ.mol^{-1}).²⁹ The usual basicity of a tertiary amine group ($pK_a (\text{R}_3\text{NH}^+/\text{R}_3\text{N}) = 11$) could be thought to clash with the proposed mechanism, suggesting that the nitrogen atom rather than F^- should abstract H^+ from the protonated oxygen. Nevertheless, the neighbouring fluorine atoms in DAST (**37**) will drastically reduce this amine's pK_a and protonating the amine would lead to additional charges throughout the resulting mechanism. These arguments along with the H-F bond strength stated above give legitimacy to the proposed mechanisms.

Still, several references have diverging opinions, about which mechanism is favoured for secondary alcohols; some would see it going through an S_N1 intermediate²⁶, while others consider S_N2 mechanisms to be the rule²⁷, both however recognising that it is a grey-zone in the case of secondary alcohols.

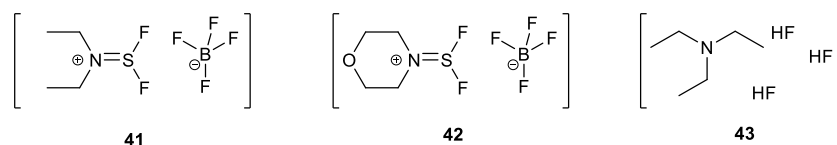


Figure 17 - Structures of XtalFluor-E (**41**)/-M (**42**) and TEA·3HF (**43**).

Nowadays, a plethora of different deoxy-fluorinating reagents have been developed, or derived from conventional ones like DAST. A common alternative to the latter would be XtalFluor-E/-M (**41** & **42** respectively in Figure 17), which is said to provide greater control over the stereochemistry and the prevention of elimination side reactions. It can also be combined with other fluoride sources like TEA·3HF (**43**), potentially increasing the overall rate of fluoro-deoxygenation.²⁷ Unfortunately, publication history on this subject seems to show that it is hard to set general rules for fluoro-deoxygenating reagents, as their actual mechanism of action is not completely known and is highly dependent upon the structure of the substrate.

1.5 - Biological Assays

1.5.1 - Thermal Shift Assay (TSA)

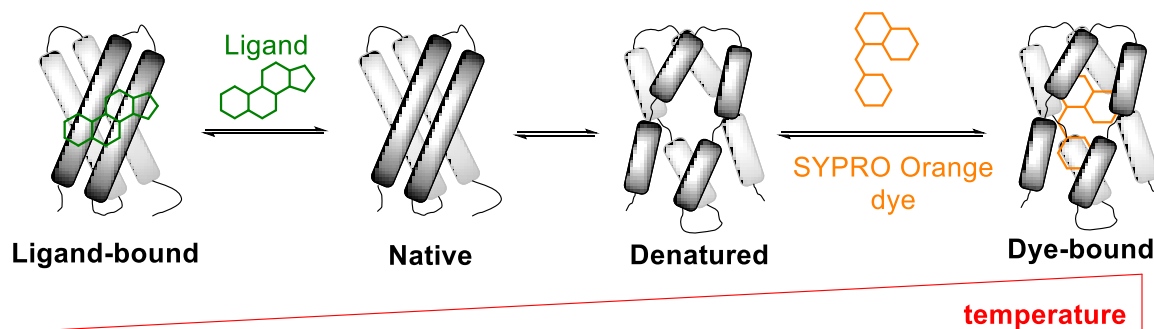


Figure 18 - Evolution of an enzyme's binding state and shape in a TSA.³⁰

Initial stages of the biological activity assessment of a compound involves binding assays to provide an idea of how strongly a compound binds to a target, however, such assays lack any information on the biological effects that it might trigger. The main advantage of using TSA however is the high throughput nature of this method; the only requirements are a correct buffer and sometimes other additives that have to be added with the protein.

A temperature gradient is employed and as the temperature increases the protein denatures from its folded structure (native state, Figure 18) to an unfolded (denatured) state, once the melting temperature T_m has been reached. When a ligand is bound to the protein it becomes stabilised, the T_m will also become proportionally dependent on the strength of this binding, the T_m can therefore be used as a method to quantify ligand binding. Even though being a quantitative method, this method has a certain degree of inaccuracy, which is why it is mostly used for relative comparisons between different ligands rather than a tool to generate absolute values for binding affinity.

In order to monitor the formation of the denatured protein, a method using a *SYPRO Orange dye* for the TSA has been outlined by K. Huynh & C. L. Partch.³⁰ Also referred to as “differential scanning fluorimetry”, this method relies on the attachment of a dye compound that can only happen on the denatured protein, making it an efficient colorimetric quantification tool. In fact, this dye binds to hydrophobic environments that become exposed during protein denaturation, thereby emitting fluorescent photons that are compatible with filter sets found on real-time PCR instruments ($\lambda_{excitation}$ 470 nm/ $\lambda_{emission}$ 570 nm).³⁰

1.5.2 - Splicing Assay

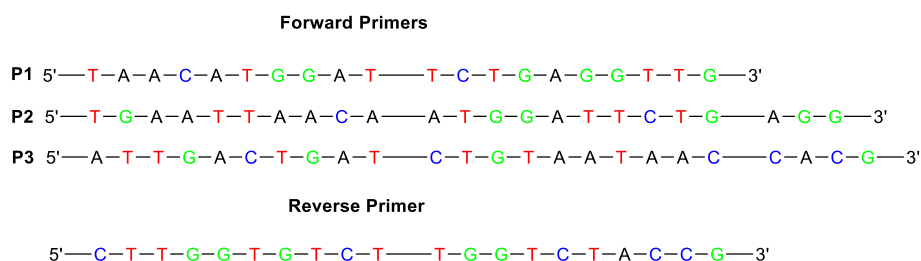


Figure 19 - Sequence of the forward primers used and the associated reverse primer.

As opposed to TSAs, the splicing assay is a functional assay, meaning that it also displays the biological effect resulting from the inhibition of a target. Functional assays typically require very specific conditions for the enzymatic machinery to operate, requiring more thoroughly elaborated procedures.

The assay developed by the O'Keefe group allowed combination of qualitative gel electrophoresis results, with quantitative qRT-PCR measurements, whereby the consistency of any output can be assessed. *In vitro* splicing assays were set up using yeast BJ2168 extract and P283 actin pre-mRNA transcript: these splicing reactions were then

treated with either compound or DMSO as control (4% final concentration). The RNA from each sample was then phenol extracted, isolated and used in a reverse-transcription (RT) reaction to synthesise the corresponding cDNA (the concentration of RNA was normalized for each RT reaction). The cDNA from each sample was then used to quantify the amount of spliced product and calculate the splicing efficiency (%) of each reaction resulting from treatment with each compound, with either PCR or qRT-PCR analysis. Three different sets of primers have been elaborated; first the *P2* primer (Figure 19) was selected to PCR amplify the cDNA used for gel electrophoresis. Amplification of the cDNA with this forward primer resulted in both the spliced and unspliced product being displayed on an agarose gel, which made it possible to qualitatively compare the activity of each compound.

On the other hand, the *P1* and *P3* primers were both developed to display exclusively the spliced product for *P1* and the unspliced product for *P3*. Having both spliced and unspliced products separated from each other was ideal for qRT-PCR measurements, as this technique can only cope with one cDNA strand at a time. The qRT-PCR technique ultimately displays values of C_T (cycle time), which are meant to be compared between the compound of interest and the control values. The higher the C_T value, the less cDNA there is in a sample, as a lower concentration of cDNA sample will require more cycles of duplication until it reaches the universally chosen concentration of cDNA. Inhibition of the target should therefore induce an increase in the C_T value for the spliced product (*P1*), since less mRNA should be produced, resulting in a smaller initial cDNA concentration.

Finally, the intensity of the bands displayed on the agarose gel had to be compared with the values generated from the qRT-PCR machine, for these results to be validated. The reverse primer used was universal to all three primers and its sequence was elaborated to base-pair on the sequence of Exon 2, which is present on the spliced as well as the unspliced product.

2.0 - Project Aims

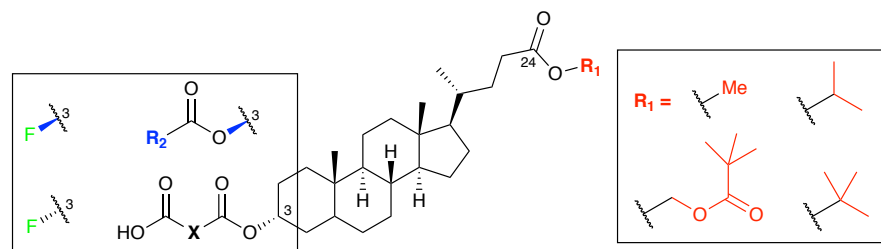


Figure 20 - Summary of the attempted modifications on lithocholic acid.

Lithocholic acid has shown promising activity for inhibition of the Snu114 sub-unit of the U5 snRNP during the splicing cycle. Conducting an SAR-study of lithocholic acid was in essence the principal aim of this project, with respect to the work already carried out on its analog fusidic acid for comparison. The *C3-OH* and *C24* carboxylic acid groups were both modified (Figure 20), while it had to be kept under consideration, that a free acid moiety at one end of the structure was believed to be crucial for effective inhibition.

Another important factor that had to be tested was the flexibility of the new structures and the importance of this factor for active site binding. In another perspective, an elevated log P and molecular weight, reaching beyond the usual range for these variables, could potentially create issues for the resulting compounds to be used as drugs. The influence of these variables was to be tested through biological (splicing) assays.

In an attempt to introduce novelty alongside other structural improvements, Mitsunobu inversion as well as fluoro-deoxygenation reactions at the *C-3* position were of interest, especially for their resulting unnatural configuration on *C-3*. A lot of effort was also to be invested in elaborating adequate purification methods, in order to maximise yields without affecting the purity of the compounds synthesized.

Alongside the synthesis of potentially active inhibitors of *Snu114*, preliminary biological assays were also set to influence the directions followed in the planning of the ongoing synthesis.

3.0 - Results & Discussion

3.1 - Protection of the C-24 Acid moiety

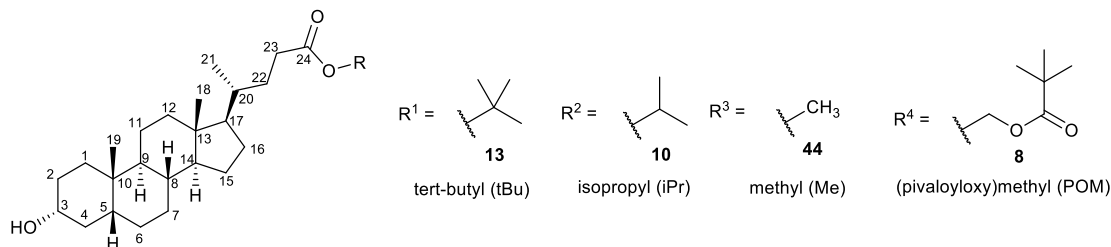


Figure 21 - Carboxylic acid protecting groups for lithocholic acid.

The project commenced with a seemingly simple protection step inspired by R.J. Soltysiak's work³ on fusidic acid. Chloromethyl pivalate (POM, **7**) was used in an attempt to protect the acid at the C-24 position of lithocholic acid (**5**, Figure 22). Even though TLC monitoring of the reaction suggested that it had succeeded, difficulties quickly appeared when it came to separating the compound of interest from the final mixture. In fact, when looking at the structure of compound **8**, it can be considered to have surfactant-like properties, where the steroid backbone would be a lipophilic tail, while the POM group would act as a polar head. This made the compound very hard to extract, due to dense emulsion formation.

After several failed attempts at this reaction, it was deemed more efficient to refocus investigations on finding alternative protecting groups. At first, the previously outlined procedure for isopropyl-protection of lithocholic acid (**10**)¹⁹ was attempted. With a 28% yield for this reaction however (also due to the need for further purification by column chromatography after extraction), a more efficient alternative had to be found, as most of the subsequent C-3 modifications carried out on lithocholic acid required the C-24 acid group to be protected.

In the end, a third attempt at protecting C-24 with *tert*-butanol²⁰ successfully provided compound **13** in a convenient manner, with extraction methods efficient enough to isolate the compound without requiring extensive purification. This allowed gram-scale production of the protected compound, with yields reaching as high as 92%, setting good ground for the upcoming C3-functionalisation step. This procedure was later used to produce the *iPr*- and *Me*- protected esters (**10** and **44** respectively, Figure 21) with good yields as well, however the focus was maintained on compound **13**, for its robustness and

tendency to form crystalline solids, which makes it easy to handle. The *isopropyl* ester (**10**) in contrast tended to form oily compounds more readily, whereas both the *methyl*- and *isopropyl*-protecting group of **44** would have been hard to remove if deprotection was required.

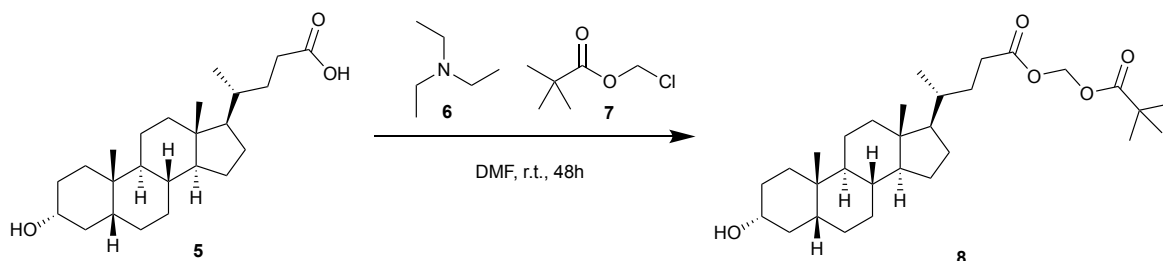


Figure 22 - Reaction conditions used to protect lithocholic acid with chloromethyl pivalate.

Another attempt at getting the original POM-protection step to succeed was carried out a few months later, once a better understanding of the chemical properties of lithocholic acid had been acquired. In fact, changing the solvent used for the extraction from diethyl ether (Et_2O) to the more polar dichloromethane (DCM) had a much better potential for retention of compound **8** in the organic phase. This change allowed careful water washes to be carried out to extract dimethylformamide (DMF) from the organic phase, without forming any emulsions. Gram-scale production of the protected ester was then feasible, with yields reaching up to 74%.

Just like compound **10**, compound **8** had a tendency to form not only oily but also very viscous compounds, which was why most of the further functionalization steps were carried out with compound **13**, even though some POM-protected analogs were later synthesized for binding affinity comparisons.

3.2 - Esterification with anhydrides

3.2.1 - DMAP mechanism in the initial procedure

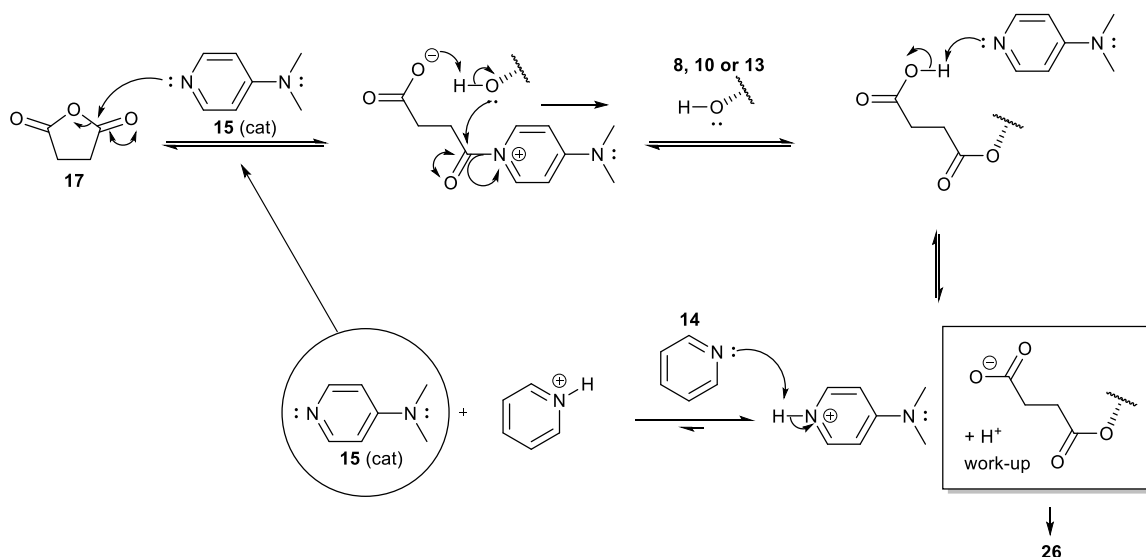


Figure 23 - Mechanism of the DMAP-catalysed cleavage of succinic anhydride (17).

Despite this reaction giving acceptable yields (48-55%), the long reaction time (3 days) and the high temperature used (115 °C reflux) were forcing conditions for a reaction that should occur rapidly because of the intrinsic reactivity of anhydride groups. A factor that would potentially limit the rate of the reaction could be the relative pK_a of DMAP **15** (pK_a(H+DMAP/DMAP) = 10.14) compared to that of Pyridine **14** (pK_a(pyridinium/pyridine) = 5.24). Considering the acidity of the pyridinium ion, it was hard to believe that the H⁺ abstraction step from the protonated DMAP would favour an equilibrium leaning towards restoration of the catalyst (last step on Figure 23). This unfavourable pK_a combination had to be overcome with additional thermal energy (to accelerate the rate of all the reactions occurring). Further investigations in order to find a better alternative to this procedure were conducted after the first 3 esters were generated (**26**, **46**, **47+48**, Table 1).

3.2.2 – Alternative reaction conditions for esterification with anhydrides

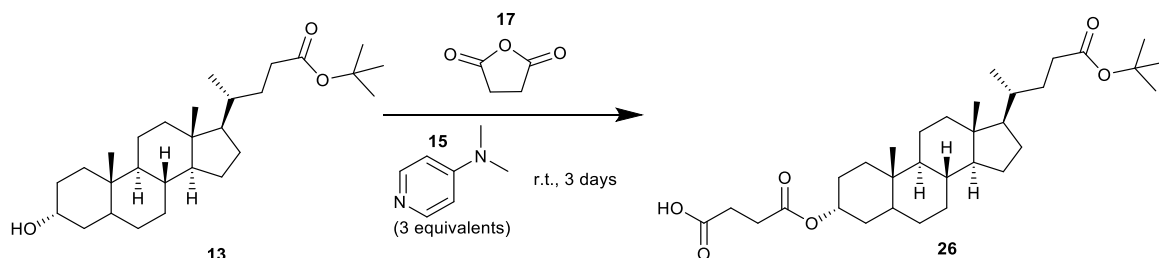


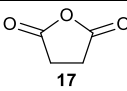
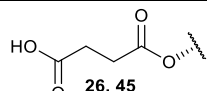
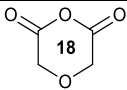
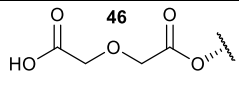
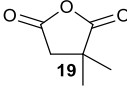
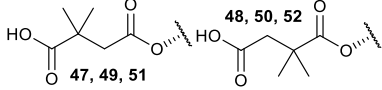
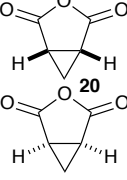
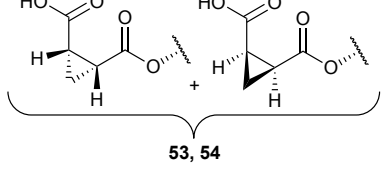
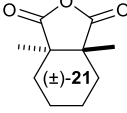
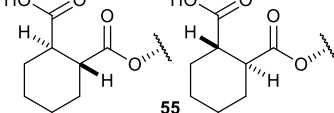
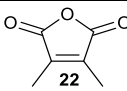
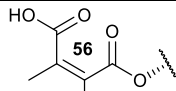
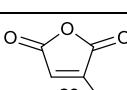
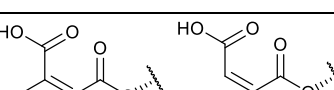
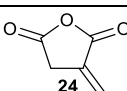
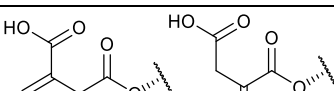
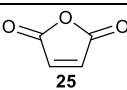
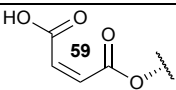
Figure 24 - Alternative procedure adopted for esterification reactions with anhydrides.

Jingxuan Ni and co-workers³¹ used a method that appeared to work much faster (10 hours instead of 72) and without the need for any added thermal energy. In fact, they introduced an excess of DMAP (3 equivalents) that now also acts as an efficient base so that pyridine could be replaced with anhydrous DCM, omitting the unfavourable last step of the previously described mechanism. Even if in terms of expense, adding 3 equivalents of DMAP would be slightly more expensive than using pyridine as a base, on plant-scale this would probably still be more advantageous than having to heat an entire vessel up to 115°C.

3.2.3 – Saturated anhydrides

All of the structures presented in Table 1 were derived from compound **13** initially. Primary TSA assays carried out on *Snu114* using the newly developed molecules showed a trend for reduction of flexibility in the side-chain to be favourable in terms of binding to the enzyme (unpublished data, Megan Eadsforth). The dimethyl- (**47** & **48**), cyclopropane- (**53** & **54**) and cyclohexane-containing derivatives (**55**) all showed promising increases in *Snu114* binding affinity (Table 1). The dimethyl-compound (**47** & **48**), which seemed to be the most promising, was derived with *isopropyl*-(**51** & **52**) as well as POM-(**49** & **50**) protecting groups, to determine if these had any influence on the binding affinity.

Table 1 - Structures resulting from all the attempted C3-functionalisations reactions with varying anhydride reagents. The corresponding C-24 protecting group is given in brackets next to the yield, where the yield reads "-" the reaction was not attempted.

| Anhydride reagent structure | Expected C3-attached structure of product | Yield (^t Bu) | Yield (POM) | Yield (ⁱ Pr) |
|---|---|-------------------------------------|-------------------------------------|--------------------------|
|  |  | 26: 55% | 45: 99% | - |
|  |  | 46: 48% | - | - |
|  |  | 47+48: 74% 47: 21% | 49+50: 55% 49: 22% | 51+52: 60% |
|  |  | 53: 61% | 54: 63% | - |
|  |  | 55: 99% | - | - |
|  |  | Not formed | - | - |
|  |  | 57: 12% | - | - |
|  |  | Not formed, 57: 9% | - | - |
|  |  | Not isolated | - | - |

In all three cases (**47-52**), the ratio between both regioisomers was about 75%(**47/49/51**)/25%(**48/50/52**) according to the splitting of certain peaks found in the ¹H NMR spectra of these mixtures. Although with commonly used separation techniques (TLC + column chromatography) the mixtures appeared as one entity, in the case of the **49+50** mixtures, a separation was successfully achieved. In fact, when column chromatography was carried out with a solvent system (hexane 2:1 ethyl acetate) slow enough for the mixture to be separated into 33 different fractions, a slight difference in retention factor (*R_f*) was observed. While most of the compound remained as a mixture (appearing as one spot on a TLC plate, resulting from the merging of two separate ones; fractions 18-47), collecting the fractions with a single spot separately made the isolation of the major regioisomer possible (fractions 14-17 for **49**). Unfortunately, compound **50** could not be recovered in a pure form, but a sample with a 50%(**49**)/50%(**50**) ratio was obtained for comparison.

Later it was found that the similar compound mixture of *tert*-butyl-protected esters (**47+48**) was separable in a comparable way, with the solvent system being changed to (hexane 4:1 ethyl acetate).

3.2.4 – Unsaturated anhydrides

From another perspective, the alkene-containing compounds (**56-59**) were also derived at a later stage of the research, in an attempt to further reduce flexibility of the side-chain, following the good results of dimethyl-compounds (**47-52**) in splicing assays. The results of all three reactions showed an overall reduction in reactivity of the anhydrides compared to their saturated analogs. Structurally speaking, both the steric hindrance added by the methyl groups and the conjugation of the double bond with the adjacent carbonyl groups were responsible for the reduced reactivity.

Unsurprisingly, compound **22** had the worst combination of both features, as illustrated by the complete lack of reactivity towards formation of the corresponding ester. In contrast, compound **25** showed a good consumption of starting material in the resulting crude mixture, which suggested that the reaction had taken place. Still, only a small amount of product could be found from ¹H NMR analysis, with the compound resisting all attempted purification methods.

Furthermore, compound **57** was effectively formed in a similar manner, despite the starting anhydride containing an additional methyl group compared to maleic anhydride (**25**). In fact, less than 10% of the starting *tert*-butyl-ester (**13**) remained in the crude product mixture, but the low yield of 12% also suggested that some by-products may have been formed during this reaction. This supposition was further reinforced by the fact that the crude mixture was appearing as a brown powder, while the isolated compound **57** was pink.

Finally, itaconic anhydride (**24**) was a particularly interesting compound, in that it didn't actually form the expected compound **58**, but instead resulted in the formation of compound **57**. Even though the yield was lower and the compound extracted was not as pure as if it was made via citraconic anhydride (**23**), this suggested that some kind of equilibrium had to take place between citraconic (**23**) and itaconic (**24**) anhydride and/or after ring opening of their structures (**57-58**).

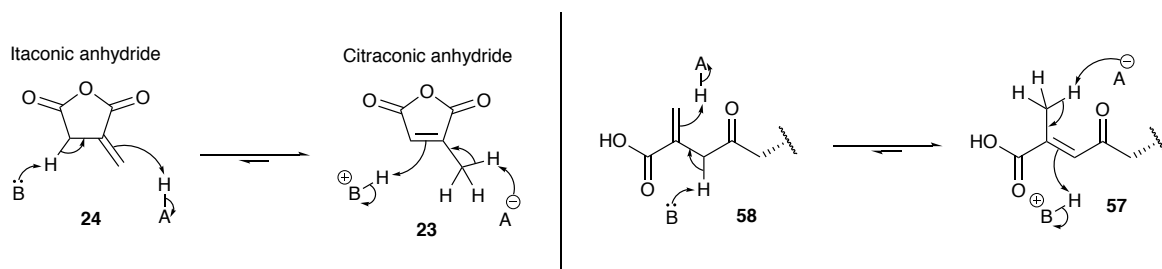


Figure 25 - Tautomerism between itaconic (**24**) & citraconic anhydrides (**23**) and their ring-opened analogs.

When looking at both structures (Figure 25), it can be postulated that a mechanism most likely to link them would be a tautomeric equilibrium. In fact, the presence of basic DMAP could provide a means for proton exchange, allowing mesomeric effects to dictate the outcome of the reaction. In compound **57**, the double bond is conjugated with both π -systems of the carbonyl bonds, generating a single extended π -system containing 6 π -electrons. As opposed to that, compound **58** has its double bond in conjugation with only one of the carbonyl groups, resulting in a decrease in stability.

From another perspective, Michael-acceptors like the exocyclic double bond present in itaconic anhydride (**24**) are not much appreciated in drug discovery, as they represent a site of potential metabolic instability.

3.3 - Esterification with acids

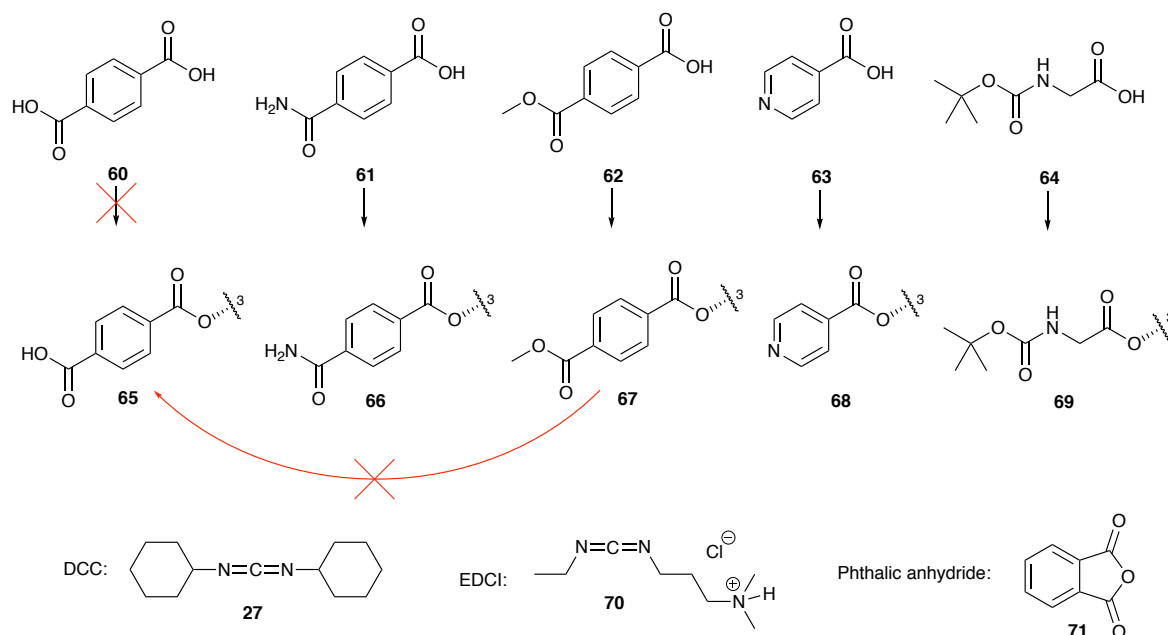


Figure 26 - Esters obtained through EDCI coupling of the corresponding carboxylic acid.

As expected earlier, purification problems quickly occurred when using DCC (**27**) along with terephthalic acid. Fortunately, more polar alternatives for the coupling agent exist: 1-ethyl-3-(3-dimethylaminopropyl)carbodiimide (EDCI) is also a commonly used coupling agent³² and is commercially available in the form of a hydrochloric salt (**70**, Figure 26). This coupling agent and its resulting side-product did effectively get driven out, in the more polar aqueous phase upon work-up.

Structures **66-69** could successfully be synthesized with this newly adapted procedure, but an issue appeared in the case of compound **65**. The reagent (terephthalic acid, **60**) could not be separated effectively from the product mixture, even though the target compound was formed. A first attempt at replacing the unsuccessful di-acid **60** led to the choice of phthalic anhydride (**71**), which would also generate a free acid group attached to a phenyl ring, while using the same method previously outlined for all other anhydrides. Unfortunately, the latter procedure led to the same outcome as previously observed for reagent **60**, with residual starting material resisting standard purification methods. Secondly, **62** was chosen as another replacement that could then be deprotected on either one or the other end of the molecule to restore the free acid group. This method was successful; however deprotection of the methyl ester to generate the corresponding carboxylic acid analog **65** was unsuccessful. Deprotection at the other end of the molecule

(C-24 'butyl-group) was the only way that ultimately regenerated a free acid group for this compound.

Furthermore, the reagent used to form compound **66** needed some additional care. In fact, terephthalic acid monoamide would not dissolve in DCM, which is why triethylamine was added to aid dissolution, inspired from a different procedure.³³ Addition of DMF instead of TEA was also suitable for complete dissolution of the starting material, however this required additional separation before column chromatography to remove solvent impurities.

3.4 - N-Acylation at C-24

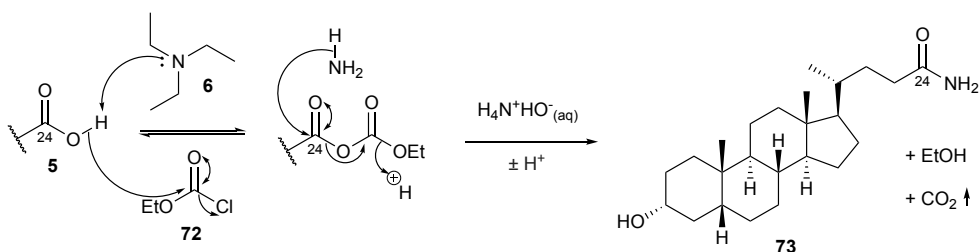


Figure 27 - Amide formation at the C-24 acid moiety of lithocholic acid.

Amide functional groups are very common in biological systems; they are known to be robust in terms of chemical stability. In fact, the similar peptide bonds that links the amino acids of proteins together, relies on the strength of that bond, to keep the plethora of enzymatic processes functioning over the course of a living system's lifetime. They also have interesting properties in terms of hydrogen bonding, being a hydrogen bond donor on the NH as well as an acceptor at the oxygen. This feature plays an important role in determining an enzyme's 3D-structure.

Fortunately, a simple two-step procedure was sufficient to convert an acid to an amide in the case of lithocholic acid.³⁴ The use of ethyl chloroformate **72** as depicted in Figure 27 was convenient because it generated CO₂, irreversibly driving the reaction forwards via the entropically favourable release of the gas, while forming the amide of interest.

When trying to predict the inhibiting activity of the amide formed in compound **73**, it was important to consider that it would not be able to interact with the Mg²⁺ ion as effectively as with the free acid group of lithocholic acid (the oxygen of a carboxylic acid group is more electron-rich than the nitrogen of an amide group). It would therefore not be

surprising to see a reduction in activity when compared to lithocholic acid itself, but this would not mean that the amide group could not potentially interact with the enzyme in an alternative way. Adding another acid group on the C3-end of the molecule (as seen previously), could then allow combination of the possible interactions of the amide group, with the already known acid-Mg²⁺ interactions.

3.5 - Mitsunobu Inversion

As explained earlier, inversion of configuration at the C3 stereocenter of lithocholic acid was one of the principal objectives of this project. Furthermore, this process also had to occur in good yield to allow gram-scale production of the inverted compound, since this also had to be further functionalised.

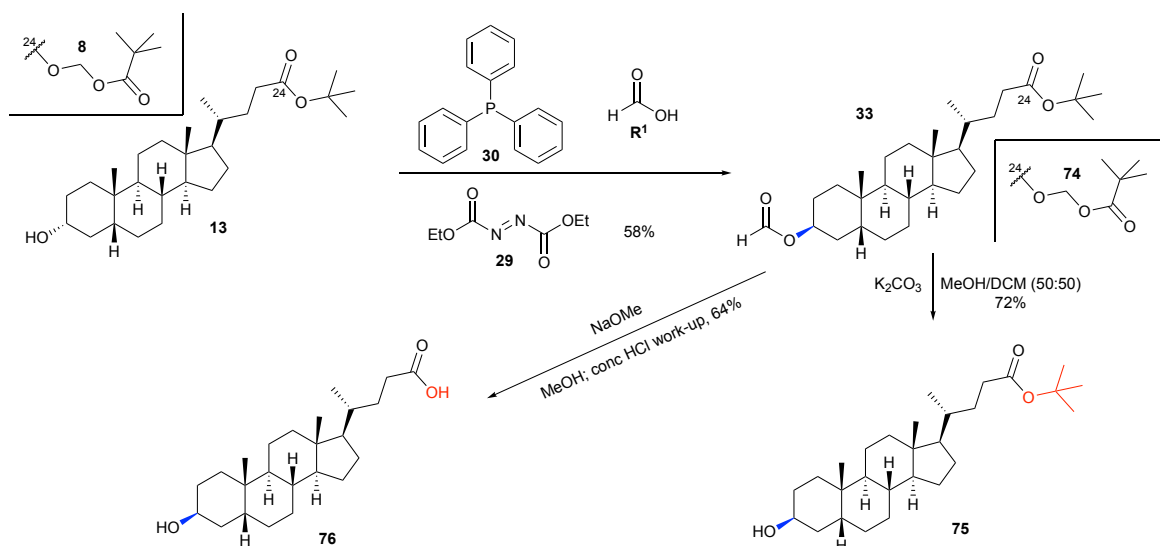


Figure 28 - The two-step Mitsunobu inversion reaction.

Several procedures found in the literature were therefore considered. In accordance with what was expected, a long reaction time ranging from 24 to 48 hours for the first step confirmed that kinetic factors limited the progress of the reaction. One procedure³⁵ suggested that the reaction should be heated at 66 °C in THF, heating to accelerate the rate of reaction. This remained relatively safe for gram scale production, as the flash point of DEAD (**29**) is as high as 85 °C. Nevertheless, the explosive nature of this compound meant that it is unlikely that this process would be suitable for plant-scale production. The highest yield reached with this procedure was 58% after column chromatography purification.

Whether or not the target compound could be purified alternatively by aqueous/organic phase separation remains to be investigated.

The first step was successful on both the *tert-butyl* (**13**) and POM-protected (**8**) lithocholic acid, although the reaction generating compound **74** only resulted in a 24% yield. Luckily, the POM-protected analog was not of great interest for the Mitsunobu inversion, as it could not be taken further than the first step, because of the POM group being base labile. The second step of the process therefore discriminated between different protecting groups, giving the advantage once more to the robust *tert-butyl*-protecting group (**13**).

Depending on the strength of the base and the work-up method used, two different products were obtained. When following the procedure described by D. Albert & M. Feigel²² (for a methyl-protected version of lithocholic acid), it turned out that upon work-up with concentrated HCl, the *C24* *tert-butyl* group underwent cleavage along with the *C3* formate ester. The resulting compound was lithocholic acid with an inverted configuration at *C3* (**76**). For most of the further reactions however, the protecting group was still required, prompting the need for this procedure to be adapted with milder conditions.

Further experimentations led to the discovery that a base as weak as K₂CO₃, could be used to completely cleave the *C3* formate ester, without removing the *C24 tert-butyl*-protecting group. Work-up of the reaction with concentrated HCl was also not necessary anymore: three water separations with the compound in a layer of diethyl ether were enough to extract and isolate the product (**75**) from the reaction mixture. The resulting inverted *tert-butyl*-lithocholate ester **75** was the compound of choice for the later envisaged fluorination reaction, as well as inverted analogs of previously synthesized molecules.

3.6 - ^tButyl deprotection to restore the C-24 acid moiety

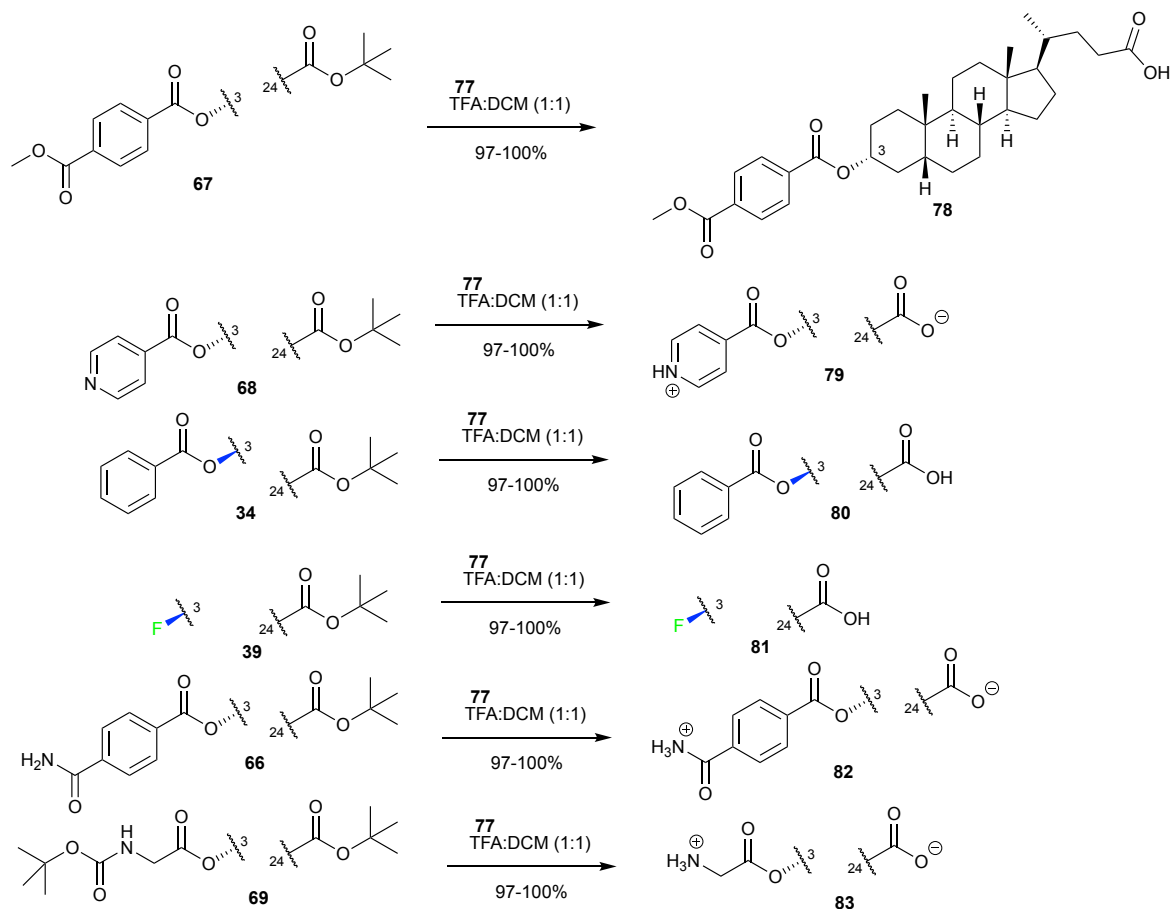


Figure 29 - Reaction conditions for the deprotection of a *tert*-butyl ester.

All biological assays carried out to-date on analogues of lithocholic acid and fusidic acid have proven unanimously that the presence of a free carboxylic acid group in their structure was the most important feature for inhibiting activity of *Snu114*. As some of the newly generated structures did not contain a free acid group at the *C3*-end of the steroid backbone, it may be necessary to restore the *C24* acid moiety by removing the protecting group. This step gave an additional reason as to why the *tert*-butyl protecting group was selected over others, since it could be selectively cleaved in a single step without requiring any extensive purification, resulting in yields as high as 100%.

Tert-butyl refers to a tertiary carbon (bearing three methyl groups), which is not prone to undergo S_N2 reaction pathways, but rather S_N1 pathways that proceed through a carbocation intermediate. Stabilising hyperconjugation effects of the neighbouring σ_{C-H} bonds (overlapping with the empty p-orbital of the carbocation) are responsible for this, which is also convenient due to S_N1 reactions more readily proceeding in acidic conditions,

where protonation of the ester would also facilitate the generation of a carbocation. Most of the esters that were introduced at the *C3* position were base labile and therefore not affected by strongly acidic conditions.

Since only liquid reagents were used in this process and the highest boiling point is that of trifluoroacetic acid (**77**, TFA, 72 °C), evaporation *in vacuo* was sufficient for product isolation.³⁶ If left at this stage however, residues of TFA tended to stick to the product, affecting its purity. For that reason, the crude product was re-dissolved and concentrated twice with toluene, whereby isolation of the pure de-protected carboxylic acid became possible, regardless of which substituent was present at the *C3* position.

3.7 - Fluoro-deoxygenation reactions

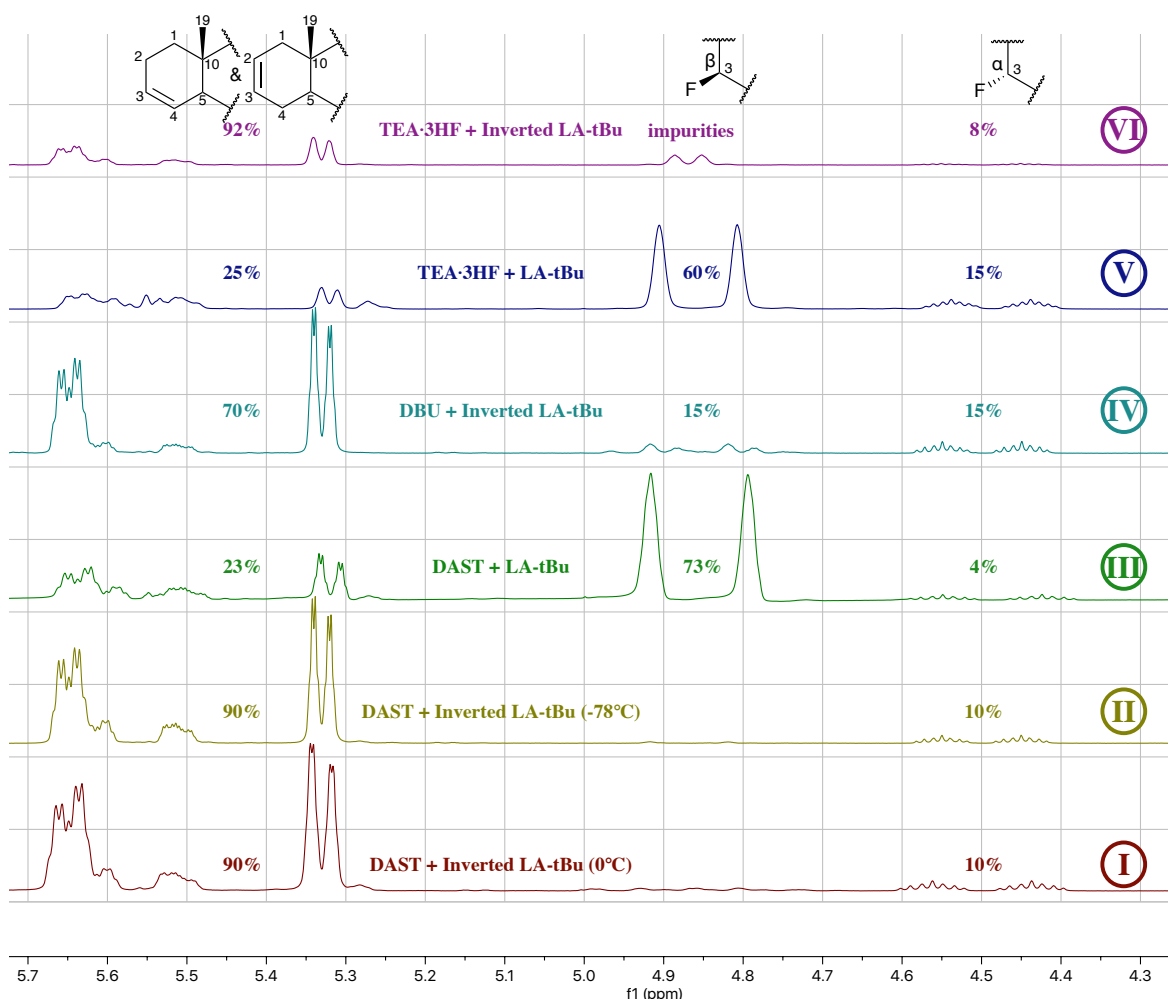


Figure 30 - Selected region of the ^1H NMR spectra of all the attempted fluoro-deoxygenations.

Although several fluoro-deoxygenation procedures were attempted, with different reagents, one particular compound was targeted from the start of the research programme: the 3α -fluoro-3-deoxy-lithocholic acid (**85**), that is to say the one with the same $C3$ -configuration as lithocholic acid itself. This compound would indeed allow direct comparison with lithocholic acid as well as fusidic acid and unlike the 3β -isomer (for which synthesis routes have previously been reported³⁷), it had good potential for novelty without any previously reported synthesis at the time of writing.

3.7.1 - DAST

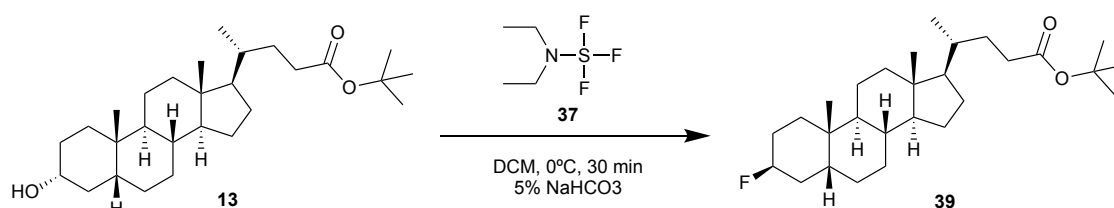


Figure 31 – Fluoro-deoxygenation reaction with DAST (**37**).

Among the plethora of fluoro-deoxygenating agents, diethylaminosulfur trifluoride (DAST, **37**) has historically been the most common one.²⁵ In the hope that an S_N2 mechanism would occur preferentially over an S_N1 mechanism, the reaction was carried out first with the unnatural β -isomer of *tert*-butyl-lithocholate (**75**). Unfortunately, this attempt resulted in an overwhelming 9:1 ratio of elimination products compared to fluoro-deoxygenation products (Figure 30, spectrum **I**).

At first it was thought that the temperature could be an issue, since elimination reactions tend to be favoured at elevated temperatures. Nevertheless, reducing the reaction temperature from 0°C to -78 °C during the addition of DAST barely changed the outcome of the reaction (spectrum **II**). Despite these reactions proceeding on a scale of about 300 mg, a 10% yield was not sufficient to separate both the eliminated and fluorinated compounds. Both compounds tended to co-elute when purified by column chromatography, even with the greatest care and solvent systems as slow as (hexane 39:1 ethyl acetate).

From a mechanistic perspective, the absence of any formation of β -fluorinated isomer in reactions **I** & **II** suggested that lithocholic acid, when combined with DAST, reacted mainly through an S_N2 mechanism, when ignoring the extent of concurrent

elimination. In an attempt to give additional evidence for this, DAST fluoro-deoxygenation was attempted on the 3α -isomer of *tert*-butyl-lithocholate (**13**).

Surprisingly, an increase in the extent of fluorination was observed when combining DAST with compound **13** (spectrum **III**), now reaching nearly a 4:1 fluoro-deoxygenation to elimination ratio. Not only did this result confirm that the S_N2 mechanism was major (through the amount of β -fluoro-deoxygenated isomer formed), it also suggested that fluoro-deoxygenation occurred differently, depending on the orientation of the *C3-hydroxyl* group in lithocholic acid.

3.7.2 - XtalFluor-E + DBU

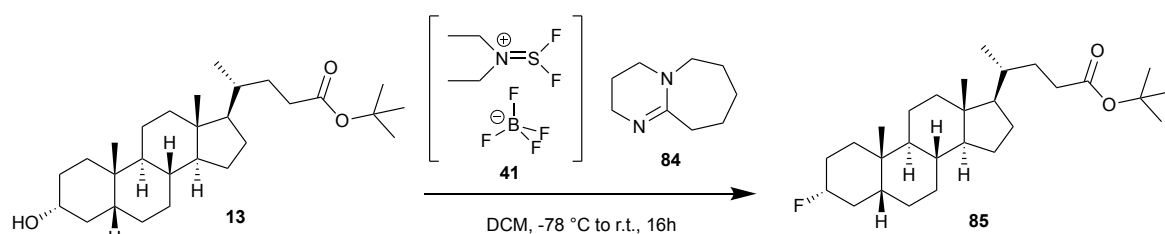


Figure 32 - Fluorination reaction with XtalFluor-E (**41**) and DBU (**84**) as an additive.

To explore the field of fluorination further with lithocholic acid, it was decided to investigate an alternative fluoro-deoxygenating agent. The use of XtalFluor-E on other steroids has been reported and shown to offer some control over the stereoselectivity of the reaction, when coupled with certain reagents. Deemed as safer to handle, DBU was chosen at first among the additives previously tested by A. L'Heureux and co-workers.²⁷

In this case however, it appeared that control over the stereoselectivity of the reaction with DBU as an additive was lost (reaction **IV**), as similar amounts of both fluorinated isomers were found in the product mixture. Furthermore, elimination was also the major reaction outcome. The high basicity of DBU (pK_a (H^+DBU/DBU) = 13.5) certainly contributed to the increase in elimination reaction occurring, however 70% of alkene (reaction **IV**) is still lower than the 90% (reaction **I/II**) found with DAST (using the unnatural 3β -isomer **75**). In fact, both the 3β -hydroxyl group and the supposedly formed 3β -fluoro-3-deoxo group were in axial position on the A-ring (Figure 34), which made them predisposed to E_2 reactions, further enhanced by the basic features of DBU.

Due to the several steps required to generate the unnatural *C3-β* configuration on lithocholic acid (**75**), scaling this reaction to 150 mg of starting material did not allow any of the fluoro-deoxygenated compounds to be efficiently isolated.

3.7.3 - XtalFluor E + TEA·3HF

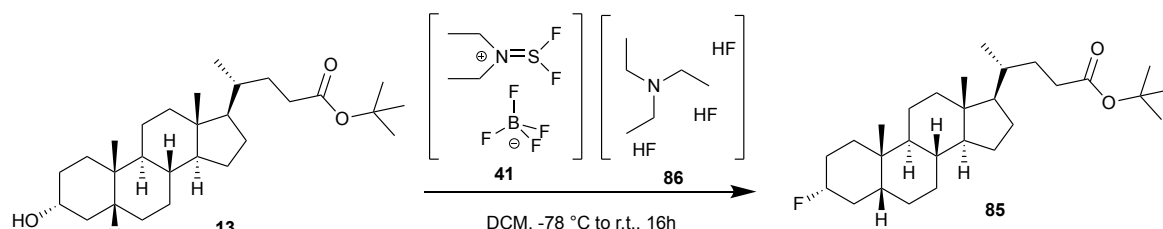


Figure 33 - Fluorination reaction with XtalFluor-E (**41**) and TEA·3HF (**86**) as an additive.

Potential alternatives to DBU as additive have also been described.²⁷ The most promising one was TEA·3HF, that was claimed as an additive that completely prevented elimination reactions from occurring, on a similar steroid structure containing a 3 α -hydroxyl group. Interestingly, this additive supposedly allowed a double S_N2 reaction to occur on carbon 3, resulting in an overall retention of configuration. This could have allowed compound **13** in its natural 3 α configuration (which can easily be produced on a large scale) to be used for the synthesis of the targeted 3 α -fluoro-LA compound (**85**). The only reasons delaying the use of this additive were the additional safety precautions that had to be taken into consideration, due to dangers associated with the use of TEA·3HF and its high concentration in the reaction mixture (4 equivalents).

Even though a substantial amount of fluoro-deoxygenation occurred with this additive compared to elimination (reaction **V**), overall only 15% of α -fluorinated compound was formed against 60% of the β -fluorinated analog. The steroid used in the study²⁸ differed from lithocholic acid in that it contains a double bond at the 5,6-position (dehydroepiandrosterone or DHEA, **87**, Figure 34), therefore altering its 3D structure, which may have resulted in a difference in stereochemical outcome of the reaction. Essentially the presence of sp^2 carbons in the steroid's B-ring was flattening the structure, when compared with lithocholic acid.

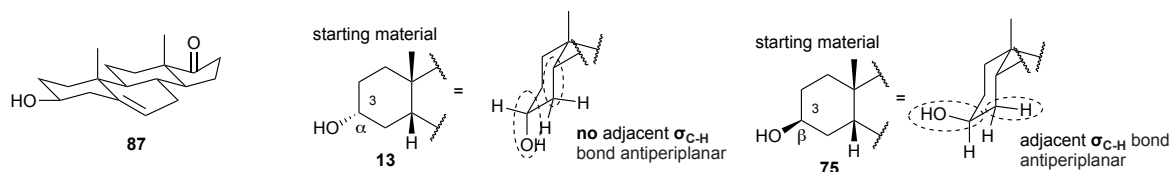


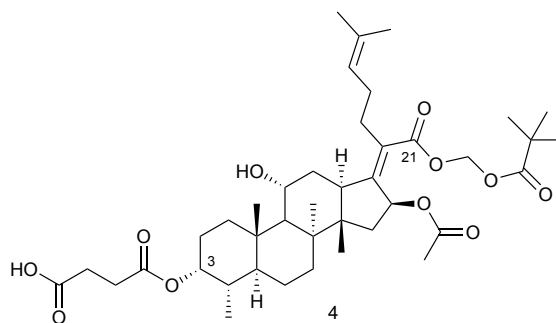
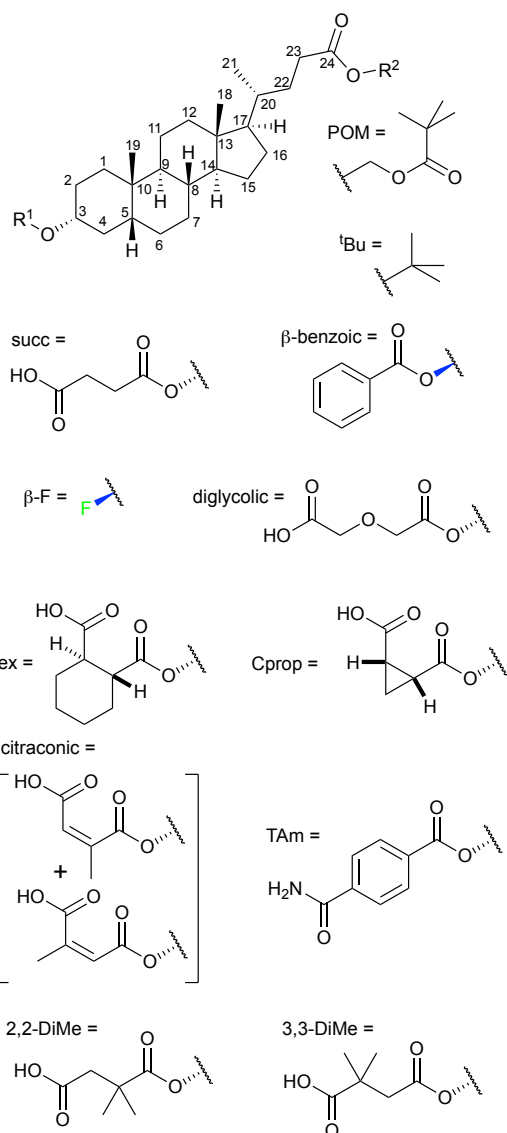
Figure 34 - 3D-Structure of DHEA (**87**) and both α -(**13**) & β -(**75**) hydroxyl groups.

In an attempt to prove what had been postulated earlier, concerning the 3β -hydroxyl (**75**) being more prone to elimination than the 3α -hydroxyl (**13**), this reaction was repeated with the inverted $C3$ -configuration (β) of *tert*-butyl-lithocholate (**75**). As expected, elimination became the dominant outcome (reaction **VI**), thus providing additional evidence to support the following explanation: the geometry of the hydroxyl group on $C3$ dictates whether or not it will be prone to eliminate, depending on the presence or not of an antiperiplanar σ_{C-H} bond (Figure 34) to allow effective orbital overlap.

3.8 - Biological Assays

Table 2 – Structures of the molecules used in thermal shift assays and splicing assays.

| Compound number | R ¹ | R ² |
|-------------------------|------------------|-----------------|
| 4 - Hit compound | | |
| 8 | H | POM |
| 13 | H | ^t Bu |
| 26 | succ | ^t Bu |
| 45 | succ | POM |
| 46 | diglycolic | ^t Bu |
| 47 | 3,3-DiMe | ^t Bu |
| 48 | 2,2-DiMe | ^t Bu |
| 49 | 3,3-DiMe | POM |
| 50 | 2,2-DiMe | POM |
| 51 | 3,3-DiMe | ⁱ Pr |
| 52 | 2,2-DiMe | ⁱ Pr |
| 54 | Cprop | POM |
| 55 | THex | ^t Bu |
| 57 | citraconic | ^t Bu |
| 80 | β -benzoic | H |
| 81 | β -F | H |
| 82 | TAm | H |



3.8.1 - Thermal Shift Assays (TSA)

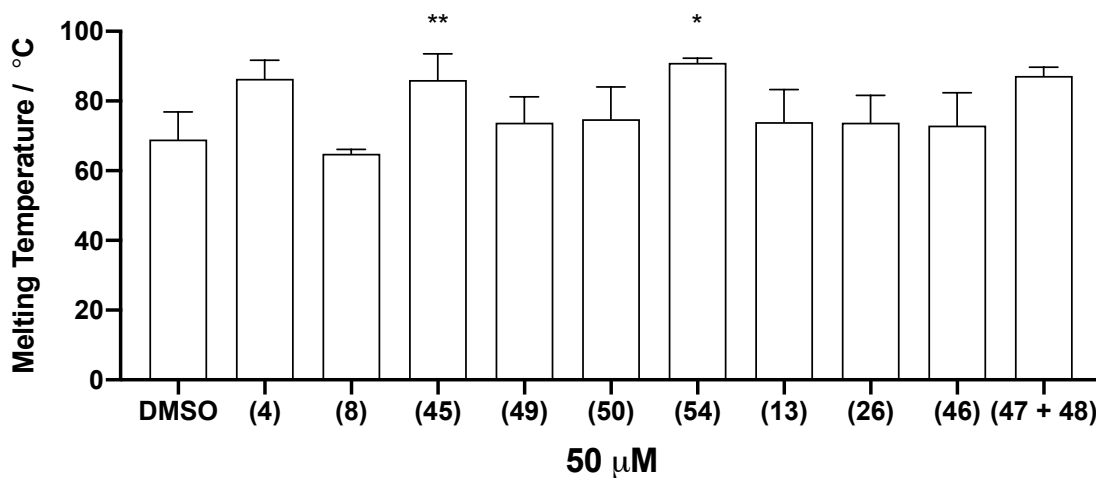


Figure 35 – Thermal shift assay results of some compounds of interest (Error bars indicate SD, $n = 3$).

Most of the compounds illustrated in Figure 35 were to be assessed comparatively with the initial hit compound **4**. The results of the assays were consistent with the idea that a reduction of flexibility in the side-chain added onto C-3 would increase the binding affinity of the compound with the target. Compounds **54** and **47+48** were the most promising molecules with increased binding affinity compared to the hit compound **4**.

On the other hand, when both *tert-butyl* and POM protecting groups were compared for their binding affinity, TSA results seemed to contradict themselves: when succinate esters of lithocholic acid (**26** & **45**) were compared, POM (**45**) seemed to offer greater affinity (**, $P = 0.0029$). Meanwhile, in the case of the supposedly more active dimethylsuccinate esters of lithocholic acid (**47+48** & **49**, **50**), *tert-butyl* derivatives (**47+48**) seemed to take the lead in terms of binding affinity.

Despite the statistical significance of these results, which relied on a sufficient number of repeats, the results may need further validation. The TSA required the protein to be in its native folded state when treated with the compounds of interest. Since purified *Snu114* was used in the assay it was possible that the nature of the isolated protein differed to the nature of the protein when in complex with U5 snRNP and other spliceosomal proteins, and this may therefore have produced false results. The TSA nevertheless served as a good tool to confirm or question the expected trends for inhibition, to keep the synthesis planning on right tracks throughout the project.

3.8.2 - Splicing assays – 1 mM

Despite splicing assays offering a more accurate picture of the inhibition as functional assays, they required more work to be set up and had to be repeated several times to generate consistent data. While all the compounds synthesized have been tested at least once at 1 mM by Megan Eadsforth (provided they were soluble in 4% DMSO), the results displayed on Figures 36 have all been carried out at least twice for increased statistical significance.

Screening the compounds at 1 mM for pre-mRNA splicing inhibition was carried out in order to rule out any compound that did not show comparable activity with lithocholic acid (**5**) and the hit compound (**4**). Compound **80** (LA- β -benzoic, Table 2) seemed to stand out on Figure 36, as it did not inhibit splicing as efficiently as all other compounds on display. Interestingly, the main structural difference between compounds **80** and **82** (which completely inhibited splicing at 1 mM), was the presence of an amide function attached to the phenyl ring of the *C*-3 substituent, which has the potential to hydrogen bond to the receptor. Although it was worth noting that the *C*-3 configuration differed between both compounds, which could also have influenced potential interactions (*C3*- β in **80**, *C3*- α in **82**).

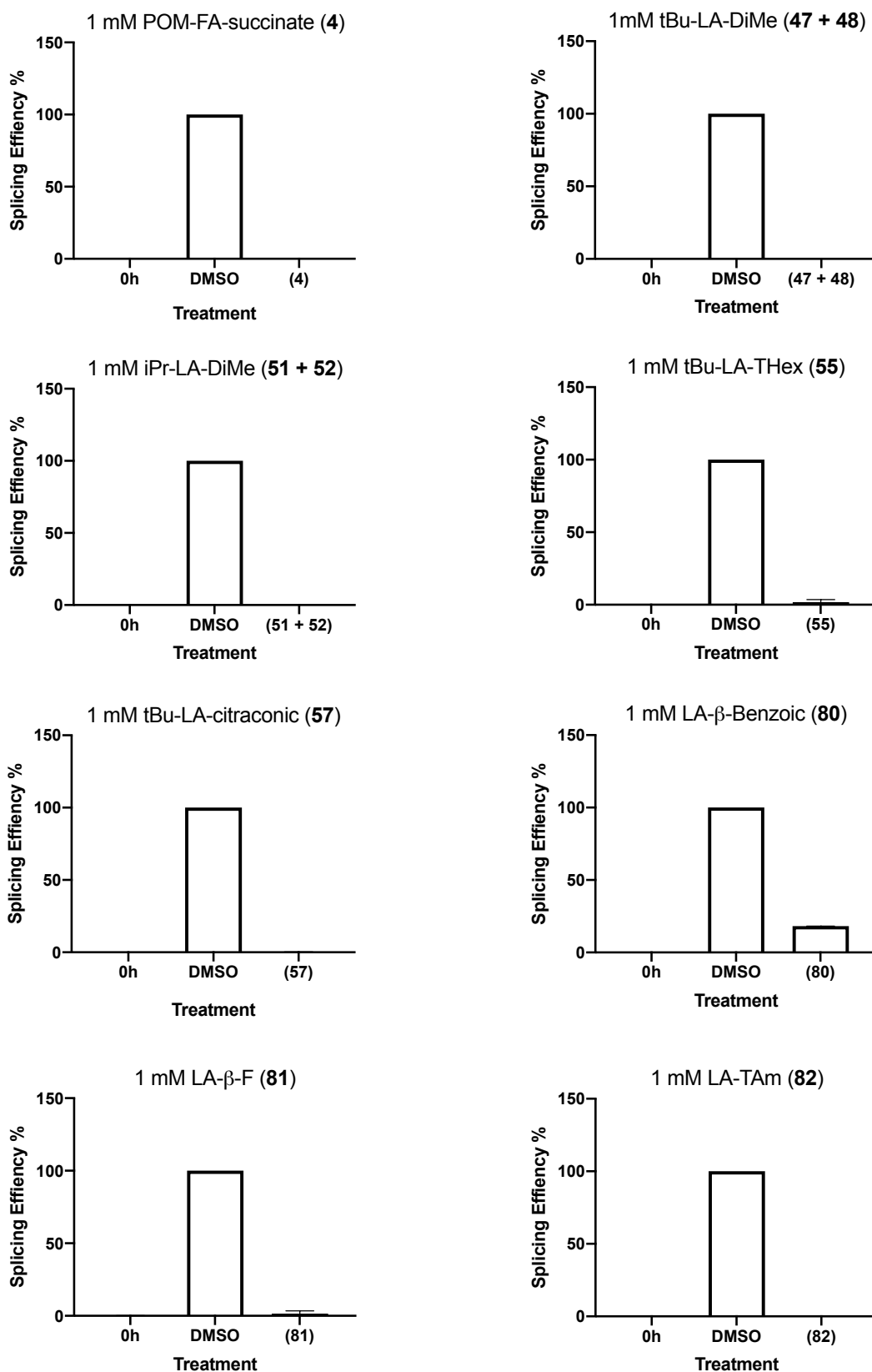


Figure 36 – Splicing inhibition displayed by some of the most promising new compounds. Splicing Efficiency (%) calculated as a percentage of the DMSO control. Error bar indicates SD, n = 2.

3.8.3 – Splicing assays - 1 mM and 100 μ M

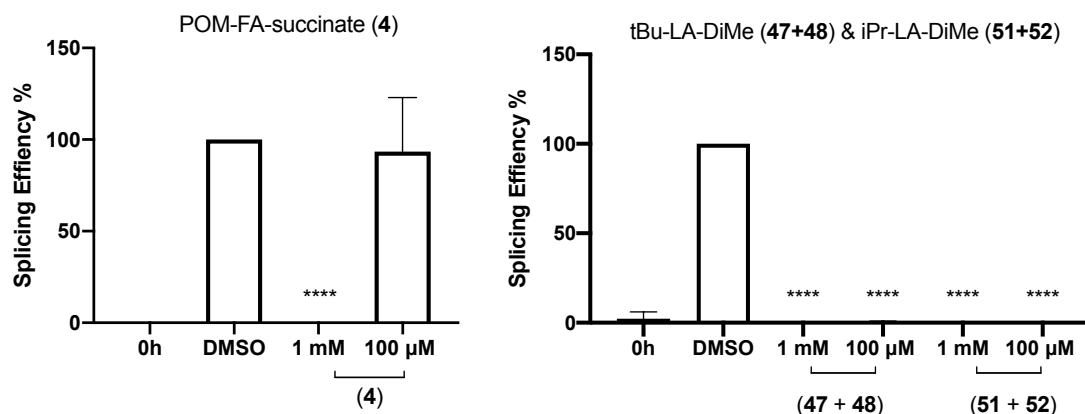


Figure 37 - Splicing inhibitory activity of the hit compound (4) compared to compounds (47+48) and (51+52). Splicing Efficiency (%) calculated as a percentage of the DMSO control. Error bars indicate SD, n = 3 (**** = $P < 0.00001$).

In addition to the results shown in Figure 36, the next step was to decrease the concentrations from 1 mM to 100 μ M for the compounds that displayed complete splicing inhibition at 1 mM in order to discriminate between the activity of each compound. Figure 37 depicts the extent of splicing efficiency for two of the most promising new compounds (47+48 and 51+52), as well as the previous hit compound 4.

In line with previous findings the hit compound (4) did not show complete inhibition of the splicing mechanism anymore, when titrated down to 100 μ M. Interestingly however, both compound mixtures (47+48) and (51+52) showed complete inhibition of splicing at 100 μ M (Figure 37). This data confirmed that among the new compounds synthesized, some have successfully surpassed the extent of inhibition previously reported for *Snu114*. The data also revealed that restricting the rotation of the succinate chain had a positive effect on activity, further supporting the idea that the carboxylate group is involved in important interactions with the receptor.

Both of the compounds displayed on Figure 37, aside from the hit compound 4, were generated as a mixture of regioisomers. Late-stage advances of the project provided compound 47 in a pure form, separated from the mixture of 47+48, setting ground for the SAR investigation with *Snu114* to be continued. Data concerning the similar POM-protected analogs, which were already provided as separate entities (49 and 49(50%)+50(50%)), could also be put into perspective with the data provided in Figure 37, in order to deduce whether the regioisomers act in concert or if one provides a more bioactive structure than the other.

4.0 - Conclusion & Future work

4.1 – New lead compound

A total of 32 molecules derived from lithocholic acid have been synthesized as part of this project. Promising new lead compounds have emerged following biological testing with the 3-dimethylsuccinate esters (**47-52**, Figure 38) that particularly stood out and laid new ground for biological analysis of the resulting inhibition of *Snu114*.

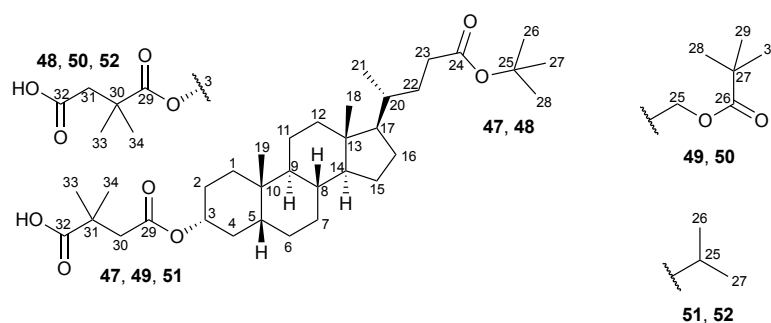


Figure 38 - Structures of the new lead compounds.

Synthesis of the new dimethyl-succinate lead compounds with unnatural 3β configuration will be of crucial importance for comparative purposes. This can be achieved via the Mitsunobu inversion reaction as described earlier and would provide additional information about the binding pocket of *Snu114*. Furthermore, the late-stage separation of isomers that was managed for compounds **47**, **49** and **50**, suggested that all other compounds generated by addition of 2,2-dimethylsuccinic anhydride (**19**) might possibly be separable. The same suggestion could be made for other anhydrides leading to mixtures of isomers like (\pm)-**20** (cyclopropyl-containing) and (\pm)-**21** (cyclohexyl-containing), however the structural differences in those cases would be much less significant than for the dimethylsuccinate-compounds.

It would also be interesting to find out whether deprotecting the *C-24* ester on compounds that also contain a free acid end at the newly functionalized *C-3* end would have any influence on the binding affinity of the resulting compounds. If no significant change in activity was measured upon restoration of the *C-24* acid moiety, then investigations into modifying this region of the molecule could be considered.

4.2 – Recently developed alternative to Mitsunobu inversion reagents

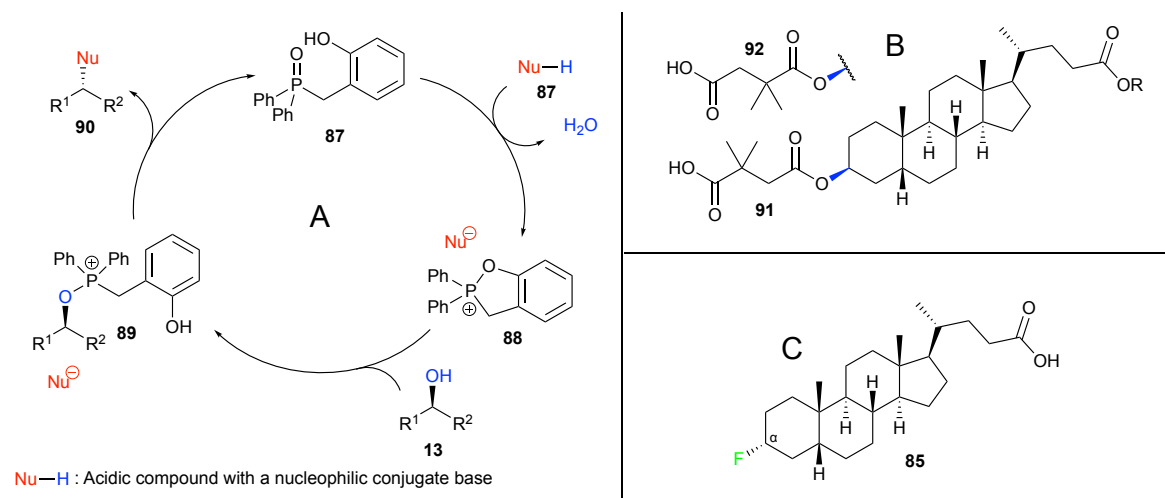


Figure 39 - (A) Newly developed organocatalyst for the Mitsunobu inversion reaction. (B) Structures of the dimethylsuccinate esters of LA with unnatural C-3 configuration. (C) Structure of the 3 α - deoxy-fluorinated compound.

Additionally, a very recent study (R. H. Beddoe, Aug. 2019) regarding the well-established Mitsunobu inversion, has described a new catalyst (Figure 39) that may make this reaction much more efficient and purification much easier.³⁸ In fact it was established during this project that a lot of side products effectively got formed while using conventional Mitsunobu inversion reagents. As soon as this catalyst become commercially available, replacing the need for the highly explosive DEAD reagent could possibly widen the array of nucleophiles used. Other reagents which may have been too dangerous to be combined with the latter reagent could now potentially be used. Besides also making large-scale production of lithocholic acid with unnatural C-3 configuration much safer and cleaner, it could also be combined with fluoro-deoxygenating reagents in an attempt to gain control over the stereochemistry of the fluoro-deoxygenation reaction.

4.3 – Stereocontrol in fluoro-deoxygenation mechanism

Despite the many attempts carried out at isolating the 3 α -fluoro- compound (**85**) having been unsuccessful, using HF or another milder alternative of nucleophilic F⁻ source in acidic medium, combined with the newly developed catalyst for Mitsunobu inversion could be a new option to investigate. This could technically already be achieved with

conventional Mitsunobu reagents but would most likely be too dangerous with DEAD being explosive as well as some of the fluoro-deoxygenating agents like DAST. The catalyst recently developed also requires acidic conditions to function (Figure 39), which would necessarily involve having HF being at least generated at some stage of the reaction, meaning that all the safety precautions related to its use would have to be taken into consideration.

In addition to that, other recently developed catalysts for fluoro-deoxygenation reactions on secondary alcohols could also be considered, as they could provide with a safer alternative to the previously quoted reaction conditions. In fact, AlkylFluor (**93**) was described as a new reagent that would selectively cause fluoro-deoxygenation of a secondary alcohol position with inversion of configuration (Figure 40, C. N. Neumann & T. Ritter, 2017).²⁸ The selectivity claims made for this reagent require confirmation and will have to be assessed, according to the observations made with XtalFluor E (Figure 40). While more complex chemical structures do usually correlate with increased selectivity, these may also come along with increased cost of production, which explains why the reagent wasn't commercially obtainable at the time of writing.

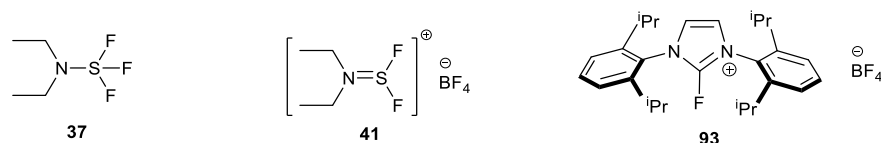


Figure 40 - Structures of DAST, XtalFluor-E and AlkylFluor.

Finally, the very last stage of this project consisted in trying to form C-3 functionalized derivatives from double-bond-containing anhydrides, which clearly left room for improvements. Regardless of the challenging separation methods required, the rate of completion for these reactions was very low, believed to be due to the conjugation induced by the double bond, which was discussed earlier. Using di-acid analogs of these anhydrides coupled with EDCI would be a potential alternative that could be studied for the generation of the same compounds of interest (**56-59**).

5.0 - Experimental

5.1 – Instrumentation, Software, Techniques and Apparatus

5.1.1 - Structures

All biology drawings, structures and compound names were generated using ChemDraw Professional 16.0 and ChemDraw 18.2.

5.1.2 - Thin Layer Chromatography (TLC)

TLC was carried out using Macherey Nagel Polygram silica TLC plates with a UV₂₅₄ fluorescent indicator and treated with solvent systems described in individual experiments. Spots were visualised using UV₂₅₄ light or phosphomolybdic acid solution with heating.

5.1.3 - Chromatography

Flash silica column chromatography was performed using silica gel (40-63 μm) and eluted with the solvent systems described in individual experiments.

5.1.4 - Nuclear Magnetic Resonance Spectroscopy (NMR)

All NMR experiments were carried out using a Bruker Avance 500 MHz or 400 MHz. Chemical shifts are reported in "parts per million" (ppm) and are relative to the reference residual solvent signal. Standard abbreviations are used for multiplicity (e.g. s = singlet, d = doublet, m = multiplet, etc) and coupling constants (J) are reported in Hertz (Hz). All carbon signals are singlets unless otherwise stated. ¹³C NMR assignment has been carried out using the 2D HSQC NMR spectroscopy technique.

5.1.5 - Infra-Red Spectroscopy

All Infra-Red Spectroscopy experiments were carried out using a Thermo Scientific Nicolet iS5 iD5 ATR spectrometer and analysed as a thin film.

5.1.6 - Melting points

All melting points measurements were carried out using a Stuart Scientific BIBBY SMP10 instrument.

5.1.7 - Optical rotation

All polarimetric measurements were carried out using a Rudolph Research Analytical, Autopol 1, Automatic Polarimeter, using sodium D line as wavelength (589.3 nm), with a 0.25 dm long cell (l). The resulting $[\alpha]_D^T$ value was calculated from the

measured value α via the following equation: $[\alpha]_D^T = \frac{\alpha}{l \cdot c}$, where c is the concentration of compound in mg.mL⁻¹ (or g.L⁻¹), T is the temperature, D the wavelength (in nm) of the sodium line and l the length of the cell (in dm).

5.1.8 - Experimental Terms

"Dry" solvents refer to anhydrous solvents, procured as anhydrous from the supplier. "Drying" with respect to organic extracts during a work-up refers to the use of magnesium sulfate (MgSO₄) to remove water, before being removed by subsequent filtration. "Concentration" of the final product refers to the removal of solvent *in vacuo*, using a rotary evaporator and a high vacuum pump.

5.1.9 - Baths

The following baths were used to achieve the corresponding temperatures:

Above 25 °C - hot water bath;

0 °C - ice and water;

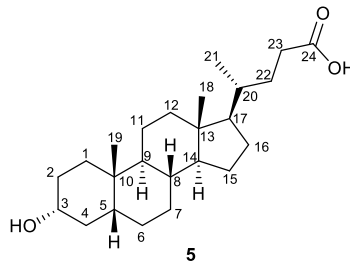
-78 °C - acetone and dry ice.

5.1.10 - Solvents and Reagents

All solvents and reagents were prepared on site or supplied by Sigma-Aldrich, Fluorochem, Acros Organics, Alfa-Aesar or Fischer.

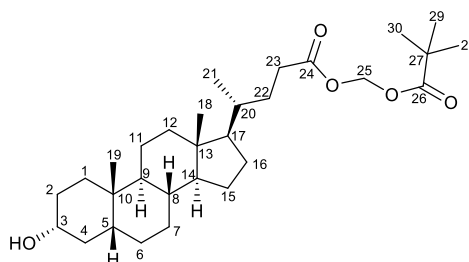
5.2 – Experimental Procedures

Lithocholic acid - (4*R*)-4-((3*R*,8*R*,9*S*,10*S*,13*R*,14*S*,17*R*)-3-hydroxy-10,13-dimethylhexadecahydro-1*H*-cyclopenta[*a*]phenanthren-17-yl)pentanoic acid (5)



M.p. 184-186 °C, [Lit³⁹: 185-187 °C]; $[\alpha]_D^{20} +34.6$ (c 1.10 in MeOH), [Lit⁴⁰: $[\alpha]_D^{20} +33.7$]; ν_{max}/cm^{-1} 3270br (O-H), 2926m (C-H), 2860m (C-H), 1699s (C=O); δ_H (CDCl₃, 400 MHz) 0.64 (3H, s, C(18)H₃), 0.92 (3H, s, C(19)H₃), 0.93 (3H, d, J = 6 Hz, C(21)H₃) 0.99 (1H, dd, J = 14.2 Hz, 3.4 Hz, C(1)H_β), 1.03-1.05 (1H, m, C(14)H_α), 1.06-1.08 (1H, m, C(15)H_α), 1.08-1.10 (1H, m, C(7)H_α), 1.11-1.13 (1H, m, C(17)H_α), 1.14-1.21 (1H, m, C(12)H_α), 1.22-1.25 (1H, m, C(11)H_β), 1.26-1.28 (1H, m, C(6)H_α), 1.29-1.32 (2H, m, C(16)H_β, C(22)H_β), 1.33-1.35 (1H, m, C(2)H_α), 1.36-1.41 (5H, m, C(11)H_α, C(8)H_β, C(20)H, C(9)H_α, C(5)H_β), 1.42-1.45 (1H, m, C(7)H_β), 1.46-1.60 (1H, m, C(4)H_β), 1.61-1.70 (1H, m, C(15)H_β, C(2)H_β), 1.71-1.89 (5H, m, C(4)H_α, C(1)H_α, C(22)H_α, C(6)H_β, C(16)H_α), 1.96 (1H, dt, J = 12 Hz, 3.2 Hz, C(12)H_β), 2.26 (1H, ddd, J = 15.8 Hz, 9.4 Hz, 6.6 Hz C(23)H_α), 2.40 (1H, ddd, J = 15.8 Hz, 10 Hz, 5.2 Hz, C(23)H_β), 3.63 (1H, tt, J = 10.8 Hz, 4.4 Hz, C(3)H), a reference was used to correlate H¹ measurements made with α,β assignments provided in the document⁴⁰; δ_C (CDCl₃, 100 MHz) 12.1 (C(18)), 18.2 (C(21)), 20.8 (C(11)), 23.4 (C(19)), 24.2 (C(15)), 26.4 (C(7)), 27.2 (C(6)), 28.2 (C(16)), 30.6 (C(2)), 30.6 (C(23)), 30.8 (C(22)), 34.6 (C(10)), 35.3 (C(20)), 35.4 (C(1)), 35.9 (C(8)), 36.5 (C(4)), 40.2 (C(12)), 40.4 (C(9)), 42.1 (C(5)), 42.8 (C(13)), 55.9 (C(17)), 56.5 (C(14)), 71.9 (C(3)), 177.8 (C(24)); LRMS ES- [M-H]⁻: 375.3 (100%); HRMS ES- calc for C₂₄H₃₉O₃ 375.2905, found 375.2905.

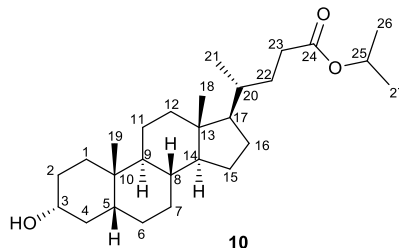
(Pivaloyloxy)methyl (4R)-4-((3R,8R,9S,10S,13R,14S,17R)-3-hydroxy-10,13-dimethyl hexadecahydro-1H-cyclopenta[a]phenanthren-17-yl)pentanoate (8)



8

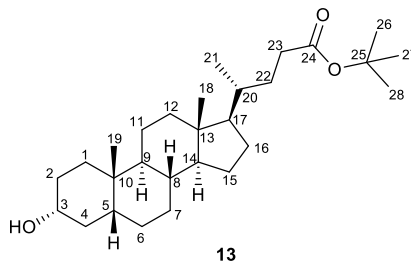
Lithocholic acid (5.00 g, 13.28 mmol) was dissolved in N,N'-dimethylformamide (25 mL), under N₂ atmosphere at 0 °C with stirring. Chloromethyl pivalate (2.02 mL, 14.00 mmol) and triethylamine (1.95 mL, 14.00 mmol) were then added. The mixture was left to stir at room temperature for 48 hours. It was then diluted with 3 x 20 mL of dichloromethane to be subsequently washed with 1M NaHCO₃ (2 x 30 mL), water (10 x 30 mL) and brine (1 x 30 mL). After drying over MgSO₄ and concentrated *in vacuo*, the residue was subjected to column chromatography (R_f = 0.44, hexane 2:1 ethyl acetate). When the amount of Lithocholic acid used exceeded 1.5 g (i.e. 5 g), instead of column chromatography purification, the residue was partitioned again between Et₂O (50 mL) and water (20 mL). It was then subsequently washed with 1M NaHCO₃ (2 x 30 mL), water (10 x 30 mL) and brine (1 x 30 mL). After drying over MgSO₄ and concentrated under reduced pressure a viscous colourless liquid was obtained (**8**, 4.8 g, 9.8 mmol, 74%). R_f = 0.44 (hexane 2:1 ethyl acetate); m.p. 69 °C; [α]_D²⁵ +26.4 (c 1.77 in DCM); ν_{max}/cm⁻¹ 2930m (C-H), 2864m (C-H), 1753s (C=O); δ_H (CDCl₃, 400 MHz) 0.59 (3H, s, C(18)H₃), 0.86 (3H, d, J = 6.8 Hz, C(21)H₃), 0.87 (3H, s, C(19)H₃), 0.88-1.14 (7H, m), 1.16 (9H, s, C(28)H₃, C(29)H₃ & C(30)H₃), 1.23-2.14 (20H, m), 2.22 (1H, ddd, J = 15.6 Hz, 9.2 Hz, 6.8 Hz, C(23)H_α), 2.34 (1H, ddd, J=15.6 Hz, 10 Hz, 5.2 Hz, C(23)H_β), 3.52-3.60 (1H, m, C(3)H), 5.69 (2H, s, C(25)H₂); δ_C (CDCl₃, 100 MHz) 12.1 (C(18)), 18.2 (C(21)), 20.8 (C(11)), 23.4 (C(19)), 24.2 (C(15)), 26.5 (C(7)), 26.9 (C(28)/C(29)/C(30)), 27.2 (C(6)), 28.2 (C(16)), 30.5 (C(2)), 30.7 (C(23)), 31.0 (C(22)), 34.6 (C(10)), 35.3 (C(20)), 35.4 (C(1)), 35.9 (C(8)), 36.4 (C(4)), 38.7 (C(27)), 40.2 (C(12)), 40.4 (C(9)), 42.1 (C(5)), 42.8 (C(13)), 56.0 (C(17)), 56.5 (C(14)), 71.7 (C(3)), 79.4 (C(25)), 172.9 (C(24)), 177.2 (C(26)); LRMS ES+ [M+Na]⁺: 513.3 (100%); HRMS ES+ calc for C₃₀H₅₀O₅Na 513.3550, found 513.3552.

Isopropyl (4R)-4-((3R,8R,9S,10S,13R,14S,17R)-3-hydroxy-10,13-dimethylhexadecahydro-1H-cyclopenta[a]phenanthren-17-yl)pentanoate (10)



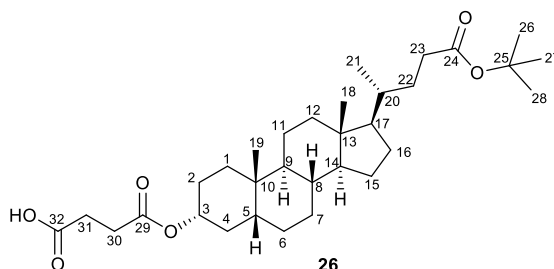
Lithocholic acid (1.00 g, 2.65 mmol) was heated at reflux in anhydrous isopropanol (150 mL) in presence of sulfuric acid (1 mL) for 24 hours. The solvent was evaporated, followed by addition of water (100 mL) and extraction with dichloromethane (3 x 30 mL). The combined extracts were washed with H₂O (3 x 60 mL), Na₂CO₃ solution (20%, 3 x 60 mL) and brine (1 x 60 mL). The organic layer was dried over MgSO₄ and evaporated under reduced pressure. The residue was purified by column chromatography on silica gel (n-hexane 80%/ethyl acetate 20%) to yield **10** as a colourless crystalline solid (0.31 g, 0.75 mmol, 28%). $R_f = 0.59$; m.p. 87-88 °C [Lit¹⁹: 78-80 °C]; $[\alpha]_D^{23} +44.9$ (c 1.66 in DCM) [Lit¹⁹: $[\alpha]_D^{20} +23.8$ (c 1.00 in CHCl₃)]; ν_{max}/cm^{-1} 3270br (O-H), 2927m (C-H), 2863m (C-H), 1729 (C=O ester); δ_H (CDCl₃, 400 MHz) 0.64 (3H, s, C(18)H₃), 0.91 (3H, d, J = 6 Hz, C(21)H₃), 0.92 (3H, s, C(19)H₃), 0.94-1.17 (7H, m), 1.22 (6H, d, J = 4.8 Hz, C(26)H₃ & C(27)H₃), 1.26-1.42 (13H, m), 1.69-2.00 (7H, m), 2.18 (1H, ddd, J = 12 Hz, 7.2 Hz, 5 Hz, C(23)H_A), 2.30 (1H, ddd, J = 12 Hz, 8 Hz, 4 Hz, C(23)H_B), 3.58-3.66 (1H, m, C(3)H); δ_C (CDCl₃, 100 MHz) 12.0 (C(18)), 18.3 (C(21)), 20.8 (C(11)), 21.9 (C(27)), 22.6 (C(26)), 23.4 (C(19)), 24.2 (C(15)), 26.4 (C(7)), 27.2 (C(6)), 28.2 (C(16)), 30.6 (C(2)), 31.0 (C(23)), 31.7 (C(22)), 34.6 (C(10)), 35.3 (C(20)), 35.3 (C(1)), 35.9 (C(8)), 36.5 (C(4)), 40.2 (C(12)), 40.4 (C(9)), 42.1 (C(5)), 42.7 (C(13)), 56.0 (C(17)), 56.5 (C(14)), 67.3 (C(25)), 71.9 (C(3)), 173.9 (C(24)); LRMS ES+ [M+Na]⁺: 441.3 (40%); HRMS ES- calc for C₂₇H₄₇O₃ 419.3520, found 419.3513.

Tert-butyl-(4R)-4-((3R,8R,9S,10S,13R,14S,17R)-3-hydroxy-10,13-dimethylhexadecahydro-1H-cyclopenta[a]phenanthren-17-yl)pentanoate (13**)**



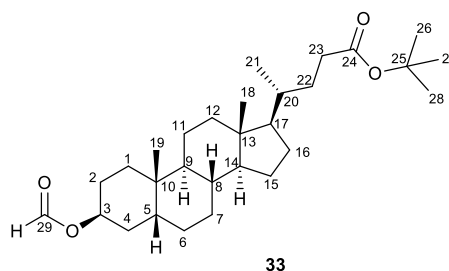
General Procedure for compounds 10, 13 and 44: Lithocholic Acid (5.0 g, 12.3 mmol) was dissolved in anhydrous THF (100 mL), the solution was stirred and cooled in an ice-bath. Trifluoroacetic anhydride (20 mL) was then added dropwise before the ice-bath was removed. The solution was left to react for 80 min. The solution was re-cooled and the corresponding anhydrous alcohol (30 mL) was added. After 7 hours at room temperature, aqueous NH_3 (20 mL, 35% w/w) was added with cooling and the solution was left for 12 hours at 0°C . Another portion of aqueous NH_3 (10 mL) was added and after a further 4 hours at room temperature, the mixture was partitioned between Et_2O (200 mL) and water (100 mL). The organic layer was washed with 1 M NaOH (2 x 100 mL) and H_2O (4 x 100 mL) respectively before being dried with MgSO_4 and evaporated to **13**, a colourless crystalline solid (4.9 g, 11.4 mmol, 92%). M.p. $122\text{--}123^\circ\text{C}$; $[\alpha]_D^{20} +24.8$ (c 1.33 in DCM); $\nu_{\text{max}}/\text{cm}^{-1}$ 3285br (O-H), 2927m (C-H), 2863m (C-H), 1730 (C=O); δ_{H} (CDCl_3 , 400 MHz) 0.64 (3H, s, C(18) $\underline{\text{H}}_3$), 0.84 (3H, d, $J = 7.6$ Hz, C(21) $\underline{\text{H}}_3$), 0.85 (3H, s, C(19) $\underline{\text{H}}_3$), 0.88-1.34 (19H, m), 1.44 (9H, s, C(26) $\underline{\text{H}}_3$, C(27) $\underline{\text{H}}_3$ & C(28) $\underline{\text{H}}_3$), 1.52-1.93 (8H, m), 2.12 (1H, ddd, $J = 15.3$ Hz, 9.8 Hz, 6.8 Hz, C(23) $\underline{\text{H}}_{\alpha}$), 2.40 (1H, ddd, $J = 15.3$ Hz, 9.6 Hz, 4.8 Hz, C(23) $\underline{\text{H}}_{\beta}$), 3.62 (1H, tt, $J = 10.8$ Hz, 4.8 Hz, C(3) $\underline{\text{H}}$); δ_{C} (CDCl_3 , 100 MHz) 12.0 (C(18)), 18.3 (C(21)), 20.8 (C(11)), 23.4 (C(19)), 24.2 (C(15)), 26.4 (C(7)), 27.2 (C(6)), 28.1 (C(26)/C(27)/C(28)), 28.2 (C(16)), 30.6 (C(2)), 31.1 (C(23)), 32.6 (C(22)), 34.6 (C(10)), 35.3 (C(20)), 35.4 (C(1)), 35.9 (C(8)), 36.5 (C(4)), 40.2 (C(12)), 40.4 (C(9)), 42.1 (C(5)), 42.7 (C(13)), 56.0 (C(17)), 56.5 (C(14)), 71.9 (C(3)), 79.9 (C(25)), 173.7 (C(24)); LRMS ES+ $[\text{M}+\text{Na}]^+$: 455.3 (100%); HRMS ES+ calc for $\text{C}_{28}\text{H}_{48}\text{O}_3\text{Na}$ 455.3496, found 455.3486.

4-(((3R,8R,9S,10S,13R,14S,17R)-17-((R)-5-(tert-butoxy)-5-oxopentan-2-yl)-10,13-dimethylhexadecahydro-1H-cyclopenta[a]phenanthren-3-yl)oxy)-4-oxobutanoic acid (26)



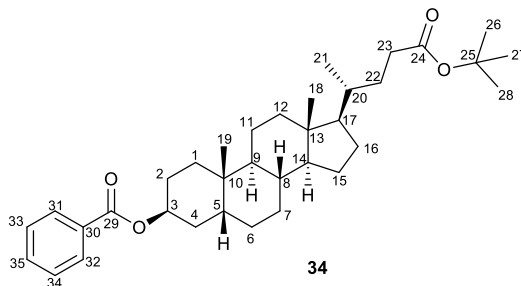
General Procedure for compounds 26, 46 and (47+48): Compound **13** (0.33 g, 0.76 mmol) was dissolved in dry pyridine (5 mL). To this was added DMAP (9.40 mg, 0.08 mmol) and the corresponding anhydride (3.17 mmol). The reaction was refluxed at 115 °C for 72 hours. After that the reaction was quenched with water (10 mL), extracted with Et₂O (20 mL) and washed with 1 M HCl (3 x 20 mL), water (3 x 20 mL) and brine (2 x 20 mL) respectively. The extracts were dried over MgSO₄ and evaporated under reduced pressure to give the ester **26** as a colourless crystalline solid (0.22 g, 0.42 mmol, 55%). M.p. : 168-170 °C [Lit⁴¹: 163-164 °C]; $[\alpha]_D^{20} +59.8$ (c 0.805 in DCM); ν_{max}/cm^{-1} 2933m (C-H), 2863m (C-H), 1732s (C=O ester), 1718s (C=O acid); δ_H (CDCl₃, 400 MHz) 0.64 (3H, s, C(18)H₃), 0.90 (3H, d, J = 6.4 Hz, C(21)H₃), 0.92 (3H, s, C(19)H₃), 1.01-1.31 (12H, m), 1.44 (9H, s, C(26)H₃, C(27)H₃ & C(28)H₃), 1.54-1.99 (15H, m), 2.05 (1H, ddd, J = 15.6 Hz, 8.8 Hz, 6.2 Hz, C(23)H_a), 2.19 (1H, ddd, J = 15.6 Hz, 10 Hz, 5.5 Hz, C(23)H_b), 2.59-2.70 (4H, m, C(30)H₃ & C(31)H₃), 4.64-4.72 (1H, m, C(3)H); δ_C (CDCl₃, 100 MHz) 12.0 (C(18)), 18.3 (C(21)), 20.9 (C(11)), 23.3 (C(19)), 24.2 (C(15)), 26.3 (C(7)), 26.6 (C(6)), 27.1 (C(2)), 28.1 (C(26)/C(27)/C(28)), 28.2 (C(16)), 28.8 (C(31)), 29.3 (C(30)), 31.1 (C(23)), 32.2 (C(22)), 32.6 (C(10)), 34.6 (C(20)), 35.0 (C(1)), 35.3 (C(8)), 35.8 (C(4)), 40.1 (C(12)), 40.4 (C(9)), 41.9 (C(5)), 42.7 (C(13)), 56.1 (C(17)), 56.5 (C(14)), 75.0 (C(3)), 79.9 (C(25)), 171.7 (C(24)), 173.8 (C(29)), 176.3 (C(32)); LRMS ES- [M-H]⁻: 531.4 (100%), ES+ [M+2Na]²⁺: 577.3 (100%); HRMS ES- calc for C₃₂H₅₁O₆ 531.3691, found 531.3692.

***tert*-butyl(4*R*)-4-((3*S*,8*R*,9*S*,10*S*,13*R*,14*S*,17*R*)-3-(formyloxy)-10,13-dimethylhexadecahydro-1*H*-cyclopenta[*a*]phenanthren-17-yl)pentanoate (33)**



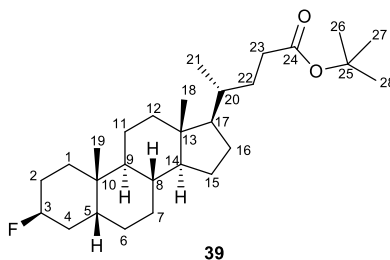
General Procedure for compounds 33, 34, 74: To a solution of **13** (1.00 g, 2.31 mmol)/**8** (1.05 g, 2.31 mmol) and PPh_3 (1.21 g, 4.62 mmol) in THF (10 mL), Formic acid (0.17 mL, 0.21 g, 4.62 mmol)/benzoic acid (0.56 g, 4.62 mmol) was slowly added. After dropwise addition of DEAD (0.73 mL, 0.81 g, 4.62 mmol), stirring was continued for 1 day at room temperature. The mixture was subjected to purification by column chromatography. The product obtained was a colourless crystalline solid (**33**, 0.62 g, 1.35 mmol, 58%). $R_f = 0.47$ (Hex 19:1 EtOAc); m.p. 76 °C; $[\alpha]_D^{23} +17.4$ (c 3.63 in DCM); $\nu_{\text{max}}/\text{cm}^{-1}$ 2930m (C-H), 2864m (C-H), 1749s (C=O), 1716s (C=O); δ_H (CDCl_3 , 500 MHz) 0.61 (3H, s, C(18) $\underline{\text{H}}_3$), 0.86 (3H, d, $J = 6.4$ Hz, C(21) $\underline{\text{H}}_3$), 0.93 (3H, s, C(19) $\underline{\text{H}}_3$), 0.97-1.38 (15H, m), 1.40 (9H, s, C(26) $\underline{\text{H}}_3$, C(27) $\underline{\text{H}}_3$ & C(28) $\underline{\text{H}}_3$), 1.41-2.00 (12H, m), 2.08 (1H, ddd, $J = 12$ Hz, 7.8 Hz, 4.6 Hz, C(23) $\underline{\text{H}}_\alpha$), 2.21 (1H, ddd, $J = 12$ Hz, 7.6 Hz, 4 Hz, C(23) $\underline{\text{H}}_\beta$), 5.18 (1H, s, C(3) $\underline{\text{H}}$), 8.02 (1H, s, C(29) $\underline{\text{H}}$); δ_C (CDCl_3 , 125 MHz) 12.1 ($\underline{\text{C}}$ (18)), 18.3 ($\underline{\text{C}}$ (21)), 21.1 ($\underline{\text{C}}$ (11)), 23.9 ($\underline{\text{C}}$ (19)), 24.2 (C(15)), 25.1 (C(7)), 26.2 (C(6)), 26.5 (C(2)), 28.2 (C(26)/C(27)/C(28)), 28.2 (C(16)), 30.6 (C(23)), 30.7 (C(22)), 31.1 (C(10)), 32.6 (C(20)), 34.9 (C(1)), 35.3 (C(8)), 35.7 (C(4)), 37.3 (C(12)), 40.0 (C(9)), 40.2 (C(5)), 42.8 (C(13)), 56.1 (C(17)), 56.6 (C(14)), 71.0 (C(3)), 79.8 (C(25)), 160.8 (C(29)), 173.6 (C(24)); LRMS ES+ $[\text{M}+\text{Na}]^+$: 583.3 (100%); HRMS ES+ calc for $\text{C}_{29}\text{H}_{48}\text{O}_4\text{Na}$ 483.3445, found 483.3446.

(3*S*,8*R*,9*S*,10*S*,13*R*,14*S*,17*R*)-17-((*R*)-5-(*tert*-butoxy)-5-oxopentan-2-yl)-10,13-dimethylhexadecahydro-1*H*-cyclopenta[*a*]phenanthren-3-yl benzoate (34**)**



34, a viscous and colourless liquid (1.1 g, 2.0 mmol, 57%, from 1.5 g of starting material). R_f = 0.40 (hexane 9:1 ethyl acetate); m.p. 87 °C; $[\alpha]_D^{24}$ +31.2 (c 1.66 in DCM); ν_{max}/cm^{-1} 2934m (C-H), 2865m (C-H), 1758s (C=O), 1715s (C=O); δ_H (CDCl₃, 500 MHz) 0.63 (3H, s, C(18)H₃), 0.88 (3H, d, J = 6.4 Hz, C(21)H₃), 0.98 (3H, s, C(19)H₃), 1.00-1.40 (15H, m), 1.42 (9H, s, C(26)H₃, C(27)H₃ & C(28)H₃), 1.47-2.06 (12H, m), 2.10 (1H, ddd, J = 12.2 Hz, 7.2 Hz, 5.2 Hz, C(23)H_a), 2.23 (1H, ddd, J=12.2 Hz, 8 Hz, 4 Hz, C(23)H_b), 5.31 (1H, s, C(3)H), 7.40 (2H, d, J = 6 Hz, C(33)H & C(34)H), 7.50 (1H, t, J = 5.6 Hz, C(35)H), 8.02 (2H, d, J = 6 Hz, C(31)H & C(32)H); δ_C (CDCl₃, 125 MHz) 12.1 (C(18)), 18.3 (C(21)), 21.1 (C(11)), 24.1 (C(19)), 24.2 (C(15)), 25.2 (C(7)), 26.2 (C(6)), 26.6 (C(2)), 28.1 (C(26)/C(27)/C(28)), 28.2 (C(16)), 30.8 (C(23)), 31.1 (C(22)), 31.1 (C(10)), 32.5 (C(20)), 35.0 (C(1)), 35.3 (C(8)), 35.7 (C(4)), 37.7 (C(12)), 39.9 (C(9)), 40.2 (C(5)), 42.8 (C(13)), 56.1 (C(17)), 56.5 (C(14)), 71.3 (C(3)), 79.7 (C(25)), 128.3 (C(33)/C(34)), 129.5 (C(31)/C(32)), 131.2 (C(30)), 132.6 (C(35)), 165.7 (C(29)), 173.5 (C(24)); LRMS ES+ $[M+Na]^+$: 559.4 (100%); HRMS ES+ calc for C₃₅H₅₂O₄Na 559.3758, found 559.3760.

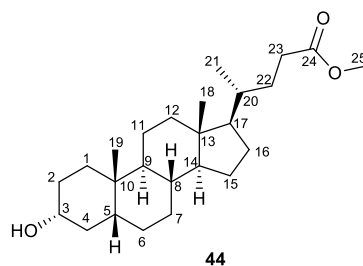
***tert*-butyl (4*R*)-4-((3*S*,8*R*,9*S*,10*S*,13*R*,14*S*,17*R*)-3-fluoro-10,13-dimethylhexadecahydro-1*H*-cyclopenta[*a*]phenanthren-17-yl)pentanoate (**39**)**



75 (0.33 mg, 0.76 mmol) was dissolved in dry DCM (5 mL) and the solution was cooled to -78 °C and stirred under N₂ atmosphere. DAST (0.13 mL, 1.00 mmol) was slowly added to the solution and the solution was allowed to heat up to room temperature while being

stirred for 1 hour. After this, the reaction was quenched with 5% NaHCO₃ solution (5 mL). The organic layer was separated and the aqueous layer was extracted twice with DCM (2 x 5 mL). The combined organic phases were washed with H₂O (3 x 10 mL) and Brine (10 mL) before being dried over MgSO₄ and evaporated to dryness. The resulting mixture was separated on a Prep TLC plate (hexane 19:1 ethyl acetate) where the silica line corresponding to the compound was scratched to a powder that was then suspended in Hexane to extract the product. The suspension was filtered and the filtrate was evaporated to yield compound **39**, a colourless crystalline solid (14.8 mg, 0.032 mmol, 4%). R_f = 0.40 (hexane 19:1 ethyl acetate); m.p. 110 °C; $[\alpha]_D^{25}$ +14.8 (c 0.72 in DCM); ν_{max}/cm^{-1} 2930m (C-H), 2863m (C-H), 1722s (C=O), 1366s (C-F); δ_H (CDCl₃, 400 MHz) 0.65 (3H, s, C(18)H₃), 0.90 (3H, d, J = 8 Hz, C(21)H₃), 0.96 (3H, s, C(19)H₃), 1.00-1.42 (17H, m), 1.44 (9H, s, C(26)H₃, C(27)H₃ & C(28)H₃), 1.48-1.54 (1H, m), 1.58-2.01 (9H, m), 2.12 (1H, ddd, J = 15.4 Hz, 8.8 Hz, 6 Hz, C(23)H_α), 2.25 (1H, ddd, J=15.4 Hz, 10 Hz, 5.2 Hz, C(23)H_β), 4.87 (1H, d, J= 48.8 Hz, C(3)FH); δ_C (CDCl₃, 100 MHz) 12.2 (C(18)), 18.4 (C(21)), 21.3 (C(11)), 23.9 (C(19)), 24.3 (C(15)), 26.1 (C(7)), 26.3 (C(6)), 26.5 (C(10)), 28.3 (C(26)/C(27)/C(28)), 28.3 (C(16)), 30.3 (C(5)), 31.2 (C(23)), 31.6 & 31.8 (C(2)), 32.7 (C(22)), 34.9 (C(20)), 35.4 (C(1)), 35.7 (C(8)), 37.0 (C(4)), 40.0 (C(12)), 40.3 (C(9)), 42.9 (C(13)), 56.2 (C(17)), 56.8 (C(14)), 80.0 (C(25)), 89.6 & 91.2 (C(3)), 173.9 (C(24)); δ_F (CDCl₃, 375 MHz) 181.9-182.3 (1F, q, J = 46.9 Hz, C(3)HF); LRMS ES+ [M+Na]⁺: 457.4 (25%); HRMS ES- calc for C₂₈H₄₈O₂F 435.3633, found 435.3625.

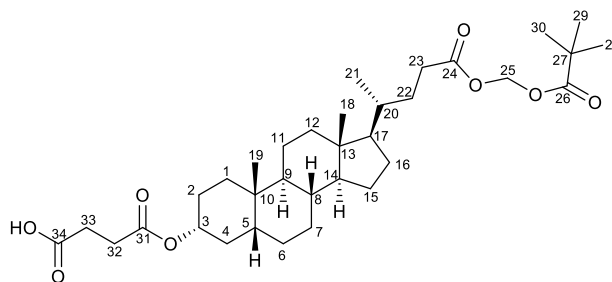
methyl(4R)-4-((3R,8R,9S,10S,13R,14S,17R)-3-hydroxy-10,13-dimethylhexadecahydro-1H-cyclopenta[a]phenanthren-17-yl)pentanoate (44)



44, a colourless crystalline solid (3.4 g, 8.7 mmol, 71%). M.p. 130 °C [Lit⁴²: 126-127 °C]; $[\alpha]_D^{25}$ +21.0 (c 2.31 in DCM); ν_{max}/cm^{-1} 3517br (O-H), 2932m (C-H), 2860m (C-H), 1733s (C=O), 1711s (C=O), 1703s (C=O); δ_H (CDCl₃, 400 MHz) 0.63 (3H, s, C(18)H₃), 0.90 (3H, d, J = 6 Hz, C(21)H₃), 0.91 (3H, s, C(19)H₃), 1.02-1.94 (27H, m), 2.21 (1H, ddd,

$J = 15.4$ Hz, 9.4 Hz, 6.2 Hz, $C(23)H_a$), 2.35 (1H, ddd, $J = 15.4$ Hz, 10 Hz, 5 Hz, $C(23)H_b$), 3.58 - 3.64 (1H, m, $C(3)H$), 3.66 (3H, s, $C(25)H$); δ_c ($CDCl_3$, 100 MHz) 12.2 ($C(18)$), 18.4 ($C(21)$), 21.0 ($C(11)$), 23.5 ($C(19)$), 24.3 ($C(15)$), 26.6 ($C(7)$), 27.3 ($C(6)$), 28.3 ($C(16)$), 30.7 ($C(2)$), 31.1 ($C(23)$), 31.2 ($C(22)$), 34.7 ($C(10)$), 35.5 ($C(20)$), 35.5 ($C(1)$), 36.0 ($C(8)$), 36.6 ($C(4)$), 40.3 ($C(12)$), 40.6 ($C(9)$), 42.2 ($C(5)$), 42.9 ($C(13)$), 51.6 ($C(25)$), 56.1 ($C(17)$), 56.6 ($C(14)$), 72.0 ($C(3)$), 174.9 ($C(24)$); LRMS ES+ $[M+Na]^+$: 413.3 (100%); HRMS ES+ calc for $C_{25}H_{42}O_3Na$ 413.3026 , found 413.3027 .

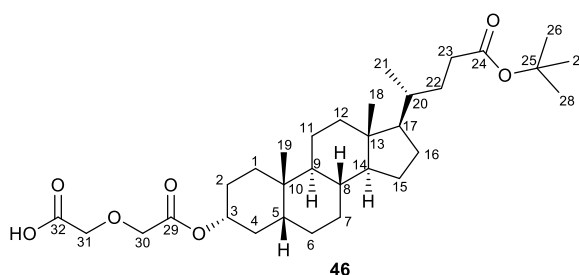
4-(((3*R*,8*R*,9*S*,10*S*,13*R*,14*S*,17*R*)-10,13-dimethyl-17-((*R*)-5-oxo-5-((pivaloyloxy)methoxy)pentan-2-yl)hexadecahydro-1*H*-cyclopenta[*a*]phenanthren-3-yl)oxy)-4-oxobutanoic acid (45**)**



General Procedure for compounds 49, 50, (51+52), 53, 54, 55, 56, 57, 58, 59: Compound **13** (0.30 g, 0.70 mmol)/**8** (0.34 g, 0.70 mmol)/**10** (0.29 g, 0.70 mmol) was dissolved in anhydrous DCM (20 mL). 2,2-dimethylsuccinic anhydride (0.45 g, 3.50 mmol) or the corresponding anhydride (3.50 mmol) and DMAP (0.26 g, 2.10 mmol) were added to the mixture with stirring, which was then left to react at room temperature for 2 days. The reaction progress was monitored by TLC. Upon reaction completion, the solvent was evaporated to dryness, the residue re-dissolved in Et_2O and washed with 1M HCl (2 x 20 mL), H_2O (4 x 20 mL) and saturated brine (2 x 20 mL). The organic phase was dried with $MgSO_4$, filtered and the solvent was evaporated under reduced pressure to yield **45**, a viscous colourless oil (0.22 g, 0.37 mmol, 99%, from 0.20 g of starting ester). M.p. 70 °C; $[\alpha]_D^{24} +17.4$ (c 1.27 in DCM); ν_{max}/cm^{-1} 2932m (C-H), 2864m (C-H), 1754s (C=O), 1731s (C=O); δ_H ($CDCl_3$, 400 MHz) 0.62 (3H, s, $C(18)H_3$), 0.88 (3H, d, $J = 6.8$ Hz, $C(21)H_3$), 0.91 (3H, s, $C(19)H_3$), 0.93-1.15 (7H, m), 1.19 (9H, s, $C(26)H_3$, $C(27)H_3$ & $C(28)H_3$), 1.30-1.97 (20H, m), 2.25 (1H, ddd, $J = 15.4$ Hz, 8.8 Hz, 6.8 Hz, $C(23)H_a$), 2.38 (1H, ddd, $J = 15.4$ Hz, 10 Hz, 5.2 Hz, $C(23)H_b$), 2.52 (4H, s, $C(32)H_2$ & $C(33)H_2$), 4.65-4.73 (1H, m, $C(3)H$), 5.72 (2H, s, $C(25)H_2$); δ_c ($CDCl_3$, 100 MHz) 12.2 ($C(18)$), 18.3

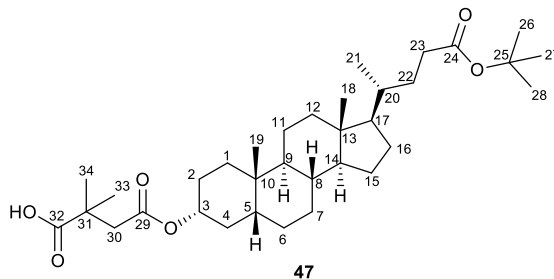
(C(21)), 20.9 (C(11)), 23.5 (C(19)), 24.3 (C(15)), 26.4 (C(7)), 26.7 (C(6)), 27.0 (C(28)/C(29)/C(30)), 27.1 (C(2)), 28.3 (C(16)), 30.1 (C(33)), 30.3 (C(32)), 30.8 (C(23)), 31.2 (C(22)), 32.3 (C(10)), 34.7 (C(20)), 35.1 (C(1)), 35.4 (C(8)), 35.9 (C(4)), 38.8 (C(27)), 40.2 (C(12)), 40.5 (C(9)), 42.0 (C(5)), 42.8 (C(13)), 56.2 (C(17)), 56.5 (C(14)), 74.8 (C(3)), 79.5 (C(25)), 172.8 (C(24)), 173.0 (C(34) & C(31)) 177.3 (C(26)); LRMS ES- $[M-H]^-$: 589.4 (100%); HRMS ES+ calc for $C_{34}H_{54}O_8Na$ 613.3711, found 613.3694.

2-(2-(((3R,8R,9S,10S,13R,14S,17R)-17-((R)-5-(tert-butoxy)-5-oxopentan-2-yl)-10,13-dimethylhexadecahydro-1H-cyclopenta[a]phenanthren-3-yl)oxy)-2-oxoethoxy)acetic acid (46)



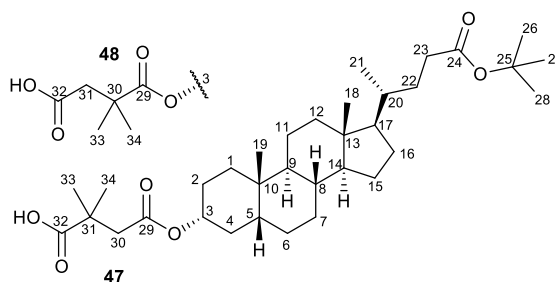
46, a colourless crystalline solid (0.19 g, 0.36 mmol, 48%); M.p. 154-156 °C; $[\alpha]_D^{20} +38.0$ (c 0.953 in DCM); ν_{max}/cm^{-1} 2932m (C-H), 2866m (C-H), 1719s (C=O acid); δ_H (CDCl₃, 400 MHz) 0.57 (3H, s, C(18)H₃), 0.83 (3H, d, J = 5.6 Hz, C(21)H₃), 0.87 (3H, s, C(19)H₃), 0.93-1.24 (15H, m), 1.37 (9H, s, C(26)H₃, C(27)H₃ & C(28)H₃), 1.60-1.94 (12H, m), 2.05 (1H, ddd, J = 12.4 Hz, 7.2 Hz, 4.8 Hz, C(23)H_a), 2.18 (1H, ddd, J = 12.4 Hz, 8 Hz, 4.4 Hz, C(23)H_b), 4.16 (4H, s, C(30)H₂ & C(31)H₂), 4.76-4.84 (1H, m, C(3)H); δ_C (CDCl₃, 100 MHz) 12.0 (C(18)), 18.3 (C(21)), 20.9 (C(11)), 23.3 (C(19)), 24.2 (C(15)), 26.5 (C(7)), 27.0 (C(6)), 27.2 (C(2)), 28.1 (C(26)/C(27)/C(28)), 28.2 (C(16)), 32.1 (C(23)), 32.6 (C(22)), 34.6 (C(4)), 34.9 (C(10)), 35.2 (C(1)), 35.3 (C(20)), 35.8 (C(8)), 40.1 (C(12)), 40.5 (C(9)), 41.9 (C(5)), 42.7 (C(13)), 56.1 (C(17)), 56.5 (C(14)), 69.8 (C(30)/C(31)), 76.5 (C(3)), 79.9 (C(25)), 170.9 (C(24)), 173.7 (C(29)/C(32)); LRMS ES- $[M-H]^-$: 547.4 (100%), ES+ $[M+3Na]^{3+}$: 619.4 (100%); HRMS ES- calc for $C_{32}H_{51}O_7$ 547.3640, found 547.3643.

4-(((3R,8R,9S,10S,13R,14S,17R)-17-((R)-5-(tert-butoxy)-5-oxopentan-2-yl)-10,13-dimethylhexadecahydro-1H-cyclopenta[a]phenanthren-3-yl)oxy)-2,2-dimethyl-4-oxobutanoic acid (47)



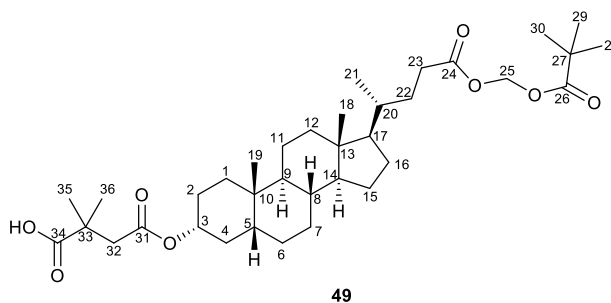
47, a colourless crystalline solid (0.03 g, 0.05 mmol, 21%, from 0.11 g, 0.26 mmol of (**47+48**)); $R_f = 0.35$ (hexane 4:1 ethyl acetate); m.p. 73-75 °C; $[\alpha]_D^{23} +28.3$ (c 1.09 in DCM); ν_{max}/cm^{-1} 2931m (C-H), 2866m (C-H), 1729s (C=O), 1704s (C=O); δ_H (CDCl₃, 400 MHz) 0.63 (3H, s, C(18)H₃), 0.90 (3H, d, J = 8 Hz, C(21)H₃), 0.91 (3H, s, C(19)H₃), 0.96-1.27 (10H, m), 1.29 (6H, s, C(33)H₃ & C(34)H₃), 1.31-1.42 (7H, m), 1.44 (9H, s, C(26)H₃, C(27)H₃ & C(28)H₃), 1.45-1.99 (10H, m), 2.11 (1H, ddd, J = 15 Hz, 8.4 Hz, 6 Hz, C(23)H_a), 2.25 (1H, ddd, J = 15 Hz, 10 Hz, 5.2 Hz, C(23)H_b), 2.57 (2H, s, C(30)H₂), 4.67-4.75 (1H, m, C(3)H); δ_C (CDCl₃, 100 MHz) 12.2 (C(18)), 18.4 (C(21)), 21.0 (C(11)), 23.5 (C(19)), 24.3 (C(15)), 25.4 (C(33)/C(34)), 26.5 (C(7)), 26.7 (C(6)), 27.1 (C(2)), 28.3 (C(26)/C(27)/C(28)), 28.3 (C(16)), 31.2 (C(23)), 32.3 (C(22)), 32.7 (C(10)), 34.7 (C(20)), 35.2 (C(1)), 35.4 (C(8)), 35.9 (C(4)), 40.3 (C(12)), 40.6 (C(9)), 42.1 (C(5)), 42.9 (C(13)), 44.6 (C(30)), 56.2 (C(17)), 56.6 (C(14)), 74.9 (C(3)), 80.0 (C(25)), 170.9 (C(29)), 173.9 (C(29)), 182.7 (C(32)); HSQC NMR: {¹H 2.57 ppm ; ¹³C 44.6 ppm; C(30)} Gem-dimethyl group on C(31); LRMS ES- [M-H]⁻: 559.5 (100%), ES+ [M+Na]⁺: 583.5 (25%) ; HRMS ES- calc for C₃₄H₅₆O₆Na 583.3969, found 583.3941.

4-(((3R,8R,9S,10S,13R,14S,17R)-17-((R)-5-(tert-butoxy)-5-oxopentan-2-yl)-10,13-dimethylhexadecahydro-1H-cyclopenta[a]phenanthren-3-yl)oxy)-2,2-dimethyl-4-oxobutanoic acid (47**(75%)+**48**(25%))**



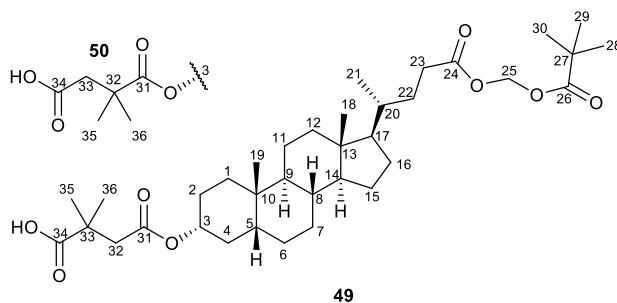
(**47**(75%)+**48**(25%)), a colourless crystalline solid (0.20 g, 0.36 mmol, 48%). M.p. 98 °C; $[\alpha]_D^{21} +50.3$ (c 0.93 in DCM); ν_{max}/cm^{-1} 2931m (C-H), 2864m (C-H), 1719s (C=O acid); δ_H (CDCl₃, 400 MHz) 0.57 (3H, s, C(18)H₃), 0.89 (3H, d, J = 8 Hz, C(21)H₃), 0.90 (3H, s, C(19)H₃), 0.95-1.25 (10H, m), 1.27 (1.5H (25%), d, J = 8 Hz, C(33)H₃ & C(34)H₃ of **48**(25%), 1.28 (4.5H, s, C(33)H₃ & C(34)H₃ of **47**(75%)), 1.32-1.42 (7H, m), 1.43 (9H, s, C(26)H₃, C(27)H₃ & C(28)H₃), 1.45-1.98 (10H, m), 2.05 (1H, ddd, J = 15.6 Hz, 8.8 Hz, 6.4 Hz, C(23)H_a), 2.18 (1H, ddd, J = 15.6 Hz, 10 Hz, 5.6 Hz, C(23)H_b), 2.54 (2H, s, C(30)H₂), 4.63-4.71 (1H, m, C(3)H); δ_C (CDCl₃, 100 MHz) 12.2 (C(18)), 18.4 (C(21)), 21.0 (C(11)), 23.5 (C(19)), 24.3 (C(15)), 25.4 (C(33)), 25.4 (C(34)), 26.5 (C(7)), 26.8 (C(6)), 27.2 (C(2)), 28.3 (C(26)/C(27)/C(28)), 29.8 (C(16)), 31.2 (C(23)), 32.2 (C(22)), 32.7 (C(10)), 34.8 (C(20)), 35.2 (C(1)), 35.5 (C(8)), 36.0 (C(4)), 40.3 (C(12)), 40.6 (C(9)), 42.1 (C(5)), 42.9 (C(13)), 44.6 (C(30)), 56.2 (C(17)), 56.6 (C(14)), 75.1 (C(3)), 80.0 (C(25)), 171.0 (C(24)), 175.9 (C(29)), 181.2 (C(32)); HSQC NMR: **47** {¹H 2.59 ppm; ¹³C 44.5 ppm; C(30)} Gem-dimethyl group on C(31), **48** {¹H 2.65 ppm; ¹³C 43.9 ppm; C(31)} Gem-dimethyl group on C(30); LRMS ES- [M-H]⁻: 559.5 (100%), ES+ [M+Na]⁺: 583.5 (100%); HRMS ES- calc for C₃₄H₅₅O₆ 559.4004, found 559.3999.

4-(((3*R*,8*R*,9*S*,10*S*,13*R*,14*S*,17*R*)-10,13-dimethyl-17-((*R*)-5-oxo-5-((pivaloyloxy)methoxy)pentan-2-yl)hexadecahydro-1*H*-cyclopenta[*a*]phenanthren-3-yl)oxy)-2,2-dimethyl-4-oxobutanoic acid (49**)**



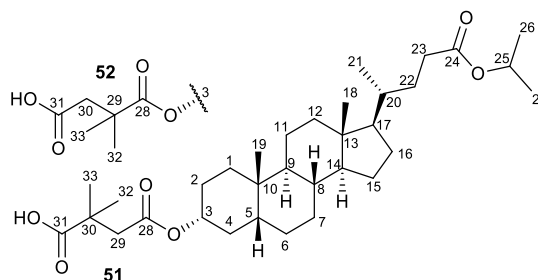
The mixture of (**49**+**50**) was subjected to column chromatography (hexane 2:1 ethyl acetate) to afford **49**, a colourless crystalline solid (57 mg, 0.09 mmol, 22%, from 260 mg, 0.41 mmol of (**49**+**50**)); R_f = 0.63 (hexane 2:1 ethyl acetate); m.p. 48 °C; $[\alpha]_D^{25}$ +50.8 (c 1.85 in DCM); ν_{max}/cm^{-1} 2927m (C-H), 2866m (C-H), 1752s (C=O), 1733s (C=O), 1703s (C=O); δ_H (CDCl₃, 400 MHz) 0.63 (3H, s, C(18)H₃), 0.90 (3H, d, J = 7.6 Hz, C(21)H₃), 0.91 (3H, s, C(19)H₃), 0.95-1.20 (7H, m), 1.21 (9H, s, C(28)H₃, C(29)H₃ & C(30)H₃), 1.24-1.28 (2H, m), 1.29 (6H, s, C(35)H₃ & C(36)H₃), 1.31-1.99 (18H, m), 2.26 (1H, ddd, J = 15.4 Hz, 8.8 Hz, 6.8 Hz, C(23)H_a), 2.38 (1H, ddd, J=15.4 Hz, 10 Hz, 5.2 Hz, C(23)H_b), 2.56 (2H, s, C(32)H₂), 4.67-4.75 (1H, m, C(3)H), 5.73 (2H, s, C(25)H₂); δ_C (CDCl₃, 100 MHz) 12.2 (C(18)), 18.4 (C(21)), 21.0 (C(11)), 23.5 (C(19)), 24.3 (C(15)), 25.4 (C(35)/C(36)), 26.5 (C(7)), 26.7 (C(6)), 27.0 (C(28)/C(29)/C(30)), 27.1 (C(16)), 28.3 (C(2)), 30.9 (C(23)), 31.2 (C(22)), 32.3 (C(10)), 34.7 (C(20)), 35.2 (C(1)), 35.4 (C(8)), 35.9 (C(4)), 38.9 (C(27)), 40.3 (C(12)), 40.6 (C(33)), 40.7 (C(9)), 42.1 (C(5)), 42.9 (C(13)), 44.6 (C(32)), 56.1 (C(17)), 56.6 (C(14)), 74.9 (C(3)), 79.5 (C(25)), 170.8 (C(31)), 173.0 (C(24)), 177.3 (C(34)), 182.8 (C(26)); HSQC NMR: **49** {¹H 2.59 ppm; ¹³C 44.5 ppm; C(32)} Gem-dimethyl group on C(33); LRMS ES- [M-H]⁻: 617.5 (55%); HRMS ES-calc for C₃₆H₅₇O₈ 617.4059, found 617.4054.

4-(((3*R*,8*R*,9*S*,10*S*,13*R*,14*S*,17*R*)-10,13-dimethyl-17-((*R*)-5-oxo-5-((pivaloyloxy) methoxy)pentan-2-yl)hexadecahydro-1*H*-cyclopenta[*a*]phenanthren-3-yl)oxy)-3,3-dimethyl-4-oxobutanoic acid (49**(50%)+**50**(50%))**



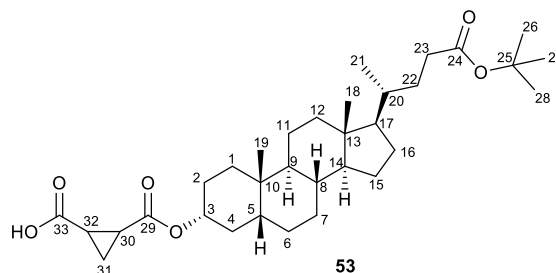
49(50%)+**50**(50%), a colourless crystalline solid (23 mg, 0.04 mmol, 9%, from 260 mg, 0.41 mmol of (**49**(75%)+**50**(25%)); $R_f = 0.53$ (hexane 2:1 ethyl acetate). M.p. 35 °C; $[\alpha]_D^{24} +23.8$ (c 0.94 in DCM); ν_{max}/cm^{-1} 2931m (C-H), 2867m (C-H), 1754s (C=O), 1732s (C=O), 1707s (C=O); δ_H (CDCl₃, 400 MHz) 0.63 (3H, s, C(18)H₃), 0.87 (3H, d, J = 6.8 Hz, C(21)H₃), 0.89 (3H, s, C(19)H₃), 0.93-1.19 (7H, m), 1.21 (9H, s, C(28)H₃, C(29)H₃ & C(30)H₃), 1.24 (3H (50%), d, J = 7.2 Hz, C(35)H₃ & C(36)H₃ of **50**(50%)), 1.25 (3H (50%), s, C(35)H₃ & C(36)H₃ of **49**(50%)), 1.29-1.98 (20H, m), 2.26 (1H, ddd, J = 15.4 Hz, 8.8 Hz, 6.8 Hz, C(23)H_α), 2.39 (1H, ddd, J=15.4 Hz, 10 Hz, 5.2 Hz, C(23)H_β), 2.57 (1H (50%), s, C(32)H₂ of **49**(50%)), 2.62 (1H (50%), s, C(32)H₂ of **50**(50%)), 4.67-4.75 (1H, m, C(3)H), 5.74 (2H, s, C(25)H₂); δ_C (CDCl₃, 100 MHz) 12.2 (C(18)), 18.4 (C(21)), 21.0 (C(11)), 22.8 (C(32)), 23.5 (C(19)), 24.3 (C(15)), 25.3 (C(35)), 25.5 (C(36)), 26.5 (C(7)), 26.6 (C(6)), 27.0 (C(28)/C(29)/C(30)), 27.2 (C(16)), 28.3 (C(2)), 30.9 (C(23)), 31.2 (C(22)), 31.7 (C(33)), 32.1 (C(10)), 34.7 (C(20)), 35.2 (C(1)), 35.5 (C(8)), 35.9 (C(4)), 38.9 (C(27)), 40.3 (C(12)), 40.5 (C(9)), 42.1 (C(5)), 42.9 (C(13)), 56.1 (C(17)), 56.6 (C(14)), 74.9 (C(3)), 79.5 (C(25)), 170.8 (C(31)), 171.3 (C(34)), 173.0 (C(24)), 177.3 (C(26)); HSQC NMR: **49** {¹H 2.59 ppm; ¹³C 44.5 ppm; C(32)} Gem-dimethyl group on C(33), **50** {¹H 2.64 ppm; ¹³C 43.9 ppm; C(33)} Gem-dimethyl group on C(32); LRMS ES- [M-H]⁻: 617.5 (100%); HRMS ES- calc for C₃₆H₅₇O₈ 617.4059, found 617.4054.

4-(((3*R*,8*R*,9*S*,10*S*,13*R*,14*S*,17*R*)-17-((*R*)-5-isopropoxy-5-oxopentan-2-yl)-10,13-dimethylhexadecahydro-1*H*-cyclopenta[*a*]phenanthren-3-yl)oxy)-2,2-dimethyl-4-oxobutanoic acid (51+52**)**



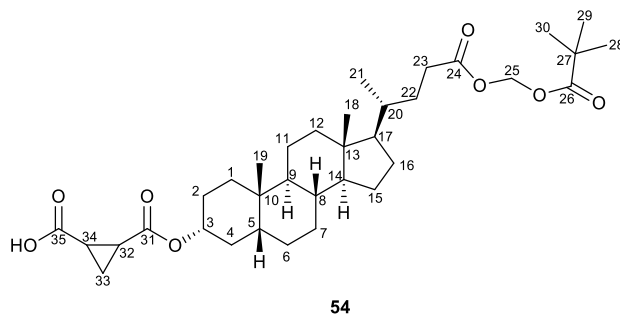
(51+52) a colourless crystalline solid (0.23 g, 0.42 mmol, 60%). M.p. 118-123 °C; $[\alpha]_D^{22} +33.9$ (c 4.74 in DCM); ν_{max}/cm^{-1} 2927m (C-H), 2866m (C-H), 1272s (C=O), 1707s (C=O); δ_H (CDCl₃, 400 MHz) 0.61 (3H, s, C(18)H₃), 0.88-0.9 (3H, d, J = 6 Hz, C(21)H₃), 0.90 (3H, s, C(19)H₃), 0.93-1.18 (7H, m), 1.20 (6H, d, J = 4.8 Hz, C(26)H₃ & C(27)H₃), 1.26 (1.5H (25%), d, J = 7.6 Hz, C(35)H₃ & C(36)H₃ of **52**(25%)), 1.27 (4.5H (75%), s, C(35)H₃ & C(36)H₃ of **51**(75%)), 1.27-1.98 (20H, m), 2.15 (1H, ddd, J = 15.2 Hz, 8.4 Hz, 5.6 Hz, C(23)H_a), 2.28 (1H, ddd, J = 15.2 Hz, 10 Hz, 5.2 Hz, C(23)H_b), 2.56 (2H, s, C(29)H₂), 4.65-4.73 (1H, m, C(3)H); δ_C (CDCl₃, 100 MHz) 12.1 (C(18)), 18.4 (C(21)), 20.9 (C(11)), 21.9 (C(26)/C(27)), 23.4 (C(19)), 24.3 (C(15)), 25.2 (C(32)), 25.3 (C(33)), 26.4 (C(7)), 26.6 (C(6)), 27.1 (C(2)), 28.2 (C(16)), 31.1 (C(22)), 31.7 (C(23)), 32.2 (C(10)), 34.7 (C(20)), 35.1 (C(1)), 35.4 (C(8)), 35.9 (C(4)), 40.2 (C(12)), 40.5 (C(30)), 40.6 (C(9)), 42.0 (C(5)), 42.8 (C(13)), 44.5 (C(29)), 56.1 (C(17)), 56.5 (C(14)), 67.4 (C(25)), 74.8 (C(3)), 170.7 (C(28)), 174.0 (C(24)), 183.3 (C(31)); LRMS ES- [M-H]⁻: 545.5 (100%); HRMS ES- calc for C₃₃H₅₃O₆ 545.3848, found 545.3849.

2-((((3*R*,8*R*,9*S*,10*S*,13*R*,14*S*,17*R*)-17-((*R*)-5-(*tert*-butoxy)-5-oxopentan-2-yl)-10,13-dimethylhexadecahydro-1*H*-cyclopenta[*a*]phenanthren-3-yl)oxy)carbonyl)cyclopropane-1-carboxylic acid (53**)**



53 a colourless crystalline solid (0.23 g, 0.43 mmol, 61%). M.p. 120 °C; $[\alpha]_D^{20} +43.2$ (c 1.07 in DCM); ν_{max}/cm^{-1} 2932m (C-H), 2865m (C-H), 1721s (C=O); δ_H (CDCl₃, 400 MHz) 0.63 (3H, s, C(18)H₃), 0.89 (3H, d, J = 6.4 Hz, C(21)H₃), 0.91 (3H, s, C(19)H₃), 0.96-1.39 (17H, m), 1.43 (9H, s, C(26)H₃, C(27)H₃ & C(28)H₃), 1.50-1.98 (10H, m), 2.01-2.13 (2H, m, C(30)H & C(32)H), 2.11 (1H, ddd, J = 15.4 Hz, 9 Hz, 6 Hz, C(23)H_a), 2.25 (1H, ddd, J = 15.4 Hz, 10 Hz, 5 Hz, C(23)H_b), 4.71-4.79 (1H, m, C(3)H); δ_C (CDCl₃, 100 MHz) 12.2 (C(18)), 18.4 (C(21)), 21.0 (C(11)), 21.7 (C(30)), 22.8 (C(32)), 23.5 (C(19) & C(31)), 24.3 (C(15)), 26.5 (C(7)), 26.6 (C(6)), 27.2 (C(2)), 28.3 (C(26)/C(27)/C(28)), 29.8 (C(16)), 31.2 (C(23)), 32.2 (C(22)), 32.7 (C(10)), 34.7 (C(20)), 35.1 (C(1)), 35.4 (C(8)), 35.9 (C(4)), 40.3 (C(12)), 40.6 (C(9)), 42.1 (C(5)), 42.9 (C(13)), 56.2 (C(17)), 56.6 (C(14)), 75.9 (C(3)), 80.0 (C(25)), 170.2 (C(29)), 173.9 (C(29)), 175.1 (C(33)); LRMS ES- [M-H]⁻: 543.4 (100%); HRMS ES- calc for C₃₃H₅₁O₆ 543.3691, found 543.3693.

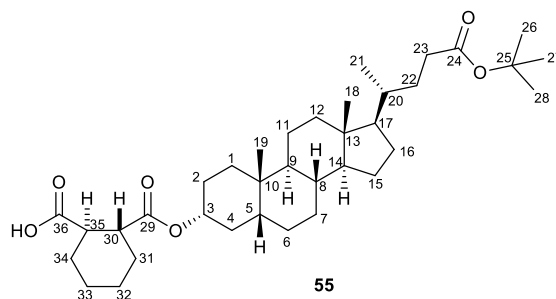
2-((((3*R*,8*R*,9*S*,10*S*,13*R*,14*S*,17*R*)-10,13-dimethyl-17-((*R*)-5-oxo-5-((pivaloyloxy)methoxy)pentan-2-yl)hexadecahydro-1*H*-cyclopenta[*a*]phenanthren-3-yl)oxy)carbonyl)cyclopropane-1-carboxylic acid (54**)**



54, a viscous colourless oil (0.16 g, 0.26 mmol, 63%, from 0.20 g of starting ester **8**). M.p. 53 °C; $[\alpha]_D^{25} +37.7$ (c 1.14 in DCM); ν_{max}/cm^{-1} 2930m (C-H), 2866m (C-H), 1738s

(C=O), 1703s (C=O); δ_H (CDCl₃, 400 MHz) 0.62 (3H, s, C(18)H₃), 0.89 (3H, d, J = 6.8 Hz, C(21)H₃), 0.90 (3H, s, C(19)H₃), 0.93-1.18 (7H, m), 1.19 (9H, s, C(28)H₃, C(29)H₃ & C(30)H₃), 1.24-1.62 (14H, m), 1.65 (2H, m, C(32)H & C(34)H), 1.76-1.96 (6H, m), 2.00-2.11 (2H, m, C(33)H₂), 2.25 (1H, ddd, J = 15.4 Hz, 8.8 Hz, 6.8 Hz, C(23)H_a), 2.37 (1H, ddd, J=15.4 Hz, 10 Hz, 5.2 Hz, C(23)H_b), 4.67-4.75 (1H, m, C(3)H), 5.72 (2H, s, C(25)H₂); δ_C (CDCl₃, 100 MHz) 12.1 (C(18)), 18.3 (C(21)), 20.9 (C(11)), 21.5 (C(32)), 22.8 (C(34)), 23.4 (C(19)), 24.3 (C(15)), 26.4 (C(7)), 26.6 (C(6)), 27.0 (C(28)/C(29)/C(30)), 27.0 (C(2)), 27.1 (C(33)), 28.3 (C(16)), 30.8 (C(23)), 31.1 (C(22)), 32.1 (C(10)), 34.7 (C(20)), 35.1 (C(1)), 35.4 (C(8)), 35.9 (C(4)), 38.8 (C(27)), 40.2 (C(12)), 40.5 (C(9)), 42.0 (C(5)), 42.8 (C(13)), 56.1 (C(17)), 56.5 (C(14)), 75.7 (C(3)), 79.5 (C(25)), 169.9 (C(31)), 173.0 (C(24)), 175.4 (C(35)) 177.3 (C(26)); LRMS ES- [M-H]⁻: 601.5 (100%); HRMS ES- calc for C₃₅H₅₃O₈ 601.3746, found 601.3742.

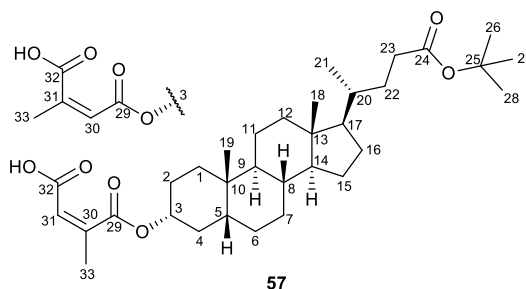
(1*R*,2*R*)-2-((((3*R*,8*R*,9*S*,10*S*,13*R*,14*S*,17*R*)-17-((*R*)-5-(*tert*-butoxy)-5-oxopent-2-yl)-10,13-dimethylhexadecahydro-1*H*-cyclopenta[*a*]phenanthren-3-yl)oxy)carbonyl) cyclohexane-1-carboxylic acid (55**)**



55, a colourless crystalline solid (0.81 g, 1.4 mmol, 99%, from 0.6058 g, 1.4 mmol of starting material **13**). M.p. 91-92 °C; $[\alpha]_D^{23} +24.7$ (c 3.52 in DCM); δ_H (CDCl₃, 400 MHz) 0.64 (3H, s, C(18)H₃), 0.91 (3H, d, J = 7.6 Hz, C(21)H₃), 0.92 (3H, s, C(19)H₃), 0.96-1.33 (15H, m), 1.44 (9H, s, C(26)H₃, C(27)H₃ & C(28)H₃), 1.60-1.98 (12H, m), 2.12 (1H, ddd, J = 15.4 Hz, 7.2 Hz, 6 Hz, C(23)H_a), 2.26 (1H, ddd, J = 15.4 Hz, 10 Hz, 5.6 Hz, C(23)H_b), 2.50-2.68 (1H, m, C(30)H), 2.79-2.86 (1H, m, C(35)H), 4.70-4.78 (1H, m, C(3)H); δ_C (CDCl₃, 100 MHz) 12.2 (C(18)), 18.5 (C(21)), 21.0 (C(11)), 23.5 (C(19)), 23.5 (C(32)), 24.1 (C(33)), 24.4 (C(15)), 26.5 (C(7)), 26.7 (C(6)), 27.2 (C(2)), 28.3 (C(26)/C(27)/C(28)), 28.4 (C(16)), 29.0 (C(31)), 31.2 (C(23)), 32.2 (C(22)), 32.7 (C(10)), 34.8 (C(20)), 35.2 (C(1)), 35.5 (C(8)), 36.0 (C(4)), 40.3 (C(12)), 40.6 (C(9)), 42.1 (C(5)), 42.9 (C(13)), 44.6 (C(35)), 45.0 (C(30)), 56.2 (C(17)), 56.6 (C(14)), 74.8 (C(3)), 80.0 (C(25)), 173.2 (C(29)),

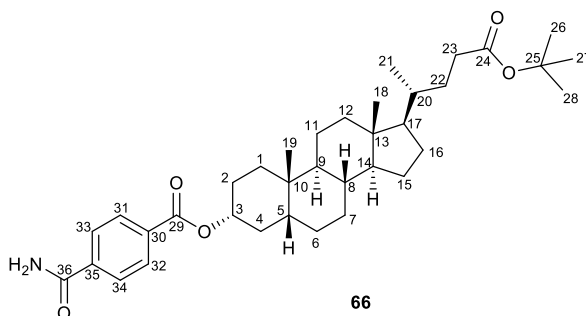
173.9 (C(24)), 174.6 (C(36)); LRMS ES- $[M-H]^-$: 585.5 (100%), ES+ $[M+Na]^+$: 609.4 (100%); HRMS ES- calc for $C_{36}H_{58}O_6Na$ 609.4126, found 609.4127.

(Z)-4-(((3R,8R,9S,10S,13R,14S,17R)-17-((R)-5-(tert-butoxy)-5-oxopentan-2-yl)-10,13-dimethylhexadecahydro-1H-cyclopenta[a]phenanthren-3-yl)oxy)-2-methyl-4-oxobut-2-enoic acid (57)



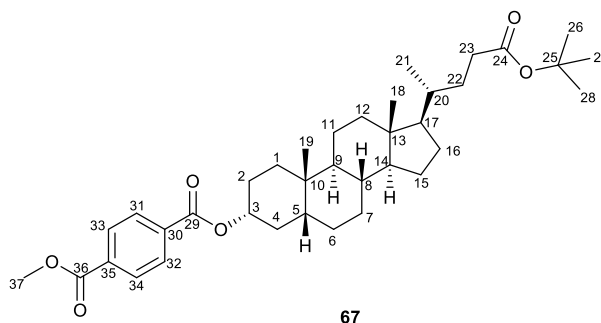
Additional column chromatography was required to isolate the compound. The silica was washed through with 500 mL of hexane 2:1 ethyl acetate, then 200 mL of pure ethyl acetate. A pink compound started separating from the colourful mixture when ethyl acetate was passed through the silica. The pink fraction of silica was carefully collected, suspended in MeOH (50 mL) and then evaporated to dryness to yield compound **57**, a pink crystalline solid (46.2 mg, 0.08 mmol, 12%); $R_f = 0$ (hexane 2:1 ethyl acetate); m.p. 180-182 °C; $[\alpha]_D^{22} +60.1$ (c 1.08 in DCM); ν_{max}/cm^{-1} 2929m (C-H), 2866m (C-H), 1728s (C=O), 1643m (C=C); δ_H (CD_3OD , 500 MHz) 0.63 (3H, s, C(18) H_3), 0.94 (3H, d, J = 5.6 Hz, C(21) H_3), 0.97 (3H, s, C(19) H_3), 1.01-1.44 (15H, m), 1.45 (9H, s, C(26) H_3 , C(27) H_3 & C(28) H_3), 1.48-2.03 (12H, m), 2.11 (1H, m, C(23) H_a), 2.26 (1H, ddd, J = 14.5 Hz, 9.5 Hz, 5.5 Hz, C(23) H_b), 4.66-4.74 (1H, m, C(3) H), 5.39 (1H, s, C(30) H); δ_C (CD_3OD , 125 MHz) 12.5 (C(18)), 18.7 (C(21)), 22.0 (C(33)), 22.0 (C(11)), 23.9 (C(19)), 25.2 (C(15)), 27.5 (C(7)), 27.6 (C(6)), 28.2 (C(2)), 28.3 (C(26)/C(27)/C(28)), 29.3 (C(16)), 32.4 (C(23)), 33.4 (C(22)), 33.5 (C(10)), 35.7 (C(20)), 36.2 (C(1)), 36.6 (C(8)), 37.2 (C(4)), 41.4 (C(12)), 41.7 (C(9)), 43.4 (C(5)), 43.9 (C(13)), 57.5 (C(17)), 57.7 (C(14)), 75.5 (C(3)), 81.3 (C(25)), 114.2 & 114.3 (C(30)) 157.1 (C(31)) 167.0 (C(29)), 175.5 (C(24)), 177.9 (C(32)); HSQC NMR { 1H 5.50 ppm; ^{13}C 112.74 ppm} methyl group on C(30), { 1H 5.50 ppm; ^{13}C 113.67 ppm} methyl group on C(31); LRMS ES- $[M-H]^-$: 543.5 (100%); HRMS ES- calc for $C_{33}H_{51}O_6$ 543.3691, found 543.3697.

(3R,8R,9S,10S,13R,14S,17R)-17-((R)-5-(tert-butoxy)-5-oxopentan-2-yl)-10,13-dimethylhexadecahydro-1H-cyclopenta[a]phenanthren-3-yl 4-carbamoylbenzoate (66)



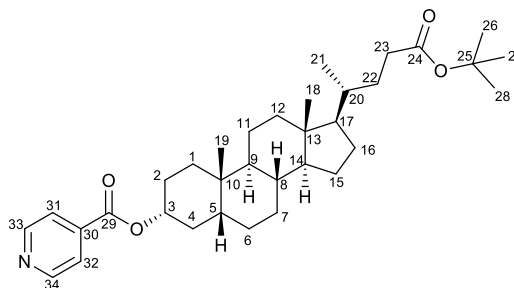
General Procedure for compounds 66, 67, 68, 69: Compound **13** (0.30 g, 0.693 mmol) was dissolved in dry DCM (8 mL). The corresponding acid (0.850 mmol) and DMAP (8.43 mg, 0.069 mmol) were added and the reaction mixture was cooled to ice-bath temperature. EDCI (0.2109 g, 1.100 mmol) was added in portions and stirring under N₂ atmosphere was continued for a further 30 min at ice-bath temperature. If the starting material had not yet been completely dissolved (**66**), addition of NEt₃ (2 mL) was proceeded, upon which complete dissolution was observed. The mixture was then allowed to warm to room temperature, at which it was stirred for a further 3 hours. The solvent was removed under reduced pressure and the residue subjected to column chromatography (hexane 2:1 ethyl acetate). A colourless crystalline product (**66**) was obtained (0.25 g, 0.43 mmol, 62%). M.p. 242-244 °C; $[\alpha]_D^{20} +20.7 \text{ dm}^{-1} \cdot \text{cm}^3 \cdot \text{g}^{-1}$ (c 0.65 g.L⁻¹ in DCM); $\nu_{\text{max}}/\text{cm}^{-1}$ 3427wk (N-H), 2927m (C-H), 2852m (C-H), 1722s (C=O), 1688s (C=O); δ_{H} (CDCl₃, 400 MHz) 0.65 (3H, s, C(18)H₃), 0.90 (3H, d, J = 6.8 Hz, C(21)H₃), 0.96 (3H, s, C(19)H₃), 1.00-1.40 (14H, m), 1.44 (9H, s, C(26)H₃, C(27)H₃ & C(28)H₃), 1.46-2.03 (13H, m), 2.13 (1H, ddd, J = 15.2 Hz, 8.4 Hz, 5.6 Hz, C(23)H_a), 2.25 (1H, ddd, J = 15.2 Hz, 10 Hz, 5.2 Hz, C(23)H_b), 4.98 (1H, tt, J = 11.2 Hz, 4.6 Hz, C(3)H), 5.90 (1H, s, NHH_a), 6.20 (1H, s, NHH_b), 7.85-7.87 (2H, m, C(31)H & C(32)H), 8.10-8.12 (2H, m, C(33)H & C(34)H); δ_{C} (CDCl₃, 100 MHz) 12.2 (C(18)), 18.4 (C(21)), 21.0 (C(11)), 23.5 (C(19)), 24.3 (C(15)), 26.5 (C(7)), 26.9 (C(6)), 27.2 (C(2)), 28.3 (C(26)/C(27)/C(28)), 28.3 (C(16)), 31.2 (C(23)), 32.5 (C(22)), 32.7 (C(1)), 34.8 (C(10)), 35.2 (C(4)), 35.4 (C(20)), 36.0 (C(8)), 40.3 (C(12)), 40.6 (C(9)), 42.1 (C(5)), 42.9 (C(13)), 56.2 (C(17)), 56.6 (C(14)), 75.8 (C(3)), 80.0 (C(25)), 127.4 (C(33)/C(34)), 130.0 (C(31)/C(32)), 134.1 (C(30)), 137.0 (C(35)), 165.4 (C(29)), 168.6 (C(36)), 173.9 (C(24)); LRMS ES- [M-C₄H₉]⁻: 523.4 (100%), ES+ [M+Na]⁺: 602.4 (100%); HRMS ES+ calc for C₃₆H₅₃O₅NNa 602.3816, found 602.3797.

(3*R*,8*R*,9*S*,10*S*,13*R*,14*S*,17*R*)-17-((*R*)-5-(*tert*-butoxy)-5-oxopentan-2-yl)-10,13-dimethylhexadecahydro-1*H*-cyclopenta[*a*]phenanthren-3-yl isonicotinate (67**)**



67, a colourless viscous liquid (0.32 g, 0.60 mmol, 90%, from 0.29 g, 0.67 mmol of starting material **13**). M.p. 143-144 °C; $[\alpha]_D^{20} +41.6$ (c 1.79 in DCM); ν_{max}/cm^{-1} 2927m (C-H), 2866m (C-H), 1715s (C=O); δ_H (CDCl₃, 400 MHz) 0.62 (3H, s, C(18)H₃), 0.92 (3H, d, J = 5.2 Hz, C(21)H₃), 0.96 (3H, s, C(19)H₃), 0.99-1.41 (13H, m), 1.44 (9H, s, C(26)H₃, C(27)H₃ & C(28)H₃), 1.47-2.04 (14H, m), 2.09 (1H, ddd, J = 15.5 Hz, 9 Hz, 6 Hz, C(23)H_a), 2.22 (1H, ddd, J = 15.5 Hz, 10 Hz, 5.2 Hz, C(23)H_b), 3.95 (3H, s, C(37)H), 4.96 (1H, tt, J = 11.2 Hz, 6.6Hz, C(3)H), 7.82 (2H, dd, J = 4.4 Hz, 1.2 Hz, C(31)H & C(32)H), 8.73 (2H, dd, J = 4 Hz, 1.4 Hz, C(33)H & C(34)H); δ_C (CDCl₃, 100 MHz) 12.1 (C(18)), 18.4 (C(21)), 21.0 (C(11)), 23.4 (C(19)), 24.2 (C(15)), 26.4 (C(7)), 26.7 (C(6)), 27.1 (C(2)), 28.2 (C(26)/C(27)/C(28)), 28.3 (C(16)), 31.1 (C(23)), 32.3 (C(22)), 32.6 (C(1)), 34.7 (C(10)), 35.1 (C(4)), 35.4 (C(20)), 35.9 (C(8)), 40.2 (C(12)), 40.6 (C(9)), 42.0 (C(5)), 42.8 (C(13)), 56.2 (C(17)), 56.6 (C(14)), 76.1 (C(3)), 79.9 (C(25)), 122.9 (C(31)/C(32)), 138.1 (C(30)), 150.6 (C(33)/C(34)), 164.6 (C(29)), 173.7 (C(24)); LRMS ES+ [M+Na]⁺: 560.4 (100%); HRMS ES+ calc for C₃₄H₅₂NO₄ 538.3891, found 538.3877.

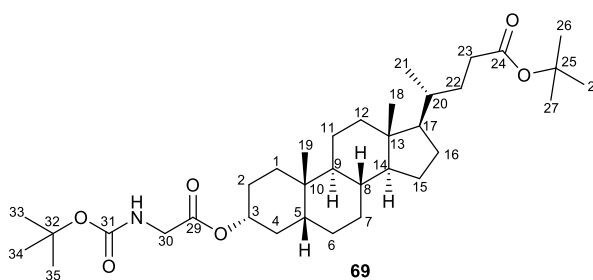
(3*R*,8*R*,9*S*,10*S*,13*R*,14*S*,17*R*)-17-((*R*)-5-(*tert*-butoxy)-5-oxopentan-2-yl)-10,13-dimethylhexadecahydro-1*H*-cyclopenta[*a*]phenanthren-3-yl methyl terephthalate (68)



68

68, a colourless crystalline solid (0.45 g, 0.75 mmol, 54%, from 0.60 g, 1.39 mmol of starting material **13**). M.p. 143-144 °C; $[\alpha]_D^{21} +42.2$ (c 1.09 in DCM); ν_{max}/cm^{-1} 2926m (C-H), 2866m (C-H), 1714s (C=O); δ_H (CDCl₃, 400 MHz) 0.65 (3H, s, C(18)H₃), 0.88 (3H, d, J = 5.2 Hz, C(21)H₃), 0.93 (3H, s, C(19)H₃), 0.95-1.39 (14H, m), 1.41 (9H, s, C(26)H₃, C(27)H₃ & C(28)H₃), 1.41-2.00 (13H, m), 2.12 (1H, ddd, J = 12 Hz, 6.8 Hz, 4.8 Hz, C(23)H_a), 2.26 (1H, ddd, J = 12 Hz, 8 Hz, 4 Hz, C(23)H_b), 3.95 (3H, s, C(37)H), 4.95-5.03 (1H, m, C(3)H), 7.81-7.82 (2H, m, C(31)H, C(32)H), 8.72-8.74 (2H, m, C(33)H & C(34)H); δ_C (CDCl₃, 100 MHz) 12.2 (C(18)), 18.5 (C(21)), 21.0 (C(11)), 23.5 (C(19)), 24.3 (C(15)), 26.5 (C(7)), 26.8 (C(6)), 27.2 (C(2)), 28.3 (C(26)/C(27)/C(28)), 28.4 (C(16)), 31.2 (C(23)), 32.5 (C(22)), 32.7 (C(1)), 34.8 (C(10)), 35.2 (C(4)), 35.5 (C(20)), 36.0 (C(8)), 40.3 (C(12)), 40.7 (C(9)), 42.1 (C(5)), 42.9 (C(13)), 52.6 (C(37)), 56.2 (C(17)), 56.6 (C(14)), 75.8 (C(3)), 80.0 (C(25)), 129.6 (C(33)/C(34)), 129.6 (C(31)/C(32)), 133.8 (C(35)), 134.9 (C(30)), 165.5 (C(29)), 166.5 (C(36)), 173.9 (C(24)); LRMS ES+ $[M+H]^+$: 595.4 (100%); HRMS ES- calc for C₃₇H₅₅O₆ 595.3993, found 595.3990.

***tert*-butyl (4*R*)-4-((3*R*,8*R*,9*S*,10*S*,13*R*,14*S*,17*R*)-3-(((*tert*-butoxycarbonyl)glycyl)oxy)-10,13 -dimethylhexadecahydro-1*H*-cyclopenta[*a*]phenanthren-17-yl)pentanoate (69)**



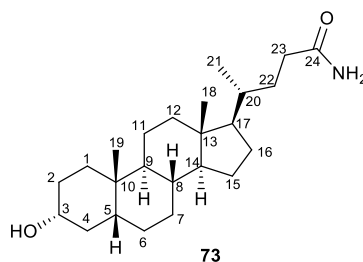
69

69, a glassy colourless solid (0.48 g, 0.81 mmol, 87%, from 0.40 g, 0.92 mmol of starting material **13**); m.p. 228-230 °C; $[\alpha]_D^{26} +23.4$ (c 1.98 in DCM); m.p. 52 °C; ν_{max}/cm^{-1}

5.0 - Experimental

3379m (N-H), 2931m (C-H), 2866m (C-H), 1720s (C=O); δ_H (CDCl₃, 400 MHz) 0.58 (3H, s, C(18)H₃), 0.84 (3H, d, J = 6.4 Hz, C(21)H₃), 0.87 (3H, s, C(19)H₃), 0.89-1.36 (16H, m), 1.38 (9H, s, C(33)H₃, C(34)H₃ & C(35)H₃), 1.39 (9H, s, C(26)H₃, C(27)H₃ & C(28)H₃), 1.40-1.99 (11H, m), 2.05 (1H, ddd, J=15.4 Hz, 8.8 Hz, 6.8 Hz, C(23)H_a), 2.18 (1H, ddd, J=15.4 Hz, 9.6 Hz, 5.2 Hz, C(23)H_b), 3.79 (2H, d, J= 5.2 Hz, C(30)H₂), 4.68-4.76 (1H, m, C(3)H), 5.09 (1H, t, J = 5.2 Hz, C(30)NH); δ_C (CDCl₃, 100 MHz) 12.0 (C(18)), 18.3 (C(21)), 20.8 (C(11)), 23.3 (C(19)), 24.2 (C(15)), 26.3 (C(7)), 26.6 (C(6)), 27.0 (C(2)), 28.1 (C(26)/C(27)/C(28)), 28.2 (C(16)), 28.3 (C(33)/C(34)/C(35)), 31.1 (C(23)), 32.2 (C(22)), 32.5 (C(10)), 34.6 (C(20)), 35.0 (C(1)), 35.3 (C(8)), 35.8 (C(4)), 40.1 (C(12)), 40.4 (C(9)), 41.9 (C(5)), 42.7 (C(30)), 42.7 (C(13)), 56.1 (C(17)), 56.5 (C(14)), 75.5 (C(3)), 79.7 (C(32)), 79.8 (C(25)), 155.7 (C(31)), 169.8 (C(29)), 173.6 (C(24)); LRMS ES+ [M+Na]⁺: 612.6 (100%); HRMS ES+ calc for C₃₅H₅₉O₆NNa 612.4235, found 612.4208.

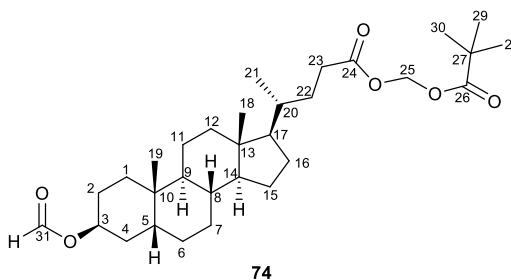
(4R)-4-((3R,8R,9S,10S,13R,14S,17R)-3-hydroxy-10,13-dimethylhexadecahydro-1H-cyclopenta[a]phenanthren-17-yl)pentanamide (73)



Lithocholic acid **5** (1.00 g, 2.65 mmol) was dissolved in chloroform (13 mL) and triethylamine (1.00 mL, 7.17 mmol) was added to the solution. The mixture was cooled to 0°C before slow dropwise addition of ethyl chloroformate (1.00 mL, 10.46 mmol) was performed, while keeping the temperature monitored with a thermometer. The mixture was allowed to react for 15 min, after which cold ammonium hydroxide (1.00 mL, 35% w/w, 8.99 mmol, 5-10 °C) was added to it. The precipitating colourless crystals were filtered and dried to yield the corresponding amide compound **73** as a colourless crystalline solid (0.81 g, 2.16 mmol, 81%). M.p.: 212 °C [Lit⁴³: 214-216 °C]; $[\alpha]_D^{22} +27.8$ (c 0.72 in DCM); ν_{max}/cm^{-1} 3440m & 3360m (N-H), 2933m (C-H), 2865m (C-H), 1666s (C=O); δ_H (CD₃OD, 400 MHz) 0.71 (3H, s, C(18)H₃), 0.96 (3H, s, C(19)H₃), 0.98 (3H, d, J = 6.4 Hz, C(21)H₃), 1.00-2.06 (27H, m), 2.09-2.16 (1H, m, C(23)H_a), 2.26 (1H, ddd, J = 15.4 Hz, 10.4 Hz, 5.2 Hz, C(23)H_b), 3.55 (1H, tt, J = 11.2 Hz, 4.8 Hz, C(3)H); δ_C (CDCl₃, 100 MHz) 12.5 (C(18)), 18.8 (C(21)), 21.9 (C(11)), 23.9 (C(19)), 25.3 (C(15)), 27.7 (C(7)), 28.4 (C(6)), 29.2 (C(16)), 31.2 (C(2)), 33.2 (C(23)), 33.5 (C(22)), 35.7 (C(10)), 36.5

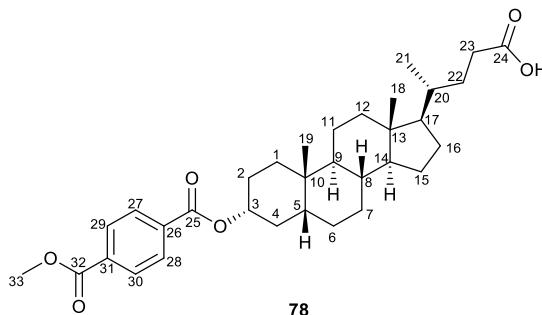
(C(20)), 36.9 (C(1)), 37.2 (C(8)), 37.2 (C(4)), 41.5 (C(12)), 41.9 (C(9)), 43.5 (C(5)), 43.9 (C(13)), 57.4 (C(17)), 57.9 (C(14)), 72.4 (C(3)), 179.8 (C(24)); LRMS ES+ $[M+Na]^+$: 398.3 (100%); HRMS ES+ calc for $C_{24}H_{41}O_2NNa$ 398.3030, found 398.3013.

(pivaloyloxy)methyl(4*R*)-4-((3*S*,8*R*,9*S*,10*S*,13*R*,14*S*,17*R*)-3-(formyloxy)-10,13-dimethyl hexadecahydro-1*H*-cyclopenta[*a*]phenanthren-17-yl)pentanoate (74)



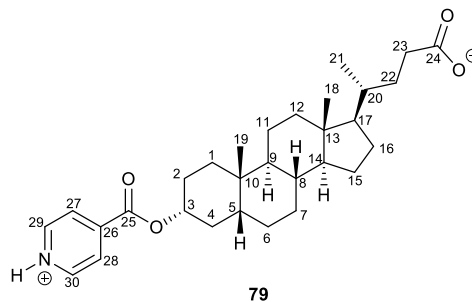
74, a viscous colourless oil (0.45 g, 0.86 mmol, 24%, from 2.0 g of starting ester **8**); R_f = 0.32 (hexane 19:1 ethyl acetate). M.p. 76 °C ; $[\alpha]_D^{26} +15.2$ (c 2.77 in DCM); ν_{max}/cm^{-1} 2933m (C-H), 2866m (C-H), 1754s (C=O), 1720s (C=O); δ_H (CDCl₃, 400 MHz) 0.65 (3H, s, C(18)H₃), 0.90 (3H, d, J = 6.4 Hz, C(21)H₃), 0.96 (3H, s, C(19)H₃), 0.99-1.19 (7H, m), 1.21 (9H, s, C(28)H₃, C(29)H₃ & C(30)H₃), 1.30-1.99 (20H, m), 2.26 (1H, ddd, J = 15.6 Hz, 9.2 Hz, 6.4 Hz, C(23)H_a), 2.39 (1H, ddd, J = 15.6 Hz, 10 Hz, 5.6 Hz, C(23)H_b), 5.22 (1H, s, C(3)H), 5.75 (2H, s, C(25)H₂), 8.07 (1H, s, C(31)H) ; δ_C (CDCl₃, 100 MHz) 12.5 (C(18)), 18.7 (C(21)), 21.5 (C(11)), 24.3 (C(19)), 24.6 (C(15)), 25.5 (C(7)), 26.6 (C(6)), 26.9 (C(2)), 27.3 (C(28)/C(29)/C(30)), 28.6 (C(16)), 31.0 (C(23)), 31.1 (C(22)), 31.2 (C(10)), 31.5 (C(20)), 35.3 (C(1)), 35.8 (C(8)), 36.1 (C(4)), 37.7 (C(12)), 39.2 (C(27)), 40.4 (C(9)), 42.6 (C(5)), 43.2 (C(13)), 56.4 (C(17)), 57.0 (C(14)), 71.5 (C(3)), 79.8 (C(25)), 161.3 (C(31)), 173.4 (C(24)), 177.7 (C(26)); LRMS ES+ $[M+Na]^+$: 541.4 (80%); HRMS ES+ calc for $C_{31}H_{50}O_6Na$ 541.3500, found 541.3480.

(4*R*)-4-((3*R*,8*R*,9*S*,10*S*,13*R*,14*S*,17*R*)-3-((4-(methoxycarbonyl)benzoyl)oxy)-10,13-dimethylhexadecahydro-1*H*-cyclopenta[*a*]phenanthren-17-yl)pentanoic acid (78)



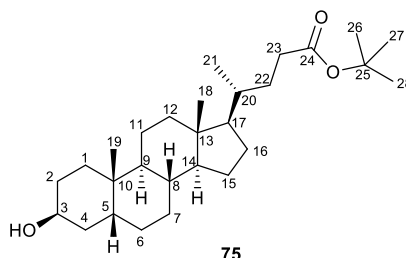
General Procedure for compounds 78, 79, 80, 81, 82 and 83: The corresponding *tert*-butyl ester (**78-83**) was dissolved in CH₂Cl₂ (4 mL) and cooled with an ice-bath to 0 °C. Dropwise addition of trifluoroacetic acid (4 mL) was proceeded and the mixture was left to react for 1 hour. The solvent was then evaporated to dryness and the residue evaporated twice with toluene (2 x 10 mL) to remove the excess TFA. A colourless crystalline product (**78**) was obtained (92 mg, 0.17 mmol, 97%). M.p. 165 °C; $[\alpha]_D^{22} +48.6$ (c 1.03 in DCM); ν_{max}/cm^{-1} 2928m (C-H), 2865m (C-H), 1709s (C=O); δ_H (CDCl₃, 400 MHz) 0.65 (3H, s, C(18)H₃), 0.92 (3H, d, J = 6 Hz, C(21)H₃), 0.96 (3H, s, C(19)H₃), 1.09-1.99 (27H, m), 2.25 (1H, ddd, J = 14 Hz, 6.8 Hz, 4.8 Hz, C(23)H_a), 2.39 (1H, ddd, J = 14 Hz, 10.4 Hz, 5.4 Hz, C(23)H_b), 3.94 (3H, s, C(33)H), 4.95-5.03 (1H, m, C(3)H), 8.09 (4H, s, C(27)H, C(28)H, C(29)H & C(30)H) ; δ_C (CDCl₃, 100 MHz) 12.2 (C(18)), 18.4 (C(21)), 21.0 (C(11)), 23.5 (C(19)), 24.3 (C(15)), 26.5 (C(7)), 26.8 (C(6)), 27.2 (C(2)), 28.3 (C(16)), 30.9 (C(23)), 31.1 (C(22)), 32.4 (C(1)), 34.8 (C(10)), 35.2 (C(4)), 35.4 (C(20)), 35.9 (C(8)), 40.2 (C(12)), 40.6 (C(9)), 42.1 (C(5)), 42.9 (C(13)), 52.5 (C(33)), 56.1 (C(17)), 56.6 (C(14)), 75.7 (C(3)), 129.6 (C(29)/C(30)), 129.6 (C(27)/C(28)), 133.8 (C(31)), 134.8 (C(26)), 165.4 (C(25)), 166.5 (C(32)), 180.5 (C(24)); LRMS ES- [M-H]⁻: 537.4 (100%), ES+ [M+Na]⁺: 561.3 (72%); HRMS ES- calc for C₃₃H₄₅O₆ 537.3222, found 537.3220.

(4*R*)-4-((3*R*,8*R*,9*S*,10*S*,13*R*,14*S*,17*R*)-10,13-dimethyl-3-((pyridin-1-ium-4-carbonyl)oxy)hexadecahydro-1*H*-cyclopenta[*a*]phenanthren-17-yl)pentanoate (79)



A colourless crystalline product (**79**) was obtained (50.3 mg, 0.105 mmol, 97%, from 58.0 mg, 0.108 mmol of **68**). M.p. 253-255 °C; $\nu_{\max}/\text{cm}^{-1}$ 2933m (C-H), 2864m (C-H), 2400-2600br (H-N⁺), 1725s (C=O), 1702s (C=O); δ_{H} (CDCl₃, 400 MHz) 0.67 (3H, s, C(18)H₃), 0.93 (3H, d, J = 6.8 Hz, C(21)H₃), 0.97 (3H, s, C(19)H₃), 1.09-1.98 (27H, m), 2.27 (1H, ddd, J = 15.4 Hz, 9.2 Hz, 5.6 Hz, C(23)H_α), 2.41 (1H, ddd, J = 15.4 Hz, 10.4 Hz, 5.2 Hz, C(23)H_β), 3.95 (3H, s, C(37)H), 5.00 (1H, tt, J = 11.2 Hz, 5.2 Hz, C(3)H), 7.90 (2H, s, C(27)H & C(28)H), 8.78 (2H, s, C(29)H & C(30)H) ; δ_{C} (CDCl₃, 100 MHz) 12.5 (C(18)), 18.7 (C(21)), 21.4 (C(11)), 23.8 (C(19)), 24.7 (C(15)), 26.8 (C(7)), 27.1 (C(6)), 27.5 (C(2)), 28.6 (C(16)), 31.1 (C(23)), 32.7 (C(22)), 32.7 (C(1)), 35.1 (C(10)), 35.5 (C(4)), 35.8 (C(20)), 36.3 (C(8)), 40.6 (C(12)), 41.0 (C(9)), 42.4 (C(5)), 43.2 (C(13)), 56.5 (C(17)), 57.0 (C(14)), 76.8 (C(3)), 123.6 (C(31)), 123.7 (C(32)), 135.0 (C(26)), 150.3 (C(29)/C(30)), 157.8 (C(25)), 176.7 (C(24)); LRMS ES- [M-H]⁻: 480.3 (100%), 480.4 (60%); HRMS ES- calc for C₃₀H₄₂NO₄ 480.3119, found 480.3117.

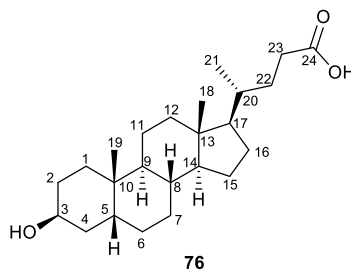
***tert*-butyl(4*R*)-4-((3*S*,8*R*,9*S*,10*S*,13*R*,14*S*,17*R*)-3-hydroxy-10,13-dimethylhexadecahydro-1*H*-cyclopenta[*a*]phenanthren-17-yl)pentanoate (75)**



Compound **33** (94.4 mg, 0.205 mmol) was dissolved in methanol 50:50 DCM (10 mL). Potassium carbonate (100 mg) was added to the solution, which was left to react with stirring for 1 hour 30 min. The mixture was then evaporated to dryness and the residue obtained was partitioned between Et₂O (20 mL) and H₂O (10 mL). The organic layer was

washed with H₂O (3*10 mL) and brine (2*10 mL), then dried over MgSO₄ and evaporated to yield compound **75**, a colourless crystalline solid (63.5 mg, 0.147 mmol, 72%). M.p. 162 °C; $[\alpha]_D^{25} +42.2$ (c 1.65 in DCM); ν_{max}/cm^{-1} 3550br (O-H), 2922m (C-H), 2880m (C-H), 1707s (C=O); δ_H (CDCl₃, 500 MHz) 0.64 (3H, s, C(18)H₃), 0.89 (3H, d, J = 7 Hz, C(21)H₃), 0.95 (3H, s, C(19)H₃), 1.03-1.40 (17H, m), 1.43 (9H, s, C(26)H₃ C(27)H₃ & C(28)H₃), 1.50-2.00 (10H, m), 2.11 (1H, ddd, J = 15.2 Hz, 8.5 Hz, 6 Hz, C(23)H_a), 2.25 (1H, ddd, J = 15.2 Hz, 10 Hz, 5 Hz, C(23)H_b), 4.10 (1H, s, C(3)H); δ_C (CDCl₃, 125 MHz) 12.2 (C(18)), 18.4 (C(21)), 21.2 (C(11)), 24.0 (C(19)), 24.3 (C(15)), 26.4 (C(7)), 26.8 (C(6)), 28.0 (C(16)), 28.3 (C(26)/C(27)/C(28)), 29.8 (C(2)), 30.1 (C(5)), 31.2 (C(23)), 32.7 (C(22)), 33.7 (C(10)), 35.3 (C(20)), 35.4 (C(1)), 35.8 (C(8)), 36.7 (C(4)), 39.9 (C(12)), 40.4 (C(9)), 42.9 (C(13)), 56.2 (C(17)), 56.8 (C(14)), 67.3 (C(3)), 80.0 (C(25)), 173.9 (C(24)); LRMS ES+ [M+Na]⁺: 455.4 (40%); HRMS ES- calc for C₂₈H₄₉O₃ 433.3676, found 433.3671.

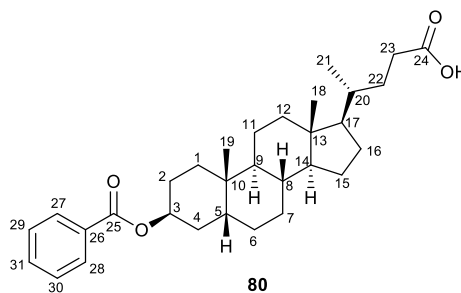
(4R)-4-((3S,8R,9S,10S,13R,14S,17R)-3-hydroxy-10,13-dimethylhexadecahydro-1H-cyclopenta[a]phenanthren-17-yl)pentanoic acid (76)



Compound **33** (0.1508 g, 0.327 mmol) was dissolved in methanol (4.33 mL). A solution of 30% w/w NaOMe/MeOH (0.66 mL) was added to the mixture and left to react with stirring for 2 hours. Then the mixture was dissolved in THF (5 mL) and stirred for a further 20 min before being evaporated to dryness. The resulting residue was partitioned between Et₂O (20 mL) and H₂O (10 mL). The organic layer was washed with HCl (3 x 10 mL), H₂O (3 x 10 mL) and brine (2 x 10 mL), then dried over MgSO₄ and evaporated to yield compound **76**, a colourless foam (78.3 mg, 0.208 mmol, 64%). M.p. 85 °C; $[\alpha]_D^{25} +24.4$ (c 1.72 in DCM); ν_{max}/cm^{-1} 2925m (C-H), 2861m (C-H), 1706s (C=O); δ_H (CDCl₃, 400 MHz) 0.65 (3H, s, C(18)H₃), 0.91 (3H, d, J = 6.4 Hz, C(21)H₃), 0.95 (3H, s, C(19)H₃), 1.09-1.99 (27H, m), 2.24 (1H, ddd, J = 15.8 Hz, 9.5 Hz, 6 Hz C(23)H_a), 2.38 (1H, ddd, J = 15.8 Hz, 11 Hz, 6 Hz, C(23)H_b), 4.11 (1H, s, C(3)H); δ_C (CDCl₃, 100 MHz) 12.2 (C(18)),

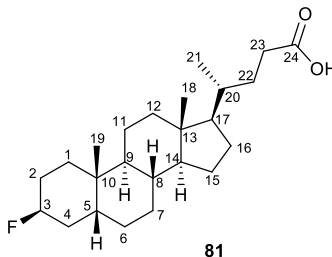
18.4 (C(21)), 21.2 (C(11)), 24.0 (C(19)), 24.3 (C(15)), 26.4 (C(7)), 26.8 (C(6)), 27.9 (C(16)), 28.3 (C(2)), 30.0 (C(5)), 30.9 (C(23)), 31.1 (C(22)), 33.6 (C(10)), 35.3 (C(20)), 35.5 (C(1)), 35.8 (C(8)), 36.7 (C(4)), 39.9 (C(12)), 40.4 (C(9)), 42.9 (C(13)), 56.1 (C(17)), 56.8 (C(14)), 67.4 (C(3)), 180.1 (C(24)) ; LRMS ES+ [M-H]⁻ : 375.3 (100%); HRMS ES-calc for C₂₄H₃₉O₃ 375.2905, found 375.2905.

(4R)-4-((3S,8R,9S,10S,13R,14S,17R)-3-(benzoyloxy)-10,13-dimethylhexadeca-1H-cyclopenta[*a*]phenanthren-17-yl)pentanoic acid (80)



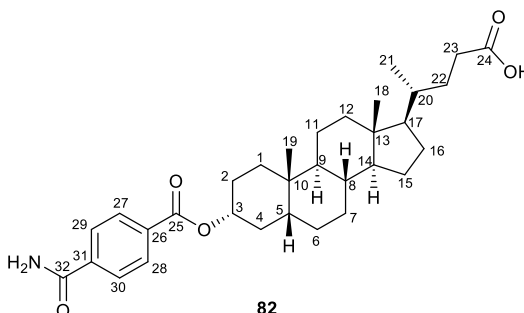
80, a colourless foam (94.4 mg, 0.196 mmol, 97%). M.p. 87 °C; [α]_D²⁶ +39.6 (c 1.52 in DCM); ν_{max}/cm^{-1} 2932m (C-H), 2863m (C-H), 1709s (C=O); δ_H (CDCl₃, 400 MHz) 0.67 (3H, s, C(18)H₃), 0.93 (3H, d, J = 6.4 Hz, C(21)H₃), 1.02 (3H, s, C(19)H₃), 1.13-2.12 (27H, m), 2.27 (1H, ddd, J = 16 Hz, 9.6 Hz, 6.4 Hz, C(23)H_a), 2.41 (1H, ddd, J = 16 Hz, 10.6 Hz, 5.4 Hz, C(23)H_b), 5.35 (1H, s, C(3)H), 7.44 (2H, t, J = 7.6 Hz, C(29)H & C(30)H), 7.55 (1H, t, J = 7.2 Hz, C(31)H), 8.05 (2H, d, J = 7.2 Hz, C(27)H & C(28)H); 9.73 (1H, s, acid OH); δ_C (CDCl₃, 100 MHz) 12.2 (C(18)), 18.4 (C(21)), 21.3 (C(11)), 24.2 (C(19)), 24.3 (C(15)), 25.3 (C(7)), 26.3 (C(6)), 26.7 (C(2)), 28.3 (C(16)), 30.9 (C(23)), 30.9 (C(22)), 31.2 (C(10)), 31.2 (C(20)), 35.1 (C(1)), 35.4 (C(8)), 35.8 (C(4)), 37.9 (C(12)), 40.1 (C(9)), 40.3 (C(5)), 42.9 (C(13)), 56.1 (C(17)), 56.7 (C(14)), 71.6 (C(3)), 128.4 (C(29)/C(30)), 129.6 (C(27)/C(28)), 131.3 (C(30)), 132.8 (C(31)), 166.1 (C(25)), 180.6 (C(24)); LRMS ES- [M-H]⁻ : 479.3 (50%) ES+ [M+Na]⁺ : 503.3 (100%); HRMS ES-calc for C₃₁H₄₃O₄ 479.3167, found 479.3171.

(4R)-4-((3S,8R,9S,10S,13R,14S,17R)-3-fluoro-10,13-dimethylhexadecahydro-1H-cyclopenta[a]phenanthren-17-yl)pentanoic acid (81)



81, a colourless crystalline solid (10.2 mg, 0.026 mmol, 84%, from 14.8 mg, 0.032 mmol of **39**). M.p. 52 °C ; $[\alpha]_D^{26} +28.3$ (c 0.81 in DCM); ν_{max}/cm^{-1} 2926m (C-H), 2864m (C-H), 1705s (C=O), 1377s (C-F); δ_H (CDCl₃, 400 MHz) 0.66 (3H, s, C(18)H₃), 0.92 (3H, d, J = 6.8 Hz, C(21)H₃), 0.96 (3H, s, C(19)H₃), 1.02-1.15 (8H, m), 1.50-2.01 (19H, m), 2.26 (1H, ddd, J = 16 Hz, 9.6 Hz, 6.4 Hz, C(23)H_α), 2.39 (1H, ddd, J=16 Hz, 10.8 Hz, 5.6 Hz, C(23)H_β), 4.86 (1H, d, J= 48.8 Hz, C(3)FH); δ_C (CDCl₃, 100 MHz) 12.2 (C(18)), 18.4 (C(21)), 21.3 (C(11)), 23.9 (C(19)), 24.3 (C(15)), 26.1 (C(7)), 26.3 (C(6)), 26.5 (C(10)), 28.3 (C(16)), 30.3 (C(5)), 30.9 (C(23)), 31.6 & 31.8 (C(2)), 32.3 (C(22)), 35.0 (C(20)), 35.5 (C(1)), 35.8 (C(8)), 37.0 (C(4)), 40.0 (C(12)), 40.4 (C(9)), 42.9 (C(13)), 56.1 (C(17)), 56.8 (C(14)), 89.6 & 91.2 (C(3)), 179.6 (C(24)); δ_F (CDCl₃, 375 MHz) (-76.0) & (-75.3) (1F, d, J = 253 Hz, C(3)HF); LRMS ES- [M-H]⁻: 377.4 (100%); HRMS ES+ calc for C₂₄H₄₀O₂F 379.3007, found 379.3003.

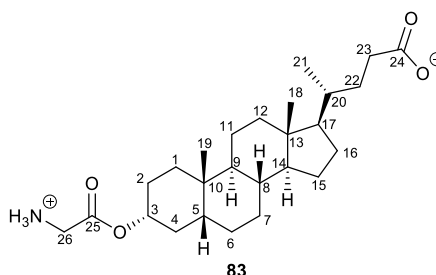
(4R)-4-((3S,8R,9S,10S,13R,14S,17R)-3-((4-carbamoylbenzoyl)oxy)-10,13-dimethylhexadecahydro-1H-cyclopenta[a]phenanthren-17-yl)pentanoic acid (82)



A brown powder (**82**) was obtained (89 mg, 0.17 mmol, 99%); m.p. 269 °C; $[\alpha]_D^{25} -35.6$ (c 1.70 in DCM); ν_{max}/cm^{-1} 3425wk (N-H), 3161br (O-H), 2927m (C-H), 2863m (C-H), 1698s (C=O), 1689s (C=O); δ_H (TFA-d, 400 MHz) 0.70 (3H, s, C(18)H₃), 1.07 (3H, d, J = 6.4 Hz, C(21)H₃), 1.10 (3H, s, C(19)H₃), 1.24-2.19 (27H, m), 2.39 (1H, ddd, J = 15.2 Hz, 9.6 Hz, 6 Hz, C(23)H_α), 2.55 (1H, ddd, J = 15.2 Hz, 10.4 Hz, 4.8 Hz, C(23)H_β), 5.03-5.11

(1H, m, C(3)H), 5.90 (1H, s, NH₃⁺), 8.00 (2H, d, J = 8 Hz, C(27)H & C(28)H), 8.21 (2H, d, J = 8 Hz, C(29)H & C(30)H); δ_C (TFA-d, 100 MHz), no distinguishable peaks apart from the solvent ones; LRMS ES- [M-H]⁻: 522.5 (100%); HRMS ES- calc for C₃₂H₄₄NO₅ 522.3225, found 522.3211.

(4R)-4-((3R,8R,9S,10S,13R,14S,17R)-3-(2-ammonioacetoxy)-10,13-dimethylhexadeca-hydro-1H-cyclopenta[*a*]phenanthren-17-yl)pentanoate (83)



83, a colourless crystalline solid (309 mg, 0.713 mmol, 99%, from 420 mg, 0.713 mmol of **69**); m.p. 228-230 °C; $[\alpha]_D^{27} +48.5$ (c 1.08 in MeOH); ν_{max}/cm^{-1} 3000-2800br (N-H, amine salt), 2925m (C-H), 2865m (C-H), 1755s (C=O), 1701s (C=O); δ_H (CD₃OD, 400 MHz) 0.72 (3H, s, C(18)H₃), 0.96 (3H, d, J = 6.8 Hz, C(21)H₃), 1.00 (3H, s, C(19)H₃), 1.02-2.09 (27H, m), 2.21 (1H, ddd, J = 15.6 Hz, 8.8 Hz, 6.8 Hz, C(23)H_a), 2.34 (1H, ddd, J = 15.6 Hz, 9.6 Hz, 5.2 Hz, C(23)H_b), 3.81 (2H, s, C(30)H₂), 4.84-4.92 (1H, m, C(3)H); δ_C (CD₃OD, 100 MHz) 12.5 (C(18)), 18.7 (C(21)), 21.9 (C(11)), 23.7 (C(19)), 25.2 (C(15)), 27.5 (C(7)), 27.5 (C(6)), 28.1 (C(2)), 29.2 (C(16)), 32.0 (C(23)), 32.3 (C(22)), 33.2 (C(10)), 35.7 (C(20)), 35.9 (C(1)), 36.7 (C(8)), 37.2 (C(4)), 41.2 (C(26)), 41.5 (C(12)), 41.8 (C(9)), 43.3 (C(5)), 43.9 (C(13)), 57.5 (C(17)), 57.9 (C(14)), 78.1 (C(3)), 168.0 (C(25)), 178.1 (C(24)); LRMS ES- [M-H]⁻: 432.4 (100%); HRMS ES- calc for C₂₆H₄₂O₄N 432.3119, found 432.3104.

5.3 - *In-Vitro* pre-mRNA Splicing Assay

5.3.1 - Yeast; Gel electrophoresis

Yeast pre-mRNA splicing extract (strain BJ2168)⁴⁴ was provided by colleagues from the O'Keefe group. Reaction mixes (10 μ L) were made up of 4 μ L of extract, 1 μ L of 3% PEG6000, 1 μ L of RNase free H₂O and 4 μ L 5X splicing buffer (300 mM K₃PO₄ pH = 7.0, 3% PEG 6000, 12.5 mM MgCl₂, 10 mM ATP) and were added. Stocks of compounds were prepared in 40% DMSO (10 mM) and 1 μ L of each were added to the reactions to give 4% final DMSO concentrations (40% DMSO alone for the controls). Pre-incubation of the reactions proceeded (5 min at 23°C). 1 μ L of β -Actin pre-mRNA (320nM/ μ L) was added to the reactions and incubated at 23°C for 60 min. The 0-hour control was processed immediately following addition of pre-mRNA. Splicing reactions were quenched by adding 4 μ L of the reaction mixes to 2 μ L stop mix (1 mg/mL proteinase K, 50 mM EDTA, 1% SDS). All reactions were then placed at 37°C for 15 min, followed by addition of 200 μ L of splicing diluent (300 mM sodium acetate pH 5.3, 1 mM EDTA, 0.1% SDS, 25 μ g/mL E. coli tRNA) and 200 μ L of PCA (Phenol Chloroform-isoamyl Alcohol). The mixtures were vortexed and spun at 13000 g for 2 min. The top-aqueous layer was extracted (190 μ L), mixed with 500 μ L of cold 100% ethanol and the samples were incubated at -20°C for at least 30 min (or overnight). All samples were spun at 13000 g for 10 min before aspirating the ethanol and allow the remaining RNA pellets to airdry. Re-suspension in 15 μ L of RNAase-free H₂O was carried out and RNA concentrations were measured using a nanodrop.

RNA was converted to cDNA using superscript (Invitrogen) and a transcript specific primer (sequence of p283-reverse). All reactions were normalised to the lowest RNA concentration (11 μ L of total volume per sample) with water dilution. To this was added 1 μ L of dNTPs and 1 μ L of gene specific primer (p283 reverse primer at 2 μ M, sequence: CCCCCTTCATCACCAACGTAGG) and the mixtures were incubated at 65°C for 5 min. Each sample then received 1 μ L of DTT (dithiothreitol), 4 μ L of SSIV buffer, 1 μ L of RNasin and 1 μ L of the superscript IV enzyme, followed by 30 min of incubation using the SSIV program. After this, cDNA amplification was carried out with 1 μ L for each reaction, mixed with 5 μ L of Phusion GC buffer, 0.5 μ L of dNTP, 1.25 μ L of P2 forward primer, 1.25 μ L of exon 2 reverse primer, 0.25 μ L of Phusion enzyme and 15.75 μ L of H₂O. The resulting mixture was incubated for 60 min using the Phusion

program. Addition of 5 μL of 6x DNA loading dye (blue) was then added to each reaction. An agarose gel (1.5%) was prepared with 1.5 g of agarose in 100 mL of TBE (Tris-Borate EDTA) and 10 μL of safeview dye. A 20 μL fraction of each sample was placed in separated wells, with 10 μL of purple 1Kb plus dye added on each side of the gel. Gel electrophoresis was carried out at 70V for 45 min, before being exposed under UV light.

5.3.2 - Yeast; qRT-PCR quantification

In addition, cDNA was quantified for spliced:unspliced abundance by qPCR using the Power SYBR green mastermix system (Thermo Fisher) and recommended protocols, using a 1/10 dilution of cDNA template, the β Act-1 spliced (P1, forward: TAACAATGGATTCTGAGGTTG; reverse: CTTGGTGTCTTGGTCTACCG) and β Act-1 un-spliced (P3, forward: ATTGACTGATCTGTAATAACCACG, reverse: CTTGGTGTCTTGGTCTACCG) primers. The relative quantity (RQ) of the spliced and unspliced transcript was calculated by normalising the abundance of spliced product (P1 primers) to that of the unspliced product (P3 primers) using the $\Delta\Delta\text{Ct}$ method.

6.0 - References

1. V. Nancollis, J. P. D. Ruckshanthi, L. N. Frazer & R.T. O'Keefe, *J. Cell. Biochem.*, 2013, **114**, 2770-2784.
2. D. L. Black, *Ann. Rev. Biochem.*, 2003, **72** (1): 291–336.
3. R. J. Soltysiak, *Arresting the Spliceosome*, PhD Thesis, The University of Manchester, 2015, 1-198.
4. C. Maeder, A. Kutasch & C. Guthrie, *Nat. Struct. Mol. Biol.*, 2009, **16**, 42-48.
5. B. Laggerbauer, T. Achsel & R. Luehrmann, *Proc. Natl. Acad. Sci. USA*, 1998, **95**, 4188-4192.
6. P. L. Raghunathan & C. Guthrie, *Curr. Biol.*, 1998, **8**, 847-855.
7. M. R. Green, *Ann. Rev. Genet.*, 1986, **20**, 671-708.
8. S. Bonnal, I. Vigevani & J. Valcarcel, *Nat. rev.*, 2012, **11**, 847-859.
9. R. Yoshimoto, D. Kaida, M. Furuno, A. M. Burroughs, S. Noma, H. Suzuki, Y. Kawamura, Y. Hayashizaki, A. Mayeda & M. Yoshida, *RNA*, **23**, 47-57.
10. G. Wu, L. Fan, M. N. Edmonson, T. Shaw, K. Boggs, J. Easton, M. C. Rusch, T. R. Webb, J. Zhang & P. M. Potter, *RNA*, **24**, 1056-1066.
11. S. M. Dehm, *Clin. Cancer Res.*, 2013, **19**, 6064-6066.
12. Unpublished communication, Ray O'Keefe, The University of Manchester, 2019.
13. E. C. Small, S. R. Leggett, A. A. Winans & J. P. Staley, *Mol. Cell.*, 2006, **23**, 389-399.
14. W. O. Godtfredsen, W. Vondaeht, L. Tybring & S. Vangedal, *J. Med. Chem.*, 1966, **9**, 15-22.
15. S. J. Harte, *Arresting the Spliceosome*, PhD Thesis, The University of Manchester, 2012, 1-201.
16. Y. Gao, M. Selmer, C. M. Dunham, A. Weixlbaumer, A. C. Kelley & V. Ramakrishnan, *Science*, 2009, **326**, 694-700.
17. D. Riber, M. Venkataramana, S. Sanyal & T. Duvold, *J. Med. Chem.*, 2006, **49**, 1503-1505.
18. D. V. Patel, E. M. Gordon, R. J. Schmidt, H. N. Weller, M. G. Young, R. Zahler, M. Barbacid, J. M. Carboni, J. L. Gullobrown, L. Hunihan, C. Ricca, S. Robinson, B. R. Seizinger, A. V. Tuomari & V. Manne, *J. Med. Chem.*, 1995, **38**, 435-442.

-
19. P. G.G. do Nascimento, T. L.G. Lemos, M. C.S. Almeida, J. M.O. de Souza, A. M.C. Bizerra, G. M.P. Santiago, J. G.M. da Costa & H. D.M. Coutinho, *Steroids, Elsevier*, 2015, **104**, 8-15.
 20. R. P. Bonar-Law, A. P. Davis & J. K. M. Sanders, *J. Chem. Soc. Perkin Trans.*, 1990, **1**, 2245-2250.
 21. B. Neises & W. Steglich, *Angew. Chem., Int. Ed. Eng.*, 1978, **17**, 522-524.
 22. D. Albert & M. Feigel, *Helv. chim. act.*, 1997, **80**, 2168-2181.
 23. S. G. Lakoud & A. Djerourou, *Arab. J. Chem.*, 2016, **9**, S889-S892.
 24. N. Muramoto, K. Yoshino, T. Misaki & T. Sugimura, *Synthesis*, 2013, **45**, 931-935.
 25. T. Liang, C. N. Neumann & T. Ritter, *Angew. Chem. Int.*, 2013, **52**, 8214-8264.
 26. D. F. Shellhamer, A. A. Briggs, B. M. Miller, J. M. Prince, D. H. Scott & V. L. Heasley, *J. Chem. Soc., Perkin Trans*, 1996, **2**, 973-977.
 27. A. L'Heureux, F. Beaulieu, C. Bennett, D. R. Bill, S. Clayton, F. LaFlamme, M. Mirmehrabi, S. Tadayon, D. Tovell & M. Couturier, *J. Org. Chem.*, 2010, **75**, 3401-3411.
 28. C. N. Neumann & T. Ritter, *Acc. Chem. Res.*, 2017, **50**, 2822-2833.
 29. S. J. Blanksby & G. Barney Ellison, *Acc. Chem. Res.*, 2003, **36**, 256-263.
 30. K. Huynh & C. L. Partch, *Curr Protoc Protein Sci*, 2016, **79**, 28.9.1-28.9.14.
 31. J. Ni, M. Guo, Y. Cao, L. Lei, K. Liu, B. Wang, F. Lu, R. Zhai, X. Gao, C. Yan, H. Wang & Y. Bi, *Europ. J. Med. Chem.*, 2019, **162**, 122-131.
 32. M. G. Simpson, M. Pittelkow, S. P. Watson & J. K. M. Sanders, *Org. Biomol. Chem.*, 2010, **8**, 1173-1180.
 33. J. C. Sheehan & S. L. Ledis, *J. Am. Chem. Soc.*, 1973, **95:3**, 875-879.
 34. K. Baburao, A. M. Costello, R. C. Petterson & G. E. Sander, *J. Chem. Soc.*, 1968, **8**, 2779-2781.
 35. T. Iida, T. Momose, T. Tamura, T. Matsumoto, F. C. Chang, J. Goto & T. Nambara, *J. Lipid R.*, 1989, **30**, 1267-1279.
 36. A. N. Butkevich, G. Y. Mitronova, S. C. Sidenstein, J. L. Klocke, D. Kamin, D. N. H. Meineke, E. D'Este, P.-T. Kraemer, J. G. Danzl, V. N. Belov & S. W. Hell, *Angew. Chem. Int. Ed.*, 2016, **55**, 3290-3294.
 37. WO 2017/035501 AI.
 38. R. H. Beddoe, K. G. Andrews, V. Magne, J. D. Cuthbertson, J. Saska, A. L. Shannon-Little, S. E. Shanahan, H. F. Sneddon & R. M. Denton, *Science*, 2019, **365**, 910-914.

-
39. H. Xiao-Long, X. Yajing ; G. Xiang-Zhong ; X. Jie-Xin, W. Ying-Ying, Y. Zhengfang & Q. Wen-Wei, *Steroids*, 2017, **125**, 54-60.
40. D. V. Waterhous, S. Barnes & D. D. Muccio, *J. Lipid Res.*, 1985, **26**, 1068-1078.
41. K. Chang, L. Lee, J. Chen & W. Li, *Chem. Comm.*, 2006, **6**, #6, 629-631.
42. Z. Zhao, X. Liu, L. Liu & G. Li, *J. Chem. Res.*, 2010, **8**, 455-458.
43. Joachimial & Roman, *J. Chem. Res.*, 2008, **5**, 260-265.
44. A. Ansari & B. Schwer, *The EMBO J.*, 1995, **14**, 4001-4009.